DESIGN AND DEVELOPMENT OF AUTO VARIABLE HITCH HEIGHT FOR 2WD TRACTORS

Submitted in partial fulfilment of the requirements of the degree of
Doctor of Philosophy

By

Tage Tapang
PhD/PT/14/AE/01

Department of Agricultural Engineering
North Eastern Regional Institute of Science and Technology
(Deemed to be University)
Nirjuli – 791109
Arunachal Pradesh, India

November 2022

DESIGN AND DEVELOPMENT OF AUTO VARIABLE HITCH HEIGHT FOR 2WD TRACTORS

Submitted in partial fulfilment of the requirements of the degree of
Doctor of Philosophy

By

Tage Tapang
PhD/PT/14/AE/01

Department of Agricultural Engineering
North Eastern Regional Institute of Science and Technology
(Deemed to be University)
Nirjuli – 791109
Arunachal Pradesh, India

November 2022

Dedicated

to my

Parents, Family, and Well wishers

पूर्वोत्तर क्षेत्रीय विज्ञान एवम् प्रौद्योगिकी संस्थान
North Eastern Regional Institute of Science & Technology
(Deemed to be University u/s 3 of the UGC Act, 1956)
Under the Ministry of Education, Govt. of India
निर्जुली - ७९१ १०९ (ईटानगर)
अरुणाचल प्रदेश, भारत
Nirjuli - 791 109 (Itanagar)
Arunachal Pradesh, India

CERTIFICATE

This is to certify that the thesis entitled **"Design and Development of Auto Variable Hitch Height for 2WD Tractors"**, submitted to the Department of Agricultural Engineering, North Eastern Regional Institute of Science and Technology, Nirjuli (Itanagar) for the award of the Degree of Doctor of Philosophy, is a record of bonafide research work carried out by **Mr. Tage Tapang** under my supervision and guidance. The thesis is, in my opinion, worthy of consideration for the award of the Doctor of Philosophy in accordance with the regulations of the Institute. The results embodied in this thesis have not been submitted to any other University or Institute for the award of any Degree or Diploma.

All helps received by him from various sources have been duly acknowledged.

(P. K. Pranav)
Supervisor

Phone : (0360) 2257401 - 11(O)
Fax : (0360) 2257872 / 2258533
Gram : NERIST, Nirjuli
E-mail : @nerist.ernet.in
@nerist.ac.in
Website : www.nerist.ac.in

NORTH EASTERN REGIONAL INSTITUTE OF SCIENCE AND TECHNOLOGY

DECLARATION

I hereby certify that the work which is being presented in the thesis entitled "Design and Development of Auto Variable Hitch Height for 2WD Tractors" in partial fulfilment of the requirements for the award of the Degree of Doctor of Philosophy and submitted in the Department of Agricultural Engineering of the NERIST, Nirjuli, is an authentic record of my own work carried out during the period from 2014 to 2022 under the supervision of Dr. P. K. Pranav, Associate Professor, RPCAU, Pusa, Samastipur, Bihar.

The matter presented in the thesis has not been submitted by me for the award of any other degree of this or any other Institute.

(Tage Tapang)
Candidate

This is to certify that the above statement made by the candidate is correct to the best of my knowledge.

Date: 30-11-2022

(P. K. Pranav)
Supervisor

The Ph.D. viva voce of Tage Tapang is held today (12-05-2023)

(P. K. Pranav)
Supervisor

(Prasanna Kumar G.V.)
Examiner

Acknowledgement

There are a lot of people who helped and supported me throughout my course of research work that led to the completion of this thesis. I am thankful to all of them and express my sincere and heartfelt gratitude to them.

Foremost, I would like to express my sincere thanks to my research supervisor, Dr. P.K. Pranav, for his continuous support, knowledge, patience, motivation, and belief in me throughout the research work. It was indeed a great privilege to work under his guidance and benefit from his expertise. This research work has been accomplished because of his unconditional support; making himself available whenever called for and guiding me throughout the journey. I am thankful and fortunate to have done my doctoral program under his guidance.

I am deeply grateful to the members of my doctoral committee, Dr. K. N. Dewangan (Chairman), Dr. S. K. Bhagat (Member), and Dr. Arnab Bandyopadhyay (Member), for their encouragement, trust, and insightful suggestions during my course of research.

I am very thankful to Dr. K. N. Dewangan, Head, Department of Agricultural Engineering, NERIST and former head, Dr. S. K. Srivastava for their constant encouragement and belief in me during the course of my research. I would also like to thank all the faculty members as well as the non-teaching staff of the Department of Agricultural Engineering, NERIST, for their love and support during my study.

I would like to express my profound and heartfelt thanks to Mr. Surya Kumar Chhetry (JPO, ESA, NERIST) for his technical support and inputs without which the thesis would not have seen the light of the day. It would be unfair if I do not mention and acknowledge my sincere thanks to Mr. Jaga Ray, Mr. Orang Megu and Mr. Jadab Saikia for their assistance throughout my research work.

I would like to extend my gratitude and thanks to my friends M. Ukil Singh, Sonu Kumar, Prem Ranjan, Sameer Mandal, Vithato Keyho for their constant support and encouragement. A very special thanks to my dear friends Mr. Duyu Byai and Mr. Gojum Nyodu for their belief, encouragement, support, and faith on me, that carried me through the difficult times.

Lastly, I would like to thank my parents, family, Winnie and almighty God for their endless love, support, and blessings.

Date: 30-11-2022

Place: Nirjuli (Tage Tapang)

Abstract

The location of the tractor hitch height plays an important role in balancing the traction and stability of a 2WD tractor, which are two vital parameters that determine its maximum pulling capacity. A lower hitch location enhances stability, whereas a higher location offers better traction. Failures in dynamic stability occur occasionally which need to be assessed and addressed by sacrificing the traction at that point of time. Hence, a project was undertaken to develop an auto variable hitch height to address such situations as per the need for stability or traction. The front axle weight was monitored to supervise the stability status of the test tractor by suitably placing a load cell under the front axle. Further, the single hitch point of the tractor was modified to enable its easy upward and downward movement using a hydraulic cylinder powered by the tractor's hydraulics. The developed variable hitch point could vary from 26 to 68 cm above the ground surface.

A microcontroller was programmed to read the front axle load continuously and send signals to solenoid operated directional control value to vary the hitch location up/down as per need. The haulage performance test was conducted with the instrumented tractor at different speeds, payloads, gradients, and surface conditions. From the field tests, it was observed that the hitch height had no considerable effect on the draft requirement; however, the vertical component of the drawbar pull had an inverse relationship with hitch height in all operating conditions. Further, lowering the hitch height reduced the weight transfer and consequently enhanced the longitudinal stability. Increase in hitch height decreased the wheel slip due to higher weight transfer from the front axle and enhanced the tractive performance. Hence it was concluded that the developed system optimized the front axle load between 20 to 25% of the total static weight of tractor by varying the hitch height. Moreover, the automatic variable hitch mechanism enabled the test tractor to operate at higher tractive efficiency without compromising the longitudinal stability within the effect of the specified range of hitch height.

Keywords: hitch height, dynamic stability, traction, front axle load, microcontroller, haulage, weight transfer.

TABLE OF CONTENTS

LIST OF FIGURES

LIST OF TABLES

LIST OF SYMBOLS AND ABBREVIATIONS

Symbol / Abbreviation	Description
°	degree
%	per cent
δ	tyre deflection
2WD	two wheel drive
3D	three dimensions
4WD	four wheel drive
ANFIS	adaptive neuro-fuzzy inference system
ASAE	American Society of Agricultural Engineers
ANN	artificial neural network
B_n	Brixius mobility number
cm	centimeter
CG	centre of gravity
DSS	decision support system
DOF	degree of freedom
DTGO	digital throttle gear optimiser
DCV	direction control valve
D	draft
et al.	et alia (and others)
etc	et cetera
G1	surface gradient type 1
G2	surface gradient type 2
G3	surface gradient type 3
GTR	gross traction ratio
H1	first gear (high)
H2	second gear (high)
H3	third gear (high)
H_v	hitch height
H_v	hitch height from the ground surface
H_d	horizontal distance between the rear axle and the hitch point
H_d	horizontal distance of the hitch point from the rear axle
i.e.	that is

Note: The unit of weight, load or force in ‘kg’ may be read as ‘N’ throughout the thesis.

kg	kilogram
km/h	kilometer per hour
kN	kilo Newton
kPa	kilo Pascal
kW	kilo Watt
L3	third gear (low)
LCD	liquid crystal display
MF399	Massey Ferguson 399 tractor
MFWD	mechanical front wheel drive
m/s	meter per second
m	meters
NERIST	North Eastern Regional Institute of Science and Technology
NTR	net traction ratio
PTO	power take off
PID	proportional integral derivative
rpm	revolution per minute
ROPS	roll over protective structure
rr	rolling radius
SVFC	specific volumetric fuel consumption
SSPM	stability of self propelled agricultural machines
TE	tractive efficiency
TS	tarmacadam surface
W_{tl}	total weight of the trailer
V	vertical force
VB	Visual Basic
US	unpaved surface
Vel (extn)	velocity during extension
Vel (retn)	velocity during retraction
WT	weight transfer
S	wheel slip
u	gradient of the surface

Note: The unit of weight, load or force in ‘kg’ may be read as ‘N’ throughout the thesis.

TABLE OF CONTENTS

Abstract

The location of the tractor hitch height plays an important role in balancing the traction and stability of a 2WD tractor, which are two vital parameters that determine its maximum pulling capacity. A lower hitch location enhances stability, whereas a higher location offers better traction. Failures in dynamic stability occur occasionally which need to be assessed and addressed by sacrificing the traction at that point of time. Hence, a project was undertaken to develop an auto variable hitch height to address such situations as per the need for stability or traction. The front axle weight was monitored to supervise the stability status of the test tractor by suitably placing a load cell under the front axle. Further, the single hitch point of the tractor was modified to enable its easy upward and downward movement using a hydraulic cylinder powered by the tractor's hydraulics. The developed variable hitch point could vary from 26 to 68 cm above the ground surface.

A microcontroller was programmed to read the front axle load continuously and send signals to solenoid operated directional control value to vary the hitch location up/down as per need. The haulage performance test was conducted with the instrumented tractor at different speeds, payloads, gradients, and surface conditions. From the field tests, it was observed that the hitch height had no considerable effect on the draft requirement; however, the vertical component of the drawbar pull had an inverse relationship with hitch height in all operating conditions. Further, lowering the hitch height reduced the weight transfer and consequently enhanced the longitudinal stability. Increase in hitch height decreased the wheel slip due to higher weight transfer from the front axle and enhanced the tractive performance. Hence it was concluded that the developed system optimized the front axle load between 20 to 25% of the total static weight of tractor by varying the hitch height. Moreover, the automatic variable hitch mechanism enabled the test tractor to operate at higher tractive efficiency without compromising the longitudinal stability within the effect of the specified range of hitch height.

Keywords: hitch height, dynamic stability, traction, front axle load, microcontroller, haulage, weight transfer.

Chapter 1
Introduction

1.1 General

India is the world's largest tractor market (Bhattarai et al., 2020) and tractors are an important aspect of farm mechanization which helps in increase of farmers profit year after year (Malik and Kohli, 2020). Tractors were first manufactured in India in the year 1961 (KhetiGaadi, 2018) and it has grown remarkably well in the previous six to seven decades. Tractors are the most important farm machines not only in India but all over the world which have traditionally been employed on farms to automate a variety of agricultural tasks.

1.2 Tractor Accidents

Tractors were invented to reduce the effort associated with agricultural work, but the use of tractors has also increased the number of farm accidents. There are various risk variables that increase the likelihood of deadly tractor accidents. This can be split into three groups, namely: tractor operator, tractor physical characteristics, and agricultural activity environment, even though it is crucial to note that these three aspects are inextricably linked (Antunes et al., 2018). Around 50 percent of the annual overall fatalities in agricultural accidents are related to tractors (Hard et al., 1999). Approximately 70 percent of these accidents are caused due to tractor rollovers which may be either sideways (lateral) or rearward (longitudinal). According to National Safety Council (1968), rearward rollovers which occur when the reaction on the front wheel becomes zero are more fatal than sideways rollovers (Figure 1.1). Tractor turnovers are the primary cause of fatal injuries on US farms and lead to about 130 deaths annually which is more than 50% of all tractor related deaths (NASD - National Agricultural Tractor Safety Initiative, 2004). Moreover, the situation is critical given the fact that 80% of rollover accidents in the US involve experienced operators which lead to permanent disability for 1 in 7 farmers, and 7 of 10 farms would go out of business within 5 years of any such accident (NASD - Tractor Overturns).

1.3 Tractor Trailer System

To ensure safety, anyone who utilizes farming equipment such as tractors must know how they work and be aware of their inherent safety issues. Tractor manufacturers design these

Figure 1.1 Lifting of front axle of a 2WD tractor and the impending longitudinal rollover (Source: Caters News Agency)

vehicles for a specific purpose. The primary design of a tractor is based on field operation mounted or trailing an equipment. The design and physical characteristics of tractors are best suited for field work rather than haulage work. Owing to the poor road conditions, especially across rural parts of the country, the tractor-trailer system mode of transportation is very popular. According to a study, haulage operation accounts to about 70 percent of the total tractor use (Kumar, 1994). But due to a lack of attention to the haulage aspect, there is a greater number of reported accidents associated with rollover during haulage operations. Various modelling and experimental data reveal that the ideal weight distribution for a conventional 2WD tractor to achieve efficient drawbar pull is around 30% on the front and 70% on the rear axle (Lankenau and Winter, 2018). The shifting of the centre of gravity which primarily occurs due to improper driving and excessive weight transfer from the front wheels is a major factor contributing to the higher number of rollovers. Weight transfer from the front axle to the rear axle is caused due to the rearward rollovers generated by the moment of the applied pull around the surface contact point of the rear wheel. This form of rollover is more common in hilly regions with sloppy ground or due to blockage in the rear wheel(s). Since more death occurs due to rollover accidents, some design intervention must be realised in this aspect to tackle this challenging issue.

1.4 Instability in 2WD Tractor

Modern tractors have become safer because of extra weighting options, wheel settings, and even dual wheel and track capability. Although, the issue of tractor stability and potential instability remains critical. Rollover mishaps are more common in tractors due to their high center of gravity (Rondelli et al., 2018). The major and predominant tractor accidents include rollovers (overturns), run-overs, collisions, and PTO injuries (Kumar et al., 1998). Poor implement hitching, moving up a steep surface, potholes or large obstacles on the road or field, sudden acceleration, extreme speed during turns, or driving too close to ditches are some of the major causes of tractor overturns.

The center of gravity (CG) plays an important role in determining the dynamic stability of a tractor. It is the point in a tractor where all of its components are assumed to be balanced. When a two-wheel drive tractor is parked on level ground with all four wheels on the ground, the CG is closer to the rear axle and normally 60 cm in front of it (Murphy, 2014). As a result, the front axle bears about 30% of the tractor's weight, while the rear axle bears 70%. The CG is slightly further forward on four-wheel drive and center-articulated tractors.

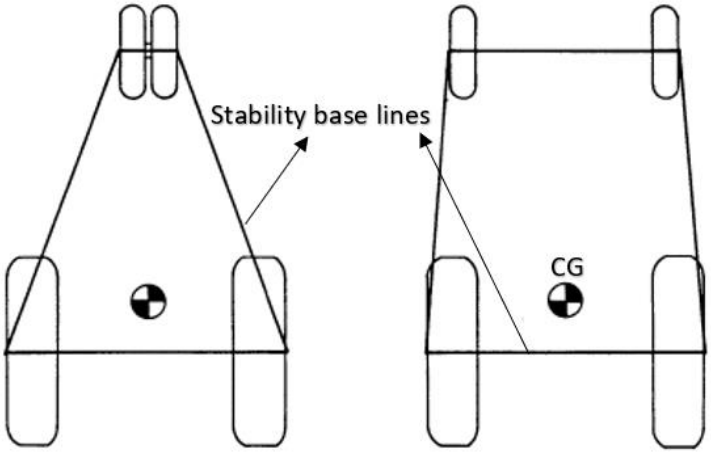

Figure 1.2 Tractor's CG and stability baselines

Centre of gravity of the tractor must lie inside the vehicle’s stability baseline in order for it to stay upright. The stability baselines are imaginary lines formed between the tractor tyres’ contact locations with the ground. The rear stability baseline is the line linking the rear tyre contact points, whereas the side stability baselines are the lines connecting the rear and front tyres on the same side. Front stability baselines exist but are rarely used in determining tractor instability. The CG and stability baselines of a tractor are depicted in Figure 1.2. The position of the CG changes drastically when the tractor travels from a level

position to a slope. The tractor rolls over if the CG-stability baseline connection changes significantly that the vehicle's CG falls beyond the stability baseline. Uneven ground terrain and load due to mounted or trailed equipment contribute to shorten the gap between the tractor's CG and stability baselines in many common working conditions. Also, the CG and the stability baseline comes closer when the tractor is on an incline surface. Centrifugal force, rear-axle torque, and drawbar leverage are the major factors in contributing towards tractor instability due to weight transfer. Each of these elements is mediated by the CG. To put it another way, any of these circumstances has the potential to cause the tractor's CG to exceed the stability baseline and result in an overturn.

1.5 Impact of Rear-Axle Torque in Tractor Stability

In two-wheel drive tractors, rear-axle torque is the energy that is transmitted from the engine to the rear axle. When the clutch of such tractor is engaged, torque is transmitted to the rear axle in the form of a twisting force. The torque is then delivered to the tractor tyre. The rear axle should rotate in typical circumstances and the tractor should drive forward. However, if the rear axle is unable to rotate, the situation becomes inverse, and the tractor chassis rotate about the rear axle. This leads to the lifting of the front-end of the tractor. If this situation prolongs until the tractor's CG goes beyond the rear stability baseline, it leads to longitudinal overturn. An operator may not recognize that a tractor is about to overturn due to rear axle torque. As a result, a tractor's CG may only have to rear up to around 75 degrees off a level surface (also known as "point of no return") before passing the rear stability baseline and rolling over. The gap between the tractor's CG and rear stability baseline is narrowed in situations like when it is in a deep hole or driving up a steep surface. The tractor will approach the "point of no return" faster if excessive rear axle torque is applied. Figure 1.4 depicts such a situation. This can occur when the rear tractor tyres are prohibited from rotating due to obstacles or due to excess drawbar load.

1.6 Impact of Drawbar Leverage in Tractor Stability

Drawbar leverage is another factor that affects dynamic stability of 2WD tractors that can result in longitudinal rollover. When such a tractor pulls any load, its rear wheels impart thrust on the ground surface. Simultaneously, the weight being trailed by the tractor tends to act in the direction opposite to the forward motion and vertically towards the ground. And as such, the load is assumed to be acting down towards the ground. The rear axle

becomes a pivot point because of this backward and downward pull, and the load acts as the force attempting to flip the tractor backward. Heavier load, surface gradient or a greater

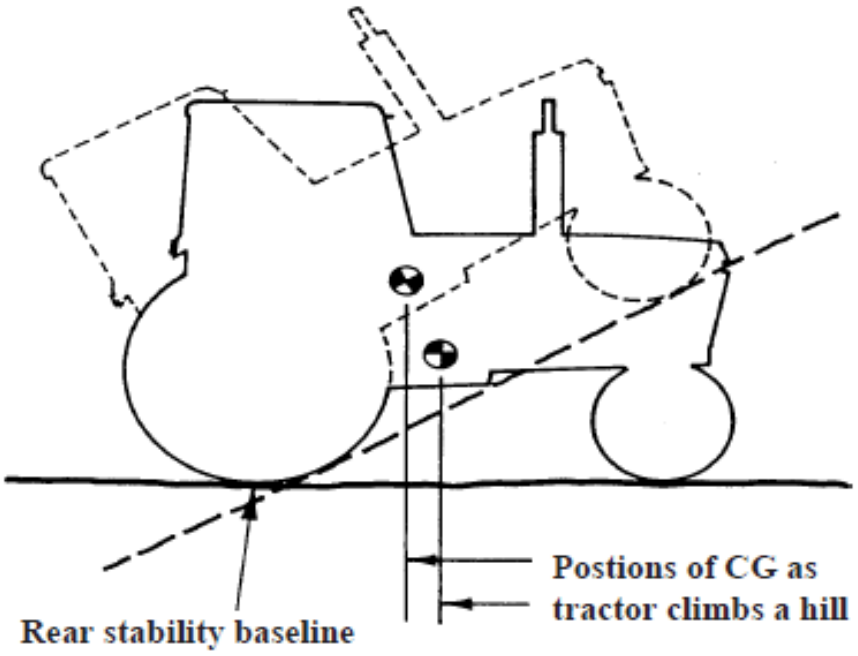

Figure 1.3 Shifting of CG of tractor when moving on an inclined surface

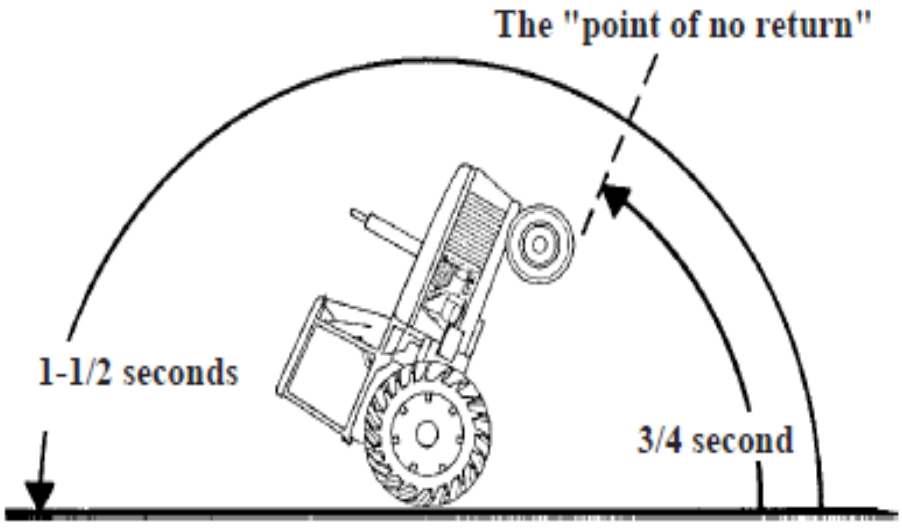

Figure 1.4 Point of no return

angle of pull between the hitch point and the ground surface result in greater leverage by the load to overturn the tractor rearward.

The drawbar of a tractor is designed to safely counter the rearward tilting effect of hauled loads (Murphy, 2014). When loads are hooked to a tractor in places other than the intended location, the tractor's design for hauling loads is compromised. The drawbar of the tractor

will descend as the front end of the tractor elevates. This is due to the tractor's geometry. As the front axle lifts, the rear drawbar is lowered. The "angle of pull" and the leverage, the load has, to tilt a tractor backward decreases when the drawbar is lowered. The reaction from the ground on the rear tyres increases at higher hitch points. This may prevent the rear tyres from slipping, but it encourages the rear axle torque to lift off the front axle. Because the tractor's CG is closer to the rear stability baseline, tractors pulling a load up an incline require less leverage to overturn the tractor rearward.

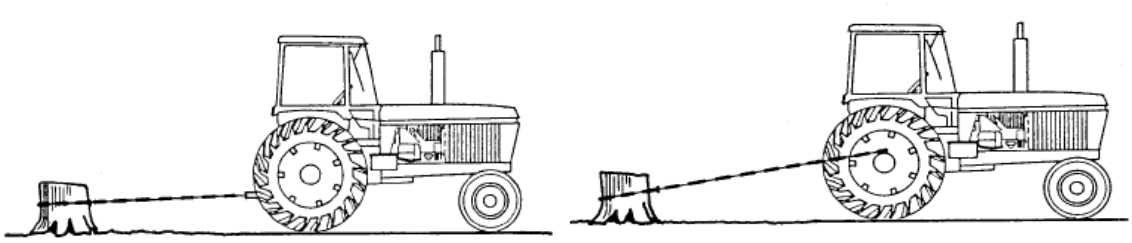

Figure 1.5 Effect of drawbar leverage in tractor stability

1.7 Hitching System in 2WD Tractor

Tractors are a widely used power source in rural areas for agricultural and transportation purposes. The drawbar connected to a trailer is very popular practice in India for transporting human in addition to carrying agricultural and non-agricultural goods. In such case, the tractor's performance is heavily influenced by the hitching mechanism. The location of the hitch point, i.e., the horizontal distance from the center line of the tractor rear axle and the vertical height from the ground, has a significant impact on the amount of weight transfer during haulage. Equation (1.1) explains the influence of hitch height on weight transfer which is expressed as:

$$WT = \frac{(H_v \times D) + (H_d \times V)}{L} \quad \ldots (1.1)$$

where,

WT = weight transfer from the front to the rear axle

H_v = hitch height from the ground surface

D = draft

H_d = horizontal distance between the rear axle and the hitch point

V = vertical force

L = wheelbase

Hitch height is critical for maintaining the tractor-trailer system's center of gravity, managing the amount of weight transfer and consequently affecting tractor rollovers. For safe operation of such tractor-trailer systems, modern tractors are equipped with adjustable hitch height points to fit diverse field and operating situations. However, because the hitch height has to be adjusted manually by the operator in addition to the process being arduous, the frequency of accidents associated with such a system could not be reduced significantly. The operator's inability to adjust the hitch height in response to field demands and operating situations such as uneven terrain, unexpected and hidden impediments in the driving wheels, sloppy surfaces etc. limits the system's effectiveness. As a result, the availability of a variable hitch point alone does not provide the necessary support to maintain tractor-trailer stability, necessitating the development of an automatic variable hitch point that can facilitate various hitching positions according to operating and field conditions, and avoiding or minimizing any unfavorable rollover incidents.

1.8 Justification and Objectives

Considering the role of tractor in haulage operations in agriculture and the related accidents, particularly longitudinal rollovers, there is a serious need to address the situation to prevent or reduce such incidents. The hitching mechanism of 2WD tractors plays a significant role in determining the amount of weight transfer that occurs from the front axle to the rear which ultimately leads to rollovers. Lower hitch heights lead to reduced weight transfer to the rear and enhances longitudinal stability (Pranav et al., 2015). The geometry (i.e., the horizontal and vertical location) of the hitch point need to properly studied to tackle this challenging issue. However, the horizontal distance of the hitch point from the tractor rear axle is limited by the physical characteristics of the tractor and hence no major change can be done in this aspect. Interestingly, the vertical distance of the hitch from the ground can be adjusted to mitigate this problem. There are three limiting factors for maximum drawbar pull: (i) longitudinal stability, (ii) traction developed and (iii) engine power. During haulage, hitch height has a considerable impact on longitudinal stability and traction. The maximum payload capacity and slope traversing ability increase with lower hitch height (Pranav et al., 2015). It's worth noting that maximum payload is restricted by vehicle stability, i.e., the tractor can pull a higher payload as long as the tractor is not limited by its stability, considering the tractor has the required engine power. On the other hand, a greater hitch height provides increase in dynamic load on the rear wheels. As a result, the wheel slip improves and increases the tractive characteristics of the tractor. Thus, suitably

changing the hitch height can provide benefits to suit the different operating condition. To facilitate this, tractor manufacturers have developed variable hitch heights that the operator can set according to their needs as shown in Figure 1.6. But if the operator selects lower hitch height to eliminate instability, which by the way occurs only occasionally, it will result in decreased traction performance. Therefore, the operator must select lower hitch height only if the dynamic weight on the front wheels falls below 20% of the static total tractor weight else, operate at a higher hitch point to encourage traction. The best-known approach for preventing rollover fatalities is to use roll over protective structures (ROPS) in conjunction with seat belts. However, these structures may not be able to prevent the damage to the vehicle or the goods being trailed behind. Moreover, in a country like India, the use of trailer for transporting human is not uncommon. As such, in an unfortunate rollover scenario, the driver may escape unhurt, but the trailer and the people on it may face sever damages. During tractor-trailer operation, field conditions vary frequently and varying the hitch height by an operator according to such variation is not possible.

Figure 1.6 Manual variable hitch height in existing tractors

In absence of auto variable hitch height, usually, a tractor operates either by compromising traction or dynamic stability. Auto variable hitch point can resolve the matter which will vary the height, primarily to meet the stability requirement during motion. Once the tractor is assumed to be stable, the auto hitch system will adjust the hitch height to enhance traction without compromising the stability below the recommended value. Hence, to maintain a stable operating condition and improve the efficiency of haulage operation in tractor-trailer system, there is a need to develop an auto variable hitch system.

From the above discussion, it is clear that the absence of auto variable hitch height makes the tractor operate either by compromising its dynamic stability or tractive efficiency. Hence, it is conceived that auto adjustable hitch point can address or minimise the problem by adjusting the height corresponding to either stability or traction requirement. Hence, to improve the efficiency of a 2WD tractor-trailer operation, there is a need to develop an auto variable hitching system considering the real time available front axle load.

The main objectives of this study are as follows:

1. To develop an instrumentation system to measure the front axle dynamic load of 2WD tractors.
2. To design and develop a variable single-point hydraulic hitch bracket.
3. To develop a microcontroller-based system for automatic hitch height variation based on the front axle dynamic load.
4. To evaluate the developed variable hitch system on various operating conditions.

Chapter 2

Review of Literature

This chapter deals with the literature survey related to the present study and systematically represents the summary of published work in the area of dynamic weight distribution of tractor, stability, microcontroller, and traction parameter prediction. The chapter also deals with haulage performance of the tractor-trailer system. The major headings in this chapter are as follows:

1. Dynamic front wheel load of 2WD tractors
2. Dynamic stability of tractor
3. Microcontroller based control in tractor
4. Traction parameter prediction
5. Haulage performance of tractor

2.1 Analysis of Dynamic Front Wheel Load of 2WD Tractors

Naderi et al. (2008) found that the use of dynamic load prediction equations is an alternative method for determining this critical parameter. Hence this study was conducted to determine the optimal equation. The dynamic rear wheel load was assumed to be equal to the tractor total static weight in equation 1, the static rear wheel load and the amount of weight transfer were considered in equation 2, and equations 3 and 4 considered the moment effect of front wheel rolling resistance in addition to static weight. The equation given by ASAE Data 497.4, which calculates wheel slip based on dynamic load, was used in this investigation. As a result, field tests were used to compare calculated magnitudes to measured levels. Although, the computational complexity increased due to manual calculations.

Van et al. (2009) explained the functional basis of instrumented strain-gauge based transducers for the farm tractor rear axle as well as the unique aspects of constructive design and calibration technique. The transducers' ability to measure dynamic axle load was confirmed using the results of ride performance tests. The experimental results showed that the suggested method of dynamic axle load measurement can monitor the vertical wheel load of a moving vehicle in real time and is used to further research vehicle dynamics and dynamic wheel-soil interaction. The dynamic axle load was highly stimulated by tire non-uniformity and tire lugs, according to the time histories and frequency compositions of the

experimental data. However, transducer based strain gauge results in non-linear measurement.

Nguyen and Inaba (2011) explained how agricultural tire parameters affected wheel load changes and vibrations conveyed from the ground to the tractor rear axle. The tests were carried out on an asphalt road and a sandy loam field using a two-wheel-drive self-propelled farm tractor at various tractor forward speeds of 0.6, 1.6, and 2.6 m/s with tire inflation pressures of 330 and 80 kPa. Using strain-gage-based transducers and a triaxial accelerometer, the vertical wheel load of the left and right rear wheels as well as the roll, bounce, and pitch accelerations of the rear axle center were measured during the experiments. Deep wheel sinkage and tire slide would increase the eccentricity of the vertical soil reaction, resulting in a significant inaccuracy for the suggested method of measuring dynamic vertical wheel load.

Kumar and Pandey (2012) developed a device to measure and display the dynamic front wheel reaction for 2WD tractors to safeguard the longitudinal stability. The display unit shows the operator a safe green zone, a warning yellow zone, and a danger red zone. These zones will assist the operator in operating the tractor in a safe manner. Under field conditions, the output of the created device was found to be quite close to the theoretical results. By uploading the entire static weight of the tractor via computer interface of the microcontroller software, the designed ring transducer, along with the display unit, which is simple in construction, allows ease of mounting on any make of 2WD tractors. The difference in weight retained on the front axle between the created device and the data acquisition system was not significant at the 1% level of significance, according to the analysis.

Abbaspour-Gilandeh and Rashidi-Mohammadabad (2013) developed and built a system to quantify dynamic load with the help of two strain gauges installed on the tractor front axle. The results of calibration tests on measurement systems provide solid proof of the measuring system's sensitivity and linearity. Through field tests, four prediction equations for dynamic load were compared using exact continuous measurements of dynamic load and other effective characteristics. Although, time complexity increases during measurement.

Battiato and Diserens (2013) investigated influence of tire inflation pressure and wheel load

engine power) on an agricultural clay Vertic Cambisol on the basis of the results of traction tests and simulations with a semi-empirical soil-tire interaction model adapted for MFWD vehicles. Four tractor configurations were used in the traction testing, with two tractor weights (40.8 kN and 50.2 kN) and two tire inflation pressures (60 kPa and 160 kPa). In relation to wheel slide, traction performance was measured in terms of drawbar pull, traction coefficient, tractive efficiency, power delivery efficiency, and specific fuel consumption. However, there is a need to reduce the root mean square error values considerably.

Kumar et al. (2017) created a microcontroller-based embedded system to measure and show the dynamic wheel axle torque and drawbar power of an agricultural tractor for tillage study. The system consists of a specific transducer that measures the tractor's dynamic drive wheel torque, an embedded wireless digital system that receives, processes, and displays data digitally, as well as an SD card module located near the tractor's dash board. An amplifier amplifies the transducer signal, a transmitter unit processes the amplifier data, and a receiver unit receives and displays the transmitter unit data which make up the embedded system. The designed technology was thoroughly tested in both the lab and in the field. Even though, it requires improvement in measuring performance by using advanced microcontrollers.

Lankenau and Winter (2018) noticed through various modeling and experimental data that the ideal weight distribution for a conventional small four wheels, rear wheel drive tractor with trailing implement, efficient drawbar pull occurs at about 30% weight on the front wheels and 70% on the rear wheels when operating on a flat ground in a straight line. Maximising the drawbar pull played a critical role in enabling the size and cost of tractors for general use among common farmers.

Peeters et al. (2018) determined that when utilising tractors on agricultural soils, the vehicle mass and tire inflation pressures must be set to the lowest possible value and matched to one another to avoid soil compaction. The same tire inflation pressure can be set on all tires due to the intended distribution of vehicle mass on the wheels based on the ratio of the expected tire contact area. A wheel load measuring system integrated into the vehicle construction is required to determine the resulting tire forces at all times during work. A measuring system can be constructed for a conventional tractor with hydro pneumatically suspended front axles employing pressure sensors in the suspension system and

magnetostrictive sensors for stiff axles. The use of reference measurement technology to validate the rear wheel vertical load measurement is not considered properly.

Shafaei et al. (2020) determined the MFWD tractor's driving lead dependency on draught force, which has yet to be addressed in the state of the art. The inflation pressure of high-lug radial tires was kept constant at 204 and 136 kPa for the front and rear wheels respectively to eliminate the effect of inflation pressure on the driving lead. The tractor was loaded with the necessary draught force for a fully mounted plough implement. The driving lead increased nonlinearly from 1.86 to 8.08 percent as the draught force increased from 7.88 to 37.81 kN. In non-uniform traction conditions, the system should aim to adjust torque distribution on the axles for the same slip produced by the front and rear wheels.

Janulevičius and Damanauskas (2022) determined tire pressures that would allow the tractor's slip to be adjusted without diverging from the predetermined driving lead of the front wheels. The study also sought to investigate the impact of front-wheel driving lead on MFWD tractor slip and fuel consumption. Experiments revealed that front/rear tire pressure combinations that produce a well-targeted driving lead of front wheels have little influence on slide on hard surface, but they do affect fuel consumption significantly. The pressure combinations in front/rear tires that produce an optimal driving lead of front wheels have a substantial impact on fuel consumption despite not changing the slip value.

2.2 Estimation of Dynamic Stability in Tractors

Abu-Hamdeh and Al-Jalil (2004) studied the mechanics of a tractor-trailer system going up and down on sloping ground under various operating situations. A computer programme was created to analyse the system and predict the impact of trailer loading weight and slope angle on tractor stability, traction, and drawbar loading. The programme was used to examine a tractor-trailer system travelling up and downhill in a consistent manner. This investigation revealed that when towing a 3750 kg trailer uphill at a 28° slope angle, the tractor becomes unstable. Trailer weights of 3750 to 750 kg corresponding to slope angles of 15° to 18°, resulted in insufficient traction. However, the analysis could not incorporate all the real world physical variations.

Nichol et al. (2005) build a new device around a simplified mathematical model of an agricultural tractor that uses low-cost sensors and microcomputers to alert the operator of potential tractor instability. This device uses a simple bar-graph display to show the current

rollover potential as well as a recent history of rollover potential to the tractor operator. A single-chip accelerometer senses the current rollover potential, and a modest microprocessor analyses the accelerometer data, compensates for temperature fluctuations, and sends the information to a visual display. The utilization of low-cost "off the shelf" components allowed for the creation of a low-cost sensor system. Because agricultural tractors have such a long service life, it was critical to make the device as inexpensive as possible. This could enable it to be sold as an aftermarket add-on for a variety of tractor models. The device is also capable of interfacing with newer on-board tractor systems via a CAN bus to make it more attractive to tractor manufacturers who may want to incorporate this device into new models. Even though, this design does not have an audio warning to notify the operator to a potential rollover scenario.

Demsar et al. (2012) studied the static stability of a tractor with an oscillating front axle in relation to its position on a slope using a mathematical model and a numerical simulation. It was followed by assessing the modifications of individual factors, such as the position of the center of gravity, the wheelbase, the wheel track width and the height of the oscillating axle mounting point, and their impact on tractor's static stability in relation to its position on a slope. The results reveal that adjusting these factors increases the tractor's static stability significantly. The increased static stability also enhanced the dynamic stability of the tractor.

Kumar et al. (2013) created a microcontroller-based digital display unit for 2WD (two-wheel drive) agricultural tractors to measure and display the weight transfer from the tractor front axle. A transducer measures the tractor's front end reaction, an amplifier amplifies the signal from the transducer, and a microcontroller calculates and displays the weight transfer from the front axle. Any make and model of 2WD tractor can be fitted with the developed device. The digital display unit was carefully tested in the laboratory as well as in the field. The tractor's weight transfer from the front axle to the rear axle was measured to determine the tractor's stability for various agricultural operations such as ploughing, harrowing, and tilling. The weight transfer was determined only for the field operations and not for the haulage purpose.

Kumar and Raheman (2015) devised a variable hitching system using tractor hydraulics, using finite element analysis and developed to give hitching heights ranging from 0.4 to 0.75 meters above the ground. This technique made it simple to connect an unbalanced

trailer to a tractor, regardless of trailer hitch position. By lowering the hitch height from 0.75 m to 0.4 m while hitching an unbalanced trailer travelling uphill on an unpaved road with payloads of 3 ton and 4 ton, the front weight utilization factor of the tractor improved on average by 6.13 % and 7.37 %, respectively. By raising the hitching, the slip of a tractor on a 9° inclined unpaved road was reduced by 4.35 % and 5.17 % for tractor with 3 ton and 4 ton payloads, respectively. However, automatic control system may be developed to further improve the dynamic stability of tractor-trailer system.

Bulgakov et al. (2016) developed a theoretical foundation for the vertical oscillation of the combined ploughing and chopping process. The certification of the tractor-implement unit's dynamic stability in the longitudinal and vertical planes has been provided. The research was carried out using methods for designing analytical mathematical models of the functioning of agricultural machines and machine assembly units based on tractor theory, vibration theory, automatic control theory, and dynamic stability theory, as well as computer programme construction and PC-assisted numerical computation. The unit's dynamics were investigated using an examination of its amplitude frequency characteristics as a dynamic system responding to external perturbations.

Sharifzadeh et al. (2017) discussed dynamic stability analysis and control of an articulated vehicle. A large vehicle is being investigated. A 3-DOF rigid body model is used to describe the lateral dynamics of an articulated heavy vehicle. The system is then treated as a linear system with a delayed steering input. The tractor unit's lateral and yaw motion, as well as the semitrailer unit's yaw motion, are the system states. As a result, for this system with time-varying delay, a less conservative stability criterion is devised. The main idea is developing a new sort of LKF with a quadruple-integral term. Furthermore, unique free-weighting matrices are added in the sufficient stability requirement to increase the degree of freedom. In terms of linear matrix inequalities, the proposed delay-dependent stability metric is described.

Sakno et al. (2018) discussed the mobility and stability of a model of a tractor-lorry-trailer combination, comprising of a two-axle tractor and a single-axle semi-trailer, as well as its various stationary states with fixed steering. The examination of a non-linear mathematical model of a two-link tractor-lorry-trailer combo is one of the research's highlights. On the basis of the developed mathematical model, a set of steady-state conditions for the movement of the tractor-lorry-trailer combination model is determined; it provides the

necessary mobility for the passage of the circular overall traffic lane. The road train's range of stable steady-state conditions is limited, and the nature of the loss of stability in direct motion (divergent, flutter) is examined.

Bietresato and Mazzetto (2019) devised a new rig for examining the static and dynamic stability of agricultural machinery, with its architecture studied and layout constructed using a special conceptual approach. The first element of the proposed design process is dedicated to test equipment and follows a 'top-down' logic that begins with the test requirements. This method alternates the analysis and synthesis phases and makes use of two key ideas in the creative design process: functional analysis and decomposition, as well as kinematic inversion. A new mechanical system's layout has been established, with the goal of guiding later and more thorough design phases suitably.

Petrovic et al. (2021) proposed an analytical algorithm with appropriate software for approximating the allowable critical slope of solid flat terrain, which ensures static and/or dynamic stability of the specified self-propelled agricultural tractors and aggregates. This algorithm considers the machine to be a rigid body with three or four contact points (specified by wheels or crawlers) moving at various constant velocities and curvature radii. The computer programme SSPM (stability of self-propelled agricultural machines) was created using this algorithm, which is based on theoretical mechanics mixed with 3D analytical geometry. However, there is a need to extend this design in order to make it suitable for real time applications.

2.3 Use of Microcontroller for Automation in Tractors

Mondal and Rao (2005) presented a digital throttle gear optimizer that can behave as a GUTC guidance system. Microcontrollers and inductive type proximity sensors were used to develop DTGO. This DTGO operator was guided by a simple signal system. DTGO successfully identifies the minimum specific fuel consumption zone for any load condition. However, there is a need to improve the system performance by including real time clock in the microcontroller.

Raheman and Jha (2007) created a microcontroller-based slip sensor for a 2WD tractor to detect slip values during on-farm operation. The 'zero condition' for the invention of the slip sensor was a tractor with enough driving torque to push any item across a tarmacadam surface with zero net traction. This sensor has four parts: a power supply, sensors for

throttle position, gear position, and wheel rpm, data processing, and a display unit. The tractor battery was used to provide power. The tractor was outfitted with a rotary potentiometer and proximity switches to measure throttle position and wheel revolution. The performance of developed slip sensor was evaluated both on tarmacadam surface as well as in the field. The variations between indicated and actual slip were found to be within 0–5% for both the surfaces, thus indicating the accuracy of slip measurement by the developed slip sensor. However, the slip values vary with increased speed.

Havasi et al. (2009) created a digital instrument for measuring slippage of farm tractor wheels based on the microprocessor 89c51. Assembly language was used to programme the 89c5l microcontroller. The infrared sensor units were mounted on the tractor's rear wheel axle and used as the source of pulse creation. Before being sent into the microcontroller, the output pulses from these two sources were filtered and amplified. The result was displayed as a percentage of slip on an LCD monitor. The instrument's performance was evaluated both in the lab and in the field. Field testing were conducted utilising an MF399 tractor with two distinct levels of drawbar pull, high and low. Data was collected through four replications of studies using both conventional and digital methods. The analysis of results showed that there was no significant difference between the manual and digital method at %1 probability level.

Pranav et al. (2010) developed a microcontroller based digital slip meter for agricultural two-wheel drive (2WD) tractors. The actual and theoretical speeds of tractor were calculated by measuring the revolutions per minute (rpm) of front and rear wheels, respectively, using optical slot sensors. A microcontroller was programmed to calculate the actual forward speed and wheel slip of the tractor. These measured values were digitally displayed on the tractor dashboard. The slip meter was fabricated in such a way that it could be mounted on any make and model of 2WD tractor. The slip meter was rigorously tested in the laboratory as well as in the field with different tractor–implement combinations. A maximum of ±2 percent variation was observed between measured and indicated wheel slip.

Pranav et al. (2012) designed a microcontroller-based automatic wheel slip control system for 2WD tractors. Under field conditions, the system continuously measures wheel slip and generates commands for depth modification if the wheel slip exceeds the specified range. The actual and theoretical speeds of the tractor were measured by measuring the rotational

speed (rpm) of the front and rear wheels, respectively. The designed system was put on a test tractor, and its performance was assessed using various implements in various field circumstances. When compared to the existing draft control system, the slip control system showed a significant reduction in fuel consumption per hectare (20–30%), an increase in field capacity (7–38%), and a gain in tractive efficiency (4–10%). The slip control system is also expected to reduce the operator's effort as it adjusts the depth control lever automatically in response to variation in the soil conditions within the field. Although, there is a need to further improve the tractive efficiency.

Gonzalez et al. (2016) examined the design, construction, and testing of an autonomously deployable ROPS. The HydraROPS prototype created two levels of help for the elevation of the foldable ROPS. The driver decides to modify the ROPS position in the first level, and does so using the manual activation on the board. In the second level, in the event of an impending rollover, the vehicle automatically switches to the operative position without the driver's assistance. This level immediately contacts emergency response workers by sending a phone message with the GPS location. The protective structure was moved using the tractor's hydraulic power. A pressure accumulator was added to the hydraulic system to speed up the deployment of the ROPS by 71%. Moreover, the electronic system could correctly predict the overturn. The developed HydraROPS can be installed on any existing tractor models equipped with a certified ROPS thus negating the need for modification of the existing ROPS.

Liu et al. (2016) showed a multipurpose automatic hydraulic steering circuit. A 5-way-3-position proportional directional valve, two pilot-controlled check valves, a pressure compensated directional valve, a pressure compensated flow regulator valve, a load shuttle valve, and a check valve are among the components included in the system design. Most open-center systems with constant flow supply and closed-center systems with load feedback can be used with it. Under load feedback, the design maintains the lowest pressure and remains in the neutral position during unloading, meeting the steering criteria. On a 51-microcontroller-unit master control chip, the steering controller is based on proportional-integral-derivative (PID). The essential properties of the system subject to stepwise inputs and sinusoidal tracking are established using an experimental platform. However, no action has been taken for minor deviations.

Wu et al. (2016) examined kinematic and dynamic parameters of the tractor-driven vehicle,

explaining why low-power motors and short-range sensors can be employed for automated heavy-duty vehicle guidance. When this tractor is equipped with various guiding sensors, such as a magnetic sensor or a camera, the corresponding magnetic or visual guided vehicle can be easily created by simply arranging tractors and other passive wheels within a vehicle frame. For example, for the tractor, a low-cost magnetic sensor is employed, and a magnetic guided vehicle prototype is built around it. This prototype is used to undertake weight carrying and path tracking experiments. The findings of the trial reveal that the tractor can operate a heavy-duty vehicle with minimal power usage.

Fedorenko and Tarkivskij (2019) created a method and technical means for real-time digital filtering of a tractor traction power (TP) strain gauge data. The IP-293 analogue signal input module was developed to process the digital strain gauge signal. It comes in a standard form and may be mounted on a DIN rail. The STM32F405RG microcontroller with inbuilt firmware executes an adaptive median filter with a changeable window and processes the incoming digital stream from the voltage-to-digital converter at a rate of 1000 times per second via two channels concurrently, which is a feature of the module. The protected MODBUS and RS485 buses were employed to ensure module connectivity with the control computer.

2.4 Prediction of Traction Parameters in Tractors

Catalán et al. (2008) built a set of programmes using the cone index as the terrain's representative parameter. Slip has been predicted for tractors with two or four wheels that use one of the four models in the present paper's software, which is written in Visual Basic. There are databases for tractors, front and rear tires, and working conditions (soil cone index and drawbar pull exerted). The output can be exported as a spreadsheet.

Yin and Lu (2010) proposed a method based on virtual prototyping technology and test the wheel type tractor slippage to indicate whether the engine power is converted by the wheels into traction. A 3D model of two-wheel drive tractor is constructed using a 3 D design software. Slip was increased with increase in the depth of operation. Less available load compared to required load caused more slip. Results show that the slippage remains almost the same at constant traction, whose averages are 10.36% and 16.69% at 5.4kN and 9.8kN, respectively.

Park and Lee (2012) employed a widely established empirical model for tractive performance prediction of single tires, Brixius, to construct a simulation programme for the prediction of tractive performance of a tractor in this study. The tractive performance prediction tool can forecast and estimate tractive performance based on a variety of soil conditions and tractor characteristics. The programme was created keeping the tractor's specifications in mind, as well as a soil characteristic (the cone index, which reflects soil strength) and the tractor's operation conditions. In addition, the programme was created to deliver tractive performance prediction results of tractors in the form of not only numerical values but also graphical depiction, such as gross traction, motion resistance, net traction, and tractive efficiency.

Patel et al. (2012) created a decision support system (DSS) for 2-wheel drive (2WD) tractors in the Visual Basic 6.0 programming language. The DSS supports tractor-implement system selection by combining datasets such as tractor parameters, tire and implement specifications, soil and operating conditions to give easy user interfaces. The DSS was tested on three distinct implements: a 2x30cm moldboard plough, a 9-23cm field cultivator, and a 7-7 offset disc harrow (1.6m». DSS can be used effectively in matching tractor implement systems of various makes and models commercially available in India, as it calculates draught, drawbar power, slip, tractive efficiency, coefficient of rolling resistance, coefficient of net traction, PTO power required, power utilization efficiency, specific fuel consumption, and so on, based on input data.

Roşca et al. (2014) proposed a semi-empirical model for forecasting traction force and efficiency for a 2WD agricultural tractor, assuming that the tire–ground contact area is shaped like a super elliptical. The model implies that the wheel sinks into the soil under vertical stress and that the force causes tire deflection; as a result, the virtual radius of the deformed tire grows as the tire–ground contact area flattens. Using an iterative procedure, a computer programme was constructed to solve the model's equations. The maximum traction force was calculated using the Mohr–Coulomb equation, with the assumption that it is only restricted by the soil shear strength. The predicted data were compared with the test data by the means of a goodness-of-fit analysis to evaluate the precision of the model.

Kumar and Pandey (2015) developed a visual simple programme for ploughing, cultivating, and harrowing operations to find the best gear and throttle position based on the lowest fuel usage per hectare. By combining databases such as tractor, tire, and

implement characteristics, draught and tractions model constants, fuel consumption model, soil, and operating conditions, the application provides an intuitive interface to anticipate the minimum fuel consumption of a specified model. PTO tests under varied throttle and load settings were used to build the fuel consumption model. The created model's coefficient of determination (R2) was determined to be close to 0.99.

Lee et al. (2016) examined how ballast, tire inflation pressure, transmission gear, engine speed, and work load affected three fuel efficiency parameters: fuel consumption per work hour (FC), fuel consumption per tilled area (FCA), and specific volumetric fuel consumption (SVFC). Computer simulation was used for moldboard ploughing and rotovating processes. Engine and power train, fuel consumption, tractive performance, and draught and power requirement were all included in the tractor model. When compared to field experiments conducted in a paddy field under the same operational conditions, the simulated fuel efficiency results were within a 3.3 to 6.5 percent error range on average. However, the effect of tire inflation pressure was seen only in the ploughing operation.

Shafaei et al. (2019) showed how to use intelligent simulation setups to anticipate tractor wheel slide in tillage operations. The impacts of numerical variables such as forward speed (2, 4, and 6 km/h) and ploughing depth (10, 20, and 30 cm) on tractor rear tire slip were intelligently simulated using data mining approaches such as artificial neural network (ANN) and adaptive neuro-fuzzy inference system (ANFIS). The ANFIS simulation framework's neuro-fuzzy potential was compared to the ANN simulation framework's neural capabilities. The results confirmed higher efficiency of the best configuration of the ANFIS simulation framework than that of the ANN simulation framework. Physical perception obtained from the ANFIS simulation results demonstrated that the wheel slip increased nonlinearly with increment of forward speed and plowing depth.

Kim et al. (2020) created a prediction model based on the traction force equation and motion resistance to determine the axle torque of an agricultural tractor. Actual field torque data was acquired through field tests, and a load measuring system was created to verify the derived prediction model. Using measured axle torque, the constructed prediction model was compared to the results of five reference prediction approaches, including weight, engine-rated torque, and three traction equations. The major criteria that were used to evaluate performance were travel speed, tillage depth, and slip ratio. At all travel speeds, tillage depths, and slip ratios, the proposed prediction model was found to be closest to the

1:1 line, meaning that it can best explain the reported torque values. However, a limitation of this study is that the data used to verify the proposed model were measured in one field only.

Janulevičius and Damanauskas (2022) developed a method for predicting tractor driving tire slippage that includes a numerical expression for tire inflation pressure. A method was devised to estimate tire slippage based on the traction coefficient by predicting the tire inflation pressure based on the results of experimental investigations of a Case Farmall 115U MFWD tractor equipped with radial-ply tires on wheat stubble on a loam soil. The empirical equation derived enables for theoretical prediction of drive tire slippage in 4WD and 2WD modes, with radial-ply tire inflation pressures ranging from 70 to 195 kPa.

2.5 Estimation of Haulage Performance in Tractors

Sahu and Pandey (2005) conducted field experiments to determine the effect of operating parameters such as gear, throttle position, payload, and type of surface on haulage performance of tractor-trailer systems with a 23 kW brake horsepower 2WD tractor employing unbalanced and balanced trailers separately. On three different surfaces, tarmacadam, moram, and firm grass surface, tests were conducted in first high (1H) and second high (2H) gears at half and full throttle positions. The payload for the unbalanced trailer was varied in four steps from 0 to 2800 kg, and for the balanced trailer from 0 to 4200 kg. Draft, vertical force, and fuel consumption were measured using two spring dynamometers and an auxiliary fuel tank.

Bietresato et al. (2012) developed a theoretical model that may be used to investigate the performance of ground vehicles using acceleration testing. The model considers all of the forces operating on a moving vehicle to determine its kinematics, including the propulsion devices' rolling friction, their slide on the ground, aerodynamic resistance, road slope, and engine traction. The experimental data obtained during acceleration tests on a flat and sloping road from a standing start to reach a set distance or a stated speed are used to calculate the average efficiency of the transmission of three tractors with various equipment in the model's application approach. Although, this design calculates vehicle performance in terms of road surface and slope only.

Kumar et al. (2012) created microcontroller-based digital display unit to measure and display weight transfer from the tractor front axle for 2WD agricultural tractors. A

transducer measures the tractor front end reaction, an amplifier amplifies the signal from the transducer, and a microprocessor calculates and displays the weight transfer from the front axle. Any brand and model of 2WD tractor can be equipped with the created gadget. Both in the lab and out in the field, the digital display unit was thoroughly tested. Between the theoretically calculated and experimentally observed weight transfer values, a maximum of + 3.5 percent variance was detected.

Bhondave et al. (2017) This system has a control valve manifold with solenoid valves, a hydraulic control unit (HCU), a position sensor, a draught sensor (load cell), and input levers with sensors. A proper wire harness is used to link them. The system has all of the traditional system's features, such as Position Control (PC), Draft Control (DC), and Quick Lift (QL). Current design has fundamental common valves such as the Pressure Relief Valve (PRV), Check Valve (CV), Shock Load Relief Valve (SLRV), Isolator valve, and Tipping trailer port. Customer contact points, such as PC, DC levers, and QL button, are kept the same as they were in the past. The study also involves Simulink Matlab analysis and optimization, as well as lab and field performance tests for proving in various soil conditions. However, the wheel parameters were not considered.

Singh and Pandey (2017) analyzed that front-mounted three-point linkage is another option for higher-powered tractors to maximize available power and speed up tillage operations. In order to design a front-mounted three-point linkage, a user-friendly computer application is created in the Visual Basic environment. The generated program's input parameters include the speed of operation, kind of implement, mast height, PTO power, angle of links, hydraulic pressure, and yield strength of materials, among others. The programme can calculate draught, linkage forces, link diameters, link points, hydraulic cylinder design, and minimum hydraulic lift capacity, among other things. To compute draught, the ASAE draught equation is employed, and horizontal and vertical forces on links are calculated to determine link safety against bending.

Kumar et al. (2020a) developed a computer software in Visual Basic 10 environment using several empirical and theoretical formulae to forecast the hauling performance of 2WD tractors. Three types of inputs linked to tractor, trailer and operational parameters were used to compute the performance parameters through empirical and theoretical formulae. Draft, slip, transport efficiency, transport productivity, fuel economy index, rear and front axle dynamic weight, and so on were among the performance parameters. The application

was used to test haulage performance under various operating situations by adjusting hitch distance (HD). Lower HD increased maximum payload, transport productivity, and maximum slope on the one hand, but it decreased rear axle dynamic load, fuel economy index, and actual engine power requirement.

Kumar et al. (2020b) created an instrumented tractor that could be used to assess the haulage performance of a tractor with a 39 kW PTO power and its dynamic behavior. Dynamic behavior is concerned with the tractor's safety, stability, and movement in various terrain conditions. Draft, vertical force, and stability are among the haulage performance factors. At a single hitch point, the tractor was equipped with two load cells with a capacity of 5 tonnes each. To determine the tractor's stability index, the wheel reactions under dynamic conditions were calculated. On a plane surface, the maximum safe haulage capacity of the test tractor was determined to be 15000 kg based on a desire stability index of 20%. However, the dynamic performance in terms of slippage and overload has to be measured.

Kumar et al. (2017) measured and displayed dynamic wheel axle torque and tractive force of several tractor-implement combinations using a mechatronic-based embedded system. It incorporated a unique transducer for measuring tractor drive wheel torque, as well as an embedded telemetry digital system for receiving, processing, and storing data on an SD card module. The measured dynamic wheel axle torque during various tillage operations with various implements was compared to theoretical values using traction models to discover the model that was best suited for sandy clay loam soils.

Shafaei et al. (2020) examined the power consumption efficiency of a mechanical front wheel drive (MFWD) tractor during the tillage process using an artificial intelligence system. Various numbers and types of input membership functions, defuzzification methods, types of output membership functions, and training cycle counts were used to construct the system. The notable system's promising performance ensured its dependability for calculating tractor power consumption efficiency based on operational variables such as tillage depth (10–30 cm), speed (2–6 km/h), and tractor driving modes (two-wheel drive (2WD) and four-wheel drive (4WD). It is advised that the intelligent fuzzy system be extended to include numerous input factors such as tillage depth and speed, tractor driving mode, implement type, and soil moisture conten

Chapter 3
Theoretical Considerations

This chapter deals with theories associated with the calculation of haulage performance parameters. The force analysis of tractor-trailer mechanics to calculate the wheel reaction is also elaborated in this chapter. The role of hitch height on tractor performance has been theoretically explained based on the draft, vertical force, coefficient of rolling radius, the location of the centre of gravity (CG) of the tractor, total weight on the trailer, wheel eccentricity, rolling resistance, wheel reactions, wheel slip and grade resistance.

3.1 Design of Hydraulic Cylinder

A double acting hydraulic cylinder was designed considering the load on the trailer and the available pump pressure. The stroke length of the cylinder was determined based on the range of the hitch height. The design of the cylinder also includes the design of the piston and piston rod, and cylinder dimensions.

3.1.1 Piston rod

The piston rod in a double acting hydraulic cylinder is subjected to a significant amount of compression load or thrust. Therefore, it is important that the rod be of sufficient diameters to prevent buckling. Euler's strut theory is used to calculate a suitable rod diameter to withstand buckling. Buckling load can be calculated using the following Euler equations:

$$K = \frac{\pi^3 E\, d^4}{64\, {L_e}^2} \quad \ldots (3.1)$$

$$F = \frac{K}{N} \quad \ldots (3.2)$$

where,

K = buckling load (maximum allowable load), kg

E = modulus of elasticity, kg/cm^2 (2.1×10^6 kg/cm^2 for steel)

d = diameter of piston rod, cm

L = length of the piston rod, cm

L_e = effective buckling length (= L/2, for fixed-fixed ends), cm

F = maximum safe working load, kg

N = factor of safety, 3.5 (Pinches and Ashby, 1988)

3.1.2 Piston head

The diameter of the piston head was designed using equations (3.3) with a minimum factor of safety of 3 (Boye et al. 2017) as follows:

$$K = P\,(A - a) \quad \ldots (3.3)$$

$$(A - a) = \frac{\pi}{4}(D^2 - d^2) \quad \ldots (3.4)$$

where,

P = available pressure, kg/cm^2

A = area of piston, cm^2

a = area of piston rod, cm^2

D = diameter of the piston, cm

d = diameter of the piston rod, cm

3.1.3 Cylinder diameter

The size of a hydraulic cylinder is specified by its diameter and closed height. In this design, Lame's equation was used to determine the outside diameter of the cylinder barrel based on the maximum working stress.

$$OD = \sqrt{\frac{D^2(\sigma_m + P)}{(\sigma_m - P)}} \quad \ldots (3.5)$$

$$\sigma_m = \frac{\sigma_t}{N} \quad \ldots (3.6)$$

where,

OD = outside diameter of cylinder, cm

σ_m = maximum working stress, kg/cm^2

P = available pressure, kg/cm^2 (measured, P = 214 kg/cm^2)

σ_t = tensile stress of material, low carbon steel (43 kg/cm^2)

N = factor of safety, 3

D = diameter of piston, cm

3.1.4 Cylinder tube thickness

The thickness of the cylinder tube can be calculated using the below given equation:

$$Thickness = \frac{OD - D}{2} \quad \ldots (3.7)$$

3.1.5 Velocity of extension and retraction strokes of the piston

In a double acting cylinder, the velocity of the extension and retraction strokes are not the same. During the extension stroke, the hydraulic pressure acts on the entire cross-sectional area of the piston head, while during the retraction stroke, the hydraulic pressure acts only on the annulus area between the piston head and the piston rod. Due to this difference, the velocity of the extension stroke is greater than that of the retraction stroke as shown in Figure 3.1

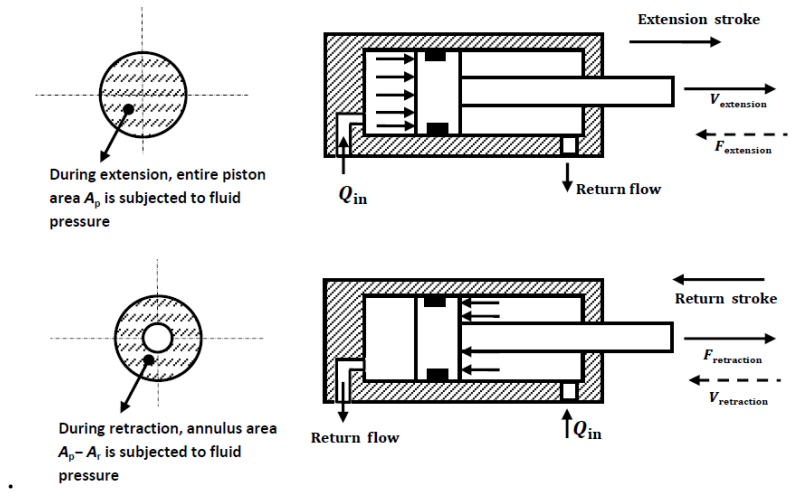

Figure 3.1 Areas subjected to pressure during extension and retraction strokes of a piston

The velocities of extension and retraction strokes can thus be calculated using the following equations:

$$Vel\ (extn),\ V_{ext} = \frac{In\ flow\ rate}{cross\ section\ area\ of\ the\ piston\ head} \quad \ldots (3.8)$$

$$Vel\ (retn),\ V_{ret} = \frac{Out\ flow\ rate}{cross\ section\ area\ of\ the\ (piston\ head - piston\ rod)} \quad \ldots (3.9)$$

3.2 Tractor Performance Parameters

3.2.1 Coefficient of rolling radius

For an automotive vehicle, the vertical distance between the center of an axle and the ground surface is called the coefficient of rolling radius. The rolling radii of the front, rear, and trailer wheels are determined by the following equation:

$$rr = \frac{2.5 * \frac{od}{2} * slr}{1.5 * \frac{od}{2} + slr} \quad \ldots (3.10)$$

where,

rr = rolling radius of the wheel, m

od = overall wheel diameter ($= 1.06 \text{ x } rd + 2 \text{ x } h$), m

slr = static loaded radius [$= (\frac{od}{2} - \delta) \times h$], m

rd = rim diameter, m

δ = tyre deflection, decimal

h = tyre section height (= 0.75 b), m

b = tyre section width, m

The radius of a wheel measured from the center of the rim to the ground surface is known as the rolling radius. Static rolling radius has been used in this study due to the difficulty in measuring the dynamic rolling radius. The tyre specifications are indicated on the tyre wall.

3.2.2 Total weight on the trailer

The total weight of the trailer includes the empty trailer weight and the payload. The total weight of the trailer can be calculated as:

$$W_{tl} = W_t + Pl \quad \ldots (3.11)$$

where,

W_{tl} = total weight of the trailer, kg

W_t = empty weight of the trailer, kg

Pl = payload, kg

3.2.3 Brixius mobility number

The Brixius mobility number which is dimensionless, represents the combination of both soil and tyre parameters. It is widely applied in the traction prediction equations to analyse

the combined effect of the soil and tyre parameters. The mobility number is applicable to bias-ply tyres only and is represented by the following equation:

$$B_n = \frac{CI \; x \; b \; x \; OD}{W/_2} \left(\frac{1+5\delta/_h}{1+3b/_h} \right) \quad \ldots (3.12)$$

where,

B_n = Brixius mobility number
CI = cone index, kPa
W = vertical load on the axle, kg

3.2.4 Wheel slip

A tractor working under any given load experiences flexing of its tractive device. Also, there is slippage between the surfaces. These result into reduction of the distance travelled or speed of operation which is often simply referred to as slip. Slip develops in any tractive device that develop some pull or a net traction. It is generally expressed as the ratio of the decrease in the actual speed to the theoretical speed and is given by:

$$s = 1 - \frac{V_a}{V_t} \quad \ldots (3.13)$$

where,

s = wheel slip, decimal
V_a = actual velocity, m/s
V_t = theoretical velocity, m/s

3.2.5 Calculation of wheel reactions

The weight of the tractor/trailer results in reaction by the ground during static and dynamic conditions. The reaction exerted by the ground is always opposite to the direction of the self-weight of the body. The wheel reactions were calculated through force analysis of tractor-trailer combination (Figure 3.2) for equilibrium condition which are as follows:

$$R_t = \frac{w_{tl} \; (CG_{dt} \; * \; cos\, u + (CG_{h'} - H_v) * (\frac{a}{g} + sin\, u) - CG_{t\,dh} * cos\, u)}{st(rr_t - H_v) - CG_{t\,dh}} \quad \ldots (3.14)$$

$$R_f = \frac{W*\cos u*(L_r - x_r) - W(\frac{a}{g} + \sin u) - (D*H_v) - (V*H_d)}{L + x_f} \quad \ldots (3.15)$$

$$R_r = \frac{W*(L + x_r - Lr)\cos u + W*(CG_h)*(\frac{a}{g} + \sin u) + V*(H_d + L + X_r) + (D*H_v)}{L + x_f - x_r} \quad \ldots (3.16)$$

where,

R_t	=	reaction at trailer wheel, kg
R_f	=	reaction at tractor front wheel, kg
R_r	=	reaction at tractor rear wheel, kg
W_{tl}	=	total weight of the trailer, kg
CG_{dt}	=	horizontal distance of CG of trailer from the tractor rear axle, m
u	=	gradient of the surface, °
$CG_{h'}$	=	new CG height of the tractor from ground, m
H_v	=	hitch height, m
a	=	acceleration of the tractor, m/s^2
g	=	acceleration due to gravity, m/s^2
CG_{tdh}	=	horizontal distance of the CG of the trailer from the hitch point, m
st	=	rolling resistance of trailer wheel
rr_t	=	rolling radius of trailer tyre, m
W	=	total weight of the tractor, kg`
CG_d	=	horizontal distance of the CG of the tractor from the rear axle, m
x_f	=	eccentricity of the rear wheel, m
x_r	=	eccentricity of the rear wheel, m
D	=	draft, kg
V	=	total vertical force, kg
H_d	=	horizontal distance of the hitch point from the rear axle, m
L	=	wheelbase of the tractor, m

L_r = horizontal distance of the CG of the tractor from the rear axle, m

CG_h = height of the CG of the tractor from the ground, m

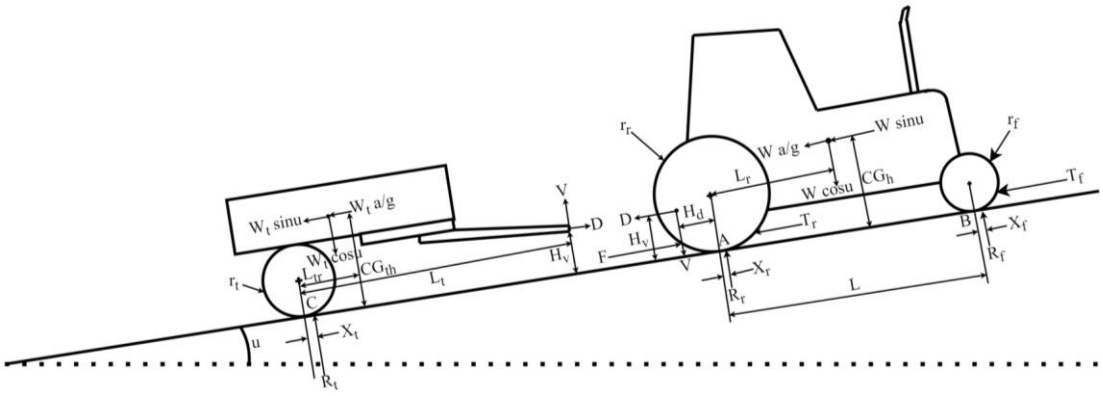

Figure 3.2 Free body diagram of 2WD tractor and trailer on an inclined surface

3.2.6 Gross Traction Ratio (GTR)

Gross traction ratio may be defined as the ratio of gross tractive force to the dynamic weight on the driving wheels. The gross traction ratio is the relationship between the tractor's gross thrust and the dynamic weight on the traction wheels and it is expressed as follows:

$$GTR = 0.88\,(1- e^{-0.1Bn})\,(1 - e^{-7.5S}) + 0.04 \quad \ldots (3.17)$$

where,

B_n = mobility number = $\frac{CI*1000*b*od}{w*g}\left(\frac{1+5*\frac{\delta}{h}}{1+3*\frac{b}{od}}\right)$

CI = cone index of soil, kPa

b = section width of tyre, m

od = overall diameter of tyre, m

w = dynamic weight on the rear axle, kg

g = acceleration due to gravity, m/s^2

h = section height of tyre, m

δ = tyre deflection (= 0.08 for driven and 0.2 for drive wheels)

3.2.7 Net Traction Ratio (NTR)

The ratio of pull to dynamic weight on the driving wheels is known as the net traction ratio and is expressed as follows:

$$NTR = GTR - sr \quad \ldots (3.18)$$

$$NTR = \frac{D}{R_r} \quad \ldots (3.19)$$

where,

sr = coefficient of rolling resistance

D = draft or horizontal component of the pull, kg

R_r = reaction at rear wheel, kg

3.2.8 Tractive efficiency

Tractive efficiency is the ratio of the drawbar power to the axle power and is expressed as:

$$TE = \left(\frac{NTR}{GTR}\right) * (1 - slip) \quad \ldots (3.20)$$

where,

TE = tractive efficiency, decimal

NTR = net traction ratio, decimal

GTR = gross traction ratio, decimal

slip = wheel slip, decimal

Chapter 4
Materials and Method

This chapter presents the various materials and methods used to achieve the objectives of the study. It encompasses the development of instrumentation systems for measuring the front axle load, microcontroller-based automated hitch height variation system and fabrication of variable single-point drawbar hitch system. It also describes the evaluation of the developed systems under various operating conditions. The various sub-headings of the chapter are as follows:

1. Front axle load measurement
2. Development of a variable single-point hydraulic hitch
3. Microcontroller-based auto variable hitch height
4. Field evaluation of the developed system

4.1 Front Axle Load Measurement

An instrumentation system was developed to measure the load on the front axle of a 2WD tractor in real time under dynamic conditions.

4.1.1 Principle of measurement

A strain gauge is a sensor that responds to any applied force by varying its resistance. When an external force is applied to a stationary object, stress and strain are created. The load cell converts force, pressure, tension, weight, and other variables into a change in electrical resistance that can be measured. In this study, the load cell takes readings based on the amount of stress (compressive or tensile) it experiences. When the load cell is initially mounted under the front axle, it is subjected to tensile stress (force) due to the tractor's self-weight, the ground's reaction on the front wheels, and partly due to the tension with which the load cell is held as shown in Figure 4.1 (a). This is the initial stress, which can be considered 0 or the starting reference stress. The tires tend to diverge away from each other towards the bottom and converge around the top in such conditions. Moreover, there is always some load transfer from the front axle to the rear axle during forward motion, i.e., the front axle load is always reduced. This occurs owing to the inertial force caused by longitudinal acceleration at the vehicle CG, which causes some amount of weight shift to the rear axle, reducing the front axle load while increasing the rear axle load. As a result, the load cell undergoes compression, and the measurement received in the load cell can be

used to calculate the reduction in front axle load. Furthermore, during longitudinal overturns, when the front tires are lifted off the ground, the soil reaction force is zero, and the load cell is compressed to its maximum as shown in Figure 4.1 (b).

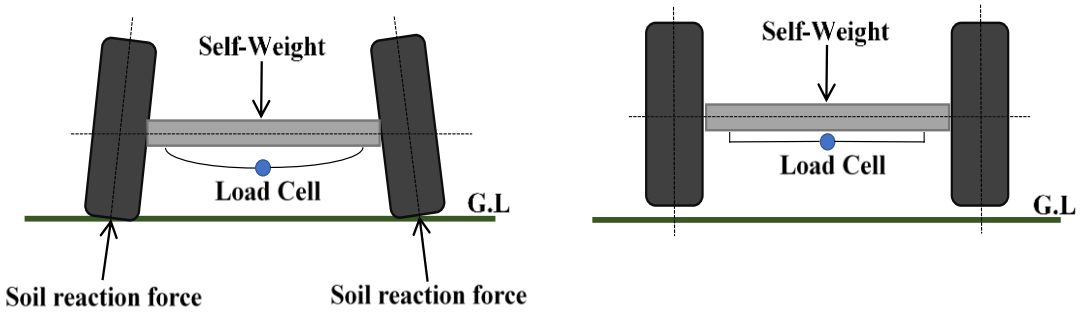

(a) Initial tensile stress on the load cell

(b) Compression stress on the load cell during lifting of the front axle

Figure 4.1 Load cell measurement under different stress conditions

4.1.2 Load cell installation

A load cell is a force transducer that can convert forces such as tension, compression, pressure, or torque into some measurable electrical signal. The electrical signal changes proportionally to the force applied to the load cell. An S-type load cell consists of four strain gauges connected using a Wheatstone bridge circuit to convert the change in strain/resistance into voltage, which is proportional to the load. It can measure both tensile and compressive forces. The circuit diagram of a Wheatstone bridge used in load cells is shown in Figure 4.2.

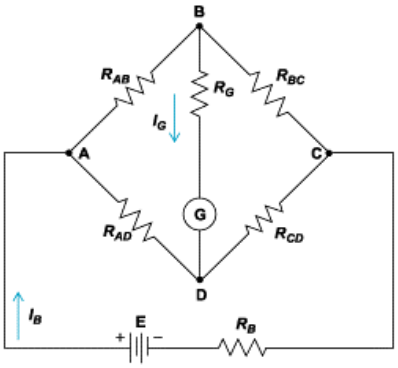

Figure 4.2 Wheatstone bridge circuit used in load cells

In this study, an S-type strain gauge-based load cell of 5 kN capacity was mounted on the tractor's front axle to determine the dynamic front axle load. The load cell was mounted below the centre of the front axle with the assistance of two iron bars as illustrated in Figure

4.3. To determine the vertical load acting on the front axle, the load cell was positioned horizontally. The load cell was mounted using two rods, one end of each rod was screwed to the load cell and the other to a U frame mounted on the axle. The ends of the two rods were welded together with screws to ease the mounting and adjustment of the load cell. The screws also helped in maintaining the required initial tension on the load cell under static conditions.

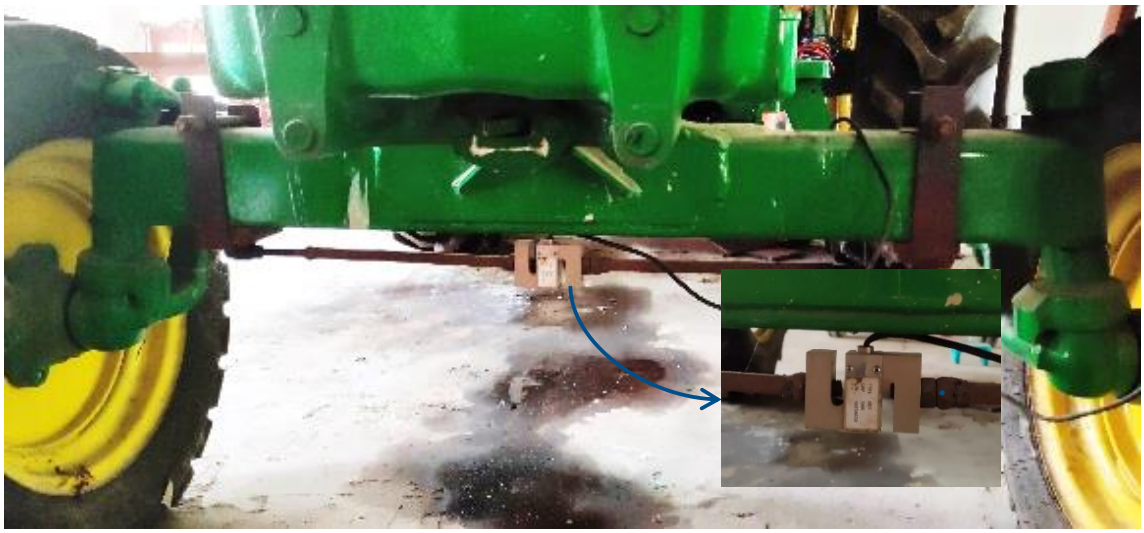

Figure 4.3 S type load cell for front axle load measurement

4.1.3 Calibration of the front axle load cell

The weight on the tractor's front axle was calibrated in the laboratory under static conditions. The test tractor was parked over weighing balances, which provided readings of the tractor's front and rear wheel weights. The initial readings on the front and rear balances (corresponding to front and rear axle loads) are recorded. The front axle was then gradually jacked up, with weighing balance measurements taken at regular intervals. With the use of a data logger (DT800), the corresponding values on the load cell (mV) resulting from the raising up of the tractor’s front wheels were recorded. The lifting procedure was continued until the front platform weight balance read 0 kg, indicating that the tractor's front axle had just been raised off the weighing balance as shown in Figure 4.4. This is the condition when the stability of the tractor fails. Under such conditions, the slightest additional rearward weight transfer can result in a longitudinal overturn of the tractor. The results obtained from the load cell and platform balance were used to establish a relationship between the load cell and front axle load as shown in Figure 4.5.

Figure 4.4 Calibration of front axle mounted load cell

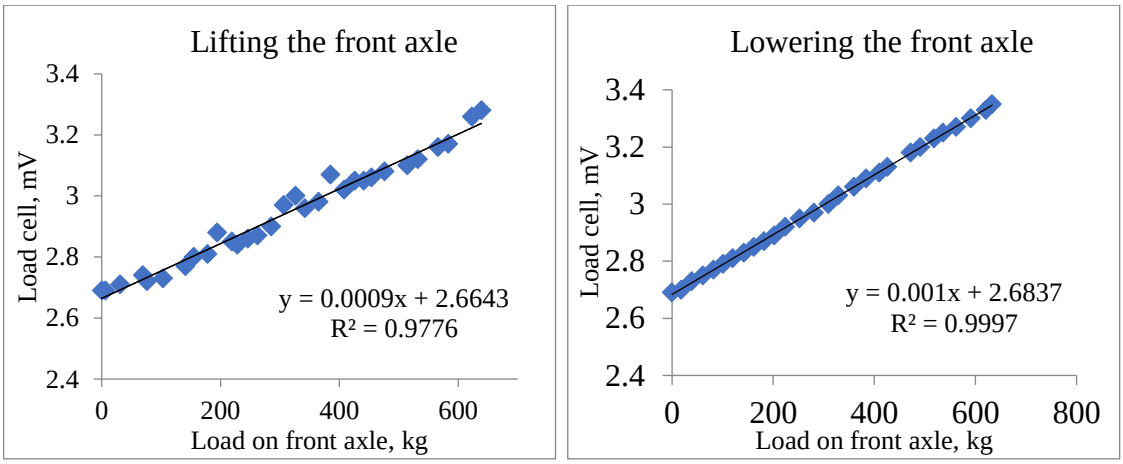

Figure 4.5 Results of the calibration of the load cell

4.1.4 Evaluation of the instrumented load cell

A 1000 kg capacity dynamometer was used in this study to test the accuracy of the calibration of the load cell mounted on the front axle. The dynamometer was mounted between the test tractor and the auxiliary tractor as shown in Figure 4.6.

(a) Application of pull on the test tractor by an auxiliary tractor

(b) Dynamometer reading

(c) Load cell reading from microcontroller

Figure 4.6 Testing of load cell mounted on the front axle under laboratory conditions

To validate the readings obtained from the load cell, the load cell was tested in laboratory conditions. The load cell-mounted tractor was placed on the platform balances with handbrakes in an engaged position. Using an auxiliary tractor, the test tractor was given some pull from the rear end, under static condition as shown in Figure 4.6 (a). Due to the applied pull, there will be some load transfer from the front axle to the rear. The change in front axle weight was recorded from the platform balance and the corresponding

observation recorded from the load cell was compared to validate the proper installation of the load cell. The process was repeated several times with different intensities of pull from the auxiliary tractor. A maximum pull of 750 kg was applied during the laboratory test. The front axle load readings from the platform balance and load cell due to the applied pull were recorded and plotted against each other as shown in Figure 4.7. The coefficient of determination (R^2) was found to be satisfactory.

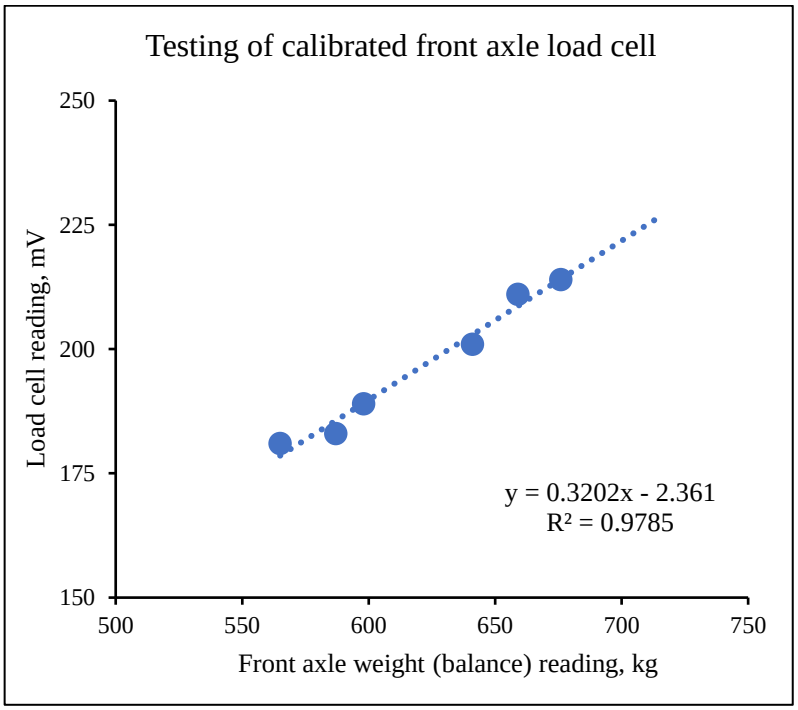

Figure 4.7 Relationship between the load cell and platform balance readings

4.2 Development of Variable Single Hitch Point

A new design of the hitch bracket was conceptualised considering the dimensions of the current hitching model and its existing mounting position to bring minimum change to the current models of tractor drawbar hitching system. The new hitch for tractor-trailer systems was provided with a sliding mechanism instead of multiple bolts so that the hitch height can be hydraulically varied to any height within the sliding range even during dynamic condition.

4.2.1 Tractor

A John Deere 5038 D tractor was taken as a test tractor in this study. It is powered by a 2.9-litre diesel engine with three cylinders that produces 38 horsepower at 2100 rpm. Without any attachments, the tractor weighed 1795 kg under static condition. The test tractor is a rear-wheel 2WD vehicle equipped with an inbuilt hydraulic system which was utilised to

get variable hitch point. The tractor's original hitch bracket was replaced with a modified hitch bracket to meet the study's objectives. This test tractor would be mounted with all the necessary sensors, an additional hydraulic cylinder, and a drawbar attached trailer.

4.2.2 Trailer

An unbalanced trailer of 3-ton capacity was selected for the present study. The trailer has a single-wheel axle towards the rear and is mounted on the tractor using a single-point drawbar hitch point. The empty trailer weighed 1150 kg.

4.2.3 Design and fabrication of sliding hitch bracket

The design and development of the new variable hitch system were done with prudence, i.e., with as few alterations as possible with respect to the original setup. The new hitch model was conceptualised with similar dimensions and mounting positions as the existing model. However, instead of the numerous hitch locations, the new design was provided with a slot on each side of the hitch bracket into which the drawbar can slide to lower or raise the trailer hitch position. The design of the proposed new sliding type hitch bracket was conceived using a computer program (CATIA). It was designed for easy hitch height manipulation as well as sufficient mechanical strength to bear the various types of loads acting on it. The new hitch bracket was designed to have an effective hitch range between 26 to 68 cm height above the ground surface. The hitch bracket and drawbar are shown in Figure 4.8 and Figure 4.9, respectively.

Structural optimization techniques and computer simulation are particularly significant in such designs. They have become an important aspect of the product design process, particularly in the automotive sector. Thus, ANSYS WORKBENCH software was used to analyse the stress developed in the proposed new hitch model due to the drawbar load as shown in Figure 4.10. The ANSYS workbench imports the CATIA models and estimates the stress distribution and structural displacement using finite element analysis (FEA). The findings of the FEA were used to assess the design's strength criterion and fatigue and identify areas that need to be improved if required. As a result, utilising ANSYS software, an approach was made to verify its structural performance.

After successfully analysing the conceptual design, the new hitch bracket model was fabricated according to the dimensions obtained from the ANSYS simulation result. The

clumsy lock and pin mechanism used on current drawbar versions was replaced by a double-acting hydraulic cylinder.

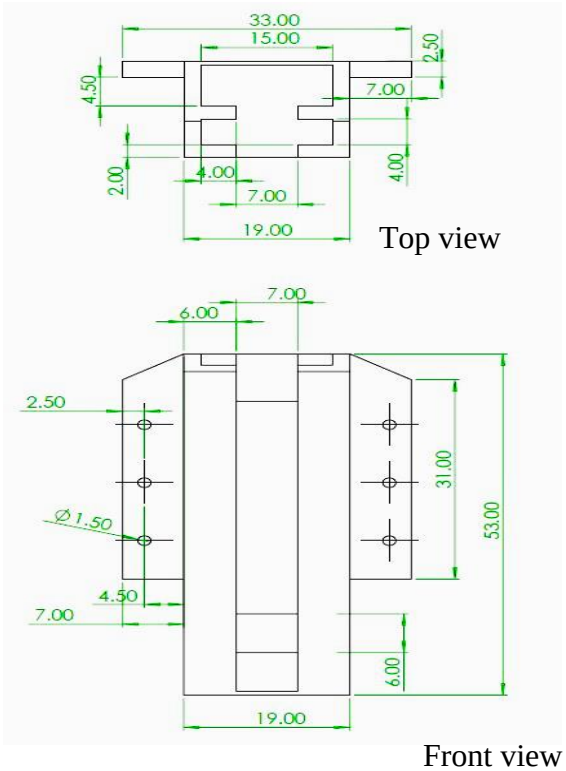

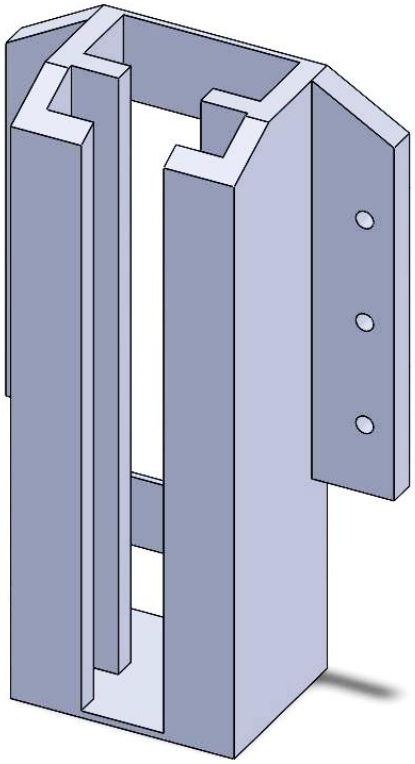

(All dimensions are in cm)

Figure 4.8 Dimensions and isometric view of the conceptualised hitch bracket

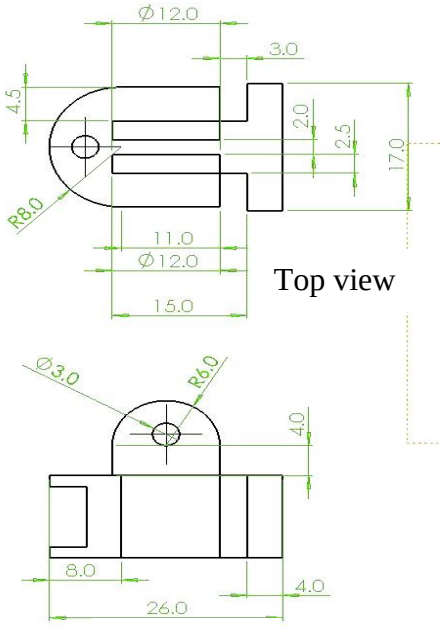

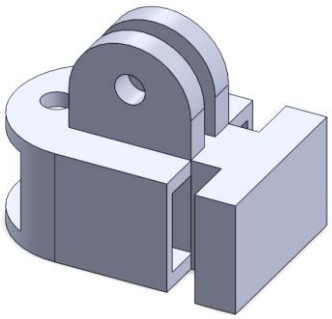

Figure 4.9 Dimensions and isometric view of the conceptualised drawbar

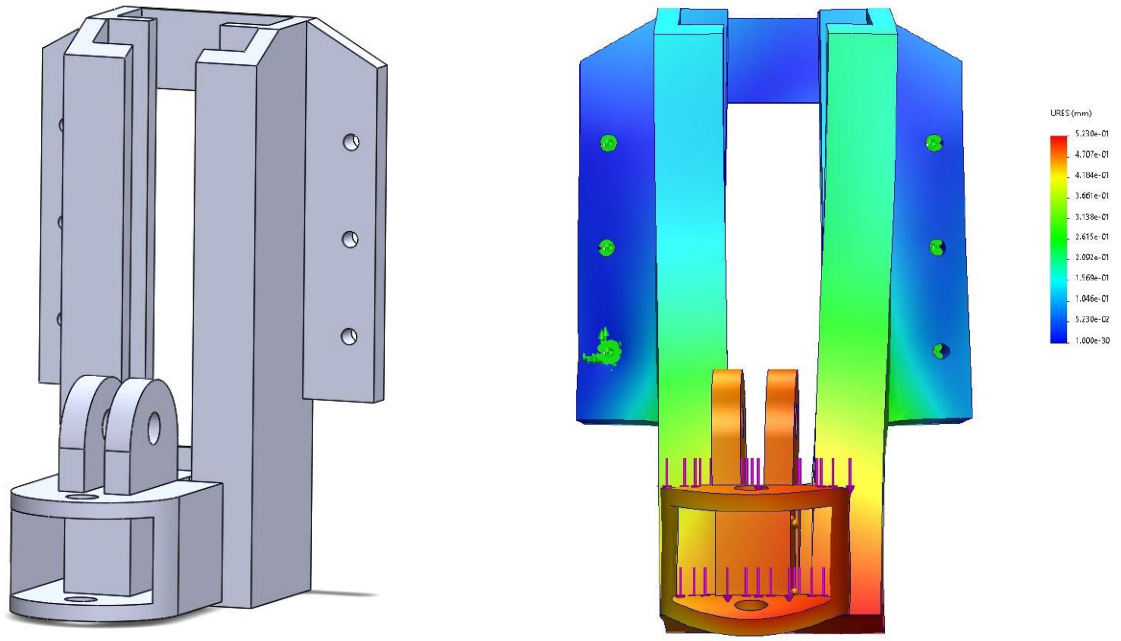

Figure 4.10 Simulated view of the conceptualised hitch and drawbar assembly

4.2.4 Hydraulic cylinder

A double acting hydraulic cylinder was selected based on the design requirements, particularly, the specifications of the inbuilt hydraulic pump of the test tractor and the expected load from the trailer on the drawbar: draft and vertical load, where ideally the latter should not exceed 20 percent of the trailer capacity. The various pump parameters namely, the rated pump pressure (214 kg/cm^2), the maximum operating speed (3000 rpm), and the minimum discharge rate (21.4 lpm, at 2000 rpm and rated pressure) were obtained from the pump manual book. Apart from these, the trailer load to be handled and the range of hitch height variation was taken into account. The vertical load on the drawbar should not exceed 20% of the trailer capacity (IS 8213:2000 Agricultural Tractor Trailer Specification). Therefore, the maximum design vertical load on the trailer was considered 1000 kg which is more than 20% of the gross trailer weight. The stroke length of the piston was determined according to the maximum range of the hitch height which is 420 mm.

Based on these above considerations, the parameters of the double-acting cylinder were calculated. The parameters included were the diameter of the piston rod and head (equations 3.3 and 3.4, respectively), the outer diameter of the cylinder (equation 3.5), and the thickness of the cylinder tube (equation. 3.7).

After the calculation of cylinder dimensions, performance characteristics of the cylinder such as speed of extension and retraction were calculated using equations 3.8 and 3.9, respectively. Specifications of the hydraulic cylinder are given in Table 4.1.

Based on the dimensions obtained from the calculation for the double-acting hydraulic cylinder, a market survey was conducted in Kolkata to select the appropriate hydraulic cylinder. A double-acting hydraulic cylinder with dimensions that were closest to the calculated specifications was purchased. As indicated in Table 4.1, the dimensions of the cylinder procured are tabulated against computed parameters.

Table 4.1 Specifications of the hydraulic cylinder

Sl. No.	Specifications	Values	
		Calculated	Procured
1	Piston rod diameter, mm	33.2	40
2	Piston diameter, mm	58.3	60
3	Cylinder outside diameter, mm	65.3	75
4	Cylinder wall thickness, mm	3.5	7.5
5	Stroke length, mm	420	520
6	Cylinder port diameter, mm	9.7	9.7
7	Mounting style	Rod eye	Rod eye
8	Eye diameter, mm	40	40
9	Pump discharge, *lpm*	20	21.4
10	Speed of extending ram, mm/s	185	162
11	Speed of retracting ram, mm/s	125	111
12	Capacity of the cylinder, ton	1	3

4.2.5 Fittings of the hydraulic cylinder

A support frame for attaching the hydraulic cylinder was conceptualised using CATIA. The frame was fabricated considering the available mounting points on the tractor's rear side, the length and size of the hydraulic cylinder to be installed, and the general sturdiness of

the drawbar hitch assembly due to the dynamic nature of the load. The frame's design was first conceived using a computer program (CATIA) and its design parameters were analysed using ANSYS software.

After the design analysis, the frame was fabricated using structural steel plates of 10 mm thickness according to the conceptualised design as shown in Figure 4.11. A pair of holes were drilled near the top of the frame for mounting one end of the hydraulic cylinder while another three sets of holes were drilled on the bottom portion of the frame corresponding to the slots available on the tractor rear for mounting the frame to the tractor. The frame was mounted on the tractor using nuts and bolts.

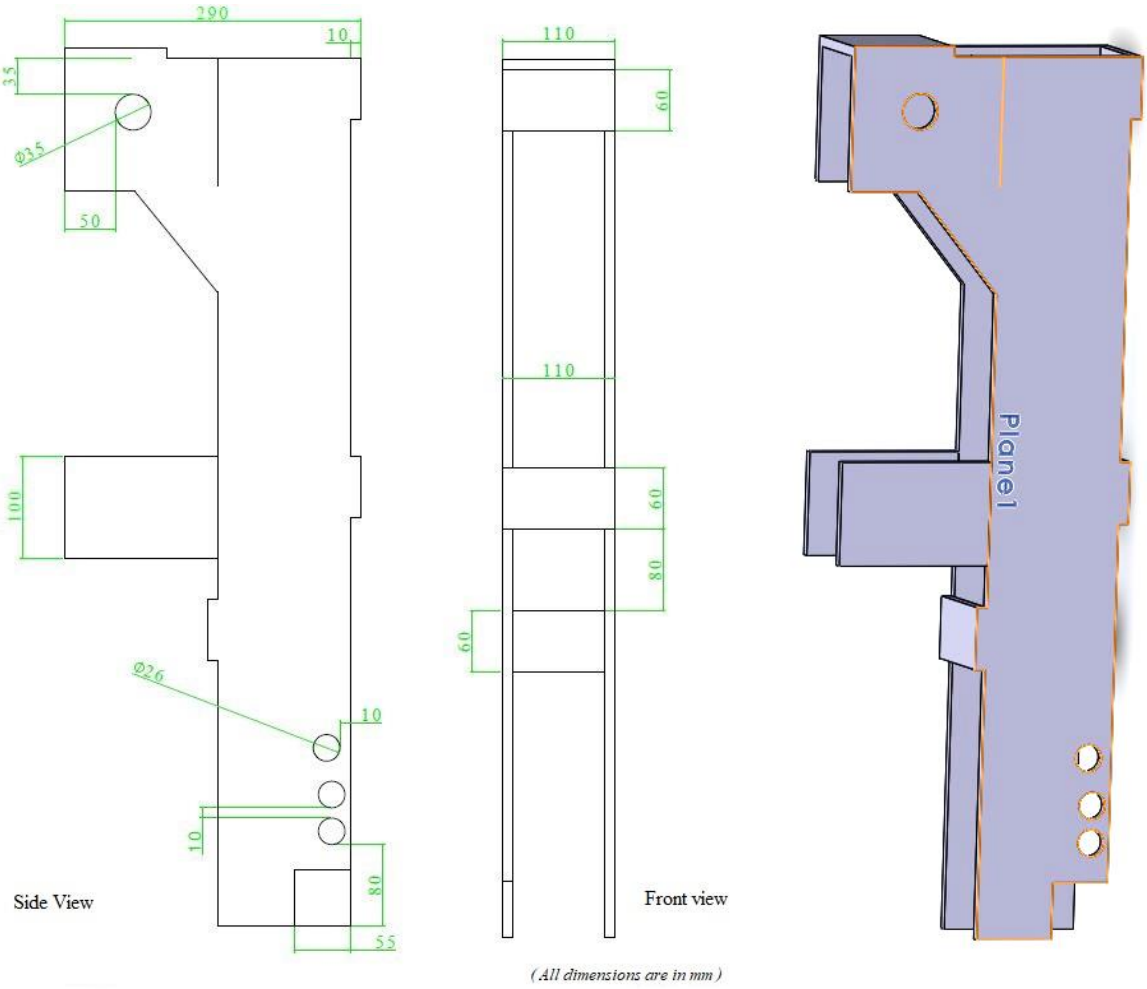

Figure 4.11 Side, front, and isometric view of the cylinder support frame

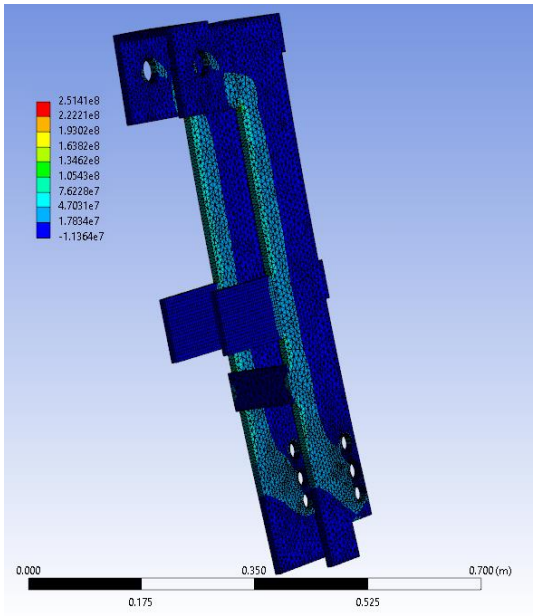

Figure 4.12 Simulated view of the cylinder support frame

The hydraulic cylinder was mounted vertically with one end bolted to a support frame and the other end (piston) to the drawbar. The extension and retraction of the piston facilitate the lowering and raising of the drawbar hitch point. The hitching system was powered using the preinstalled hydraulic system of the tractor. Varying the hitch height is executed by sliding the drawbar hydraulically through the slots of the hitch bracket. The sliding mechanism ensures easy and smooth variation of the drawbar over the conventional burdensome bolt and pin mechanism. The developed hitch bracket with drawbar in its highest and lowest positions are shown in Figure 4.13 and Figure 4.14, respectively.

Figure 4.13 Highest hitch position

Figure 4.14 Lowest hitch position

4.2.6 Hydraulic hose pipes with adapters

Hydraulic hose pipes are employed in a hydraulic system to transmit hydraulic power between two fluid ports. They are generally made of a synthetic rubber tube that is wrapped in a flexible strength-enhancing wrapping, such as metal or fiber, and then covered in another rubber carcass. Hydraulic hose pipes are sturdy pipes used to convey hydraulic fluids in a hydraulic system under high pressure.

In this study, hose pipes were used to transfer the hydraulic energy through hydraulic oil from reservoir to cylinder via the hydraulic pump and transfer the oil from cylinder to reservoir. They are generally designated according to the hydraulic pressure it can handle and the size of the adapter at the two ends of the hose. To bear the working load of the pressurized oil i.e., 214 kg/cm^2, a hose pipe with a pressure bearing capacity of 225 kg/cm^2 (based on the availability in the market) having an inner pipe diameter of 6.35 mm was selected to suit the ports of the existing hydraulic pump, direction control valve, and hydraulic cylinder.

4.2.7 Direction control valve

A direction control valve (DCV) is a hydraulic valve that regulates the flow direction in a hydraulic system. They are usually designated by the number of ports and the number of switching positions. A 4/3-way (4 ports and 3 positions) solenoid-operated DCV was employed in this study to open, close, or change the direction of fluid flow in the hydraulic circuit. It consists of a solenoid and valve. The solenoid is an electric coil that is wound around a ferromagnetic core at its center and is used to control the valve. The valve consists of several chambers known as ports. The solenoid is used to open or close the ports by sliding the spool within the valve. A spool is a cylindrical component that serves as a valve by either blocking or allowing liquid flow via these ports, depending on its position. The DCV required in the study was selected based on the following criteria:

(a) Positions: The current study required the DCV to facilitate three positions to manipulate the fluid flow. One position would allow the hitch point to be raised, the second would direct the hitch to be lowered, while the third or neutral position would allow the height to be maintained at a fixed (existing) position as per the requirement.

(b) Ports: There are four ports in this DCV model. Two ports were connected to either end of the cylinder through which the hydraulic oil enters or exits the cylinder

during the extension or retraction of the piston. While the other two ports were connected to the pump and tank for drawing and returning the oil, respectively. Thus, a 4/3 DCV was required in the study.

(c) Operation: The opening and closing of valves to navigate the direction of fluid flow are accomplished by an electric solenoid.

(d) Power source: The available battery of the tractor with a 12 V DC supply was stepped up to the required 24 V DC with the help of a converter. Hence, the available tractor battery along with a suitable converter was employed to operate the DCV.

The specifications for solenoid operated directional control valve are given in Table 4.2.

Table 4.2 Specifications of the solenoid-operated directional control valve

Sl. No.	Items	Specification
1.	Make	YUKEN
2.	Model	DSG-01-3C4-24-N1-50
3.	Positions	3
4.	Ports	4
5.	Pressure	315 kg/cm^2
6.	Discharge rate	40 l/min.
7.	Power source	24 V (DC)

4.2.8 Installation of the DCV

The DCV was mounted on the body of the tractor towards the operator's right-hand side for easy reach and operation. The hose pipes were connected to the DCV as shown in the circuit diagram (Figure 4.15). The DCV has 4 ports namely: P, T, A, and B. The hose pipe connected to port 'P' of the DCV is connected to the hydraulic pump which is further connected to the reservoir. The hydraulic oil is drawn from the reservoir through this port. Ports 'A' and 'B' of the DCV are connected to the two ends (cap end side and rod end side) of the hydraulic cylinder through which the oil enters or leaves the hydraulic cylinder. Port 'T' of the DCV is connected to the reservoir and acts as a passage to deposit the oil back into the reservoir tank. A pressure relief valve is linked to the two hose pipes connected to

the reservoir. Thus, the fluid that comes from the oil reservoir passes through the safety valve, goes to one end of the hydraulic ram via the DCV, actuates the piston, and from the other end, the fluid comes out through another hose pipe and exits to the oil tank via the DCV. Another pressure gauge was mounted on the hose pipe between the pump and the DCV to monitor the line pressure of the system. An additional switch was provided so that the operator can manually control the DCV irrespective of the load on the front axle.

(a) A pressure relief valve was installed considering the safety of the designed system. An adjustable pressure relief valve of 300 kg/cm^2 was mounted in the hydraulic line in series between the pump and the DCV and set at 180 kg/cm^2.

(b) A pressure gauge was used to monitor the line pressure in the hydraulic circuit. A pressure gauge of 200 kg/cm^2 capacity was used in the system for continuous monitoring of the pressure developed during the lowering and lifting of the hydraulic cylinder. This gauge helped measure the maximum oil pressure of the pump while selecting the other components of the hydraulic system.

(c) After selection of the specific size of hydraulic components, all the components were installed in series as per the hydraulic circuit shown in Figure 4.15 for easy manipulation of the trailer hitch height.

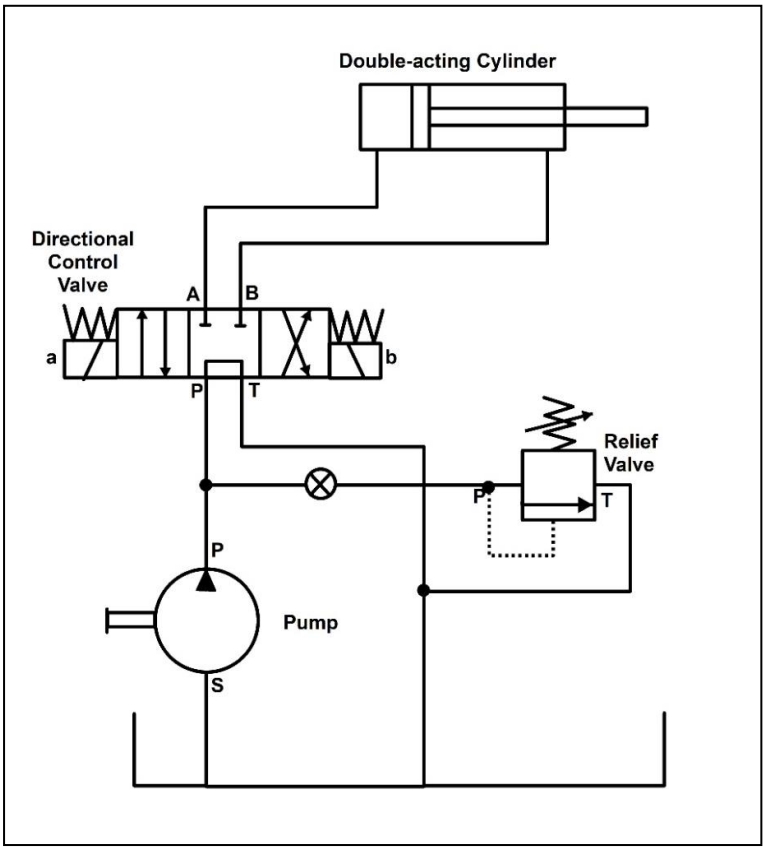

Figure 4.15 Hydraulic circuit of a double-acting cylinder

Figure 4.16 Solenoid operated DCV connected to hydraulic cylinder

4.2.9 Evaluation of the new hitch bracket

The new hitch bracket was mounted in place of the original hitch bracket of the test tractor. The existing drawbar was replaced with the newly fabricated drawbar and slid into the designated slot. The drawbar, as shown in Figure 4.17, was bolted to the rod eye end of the piston. The hydraulic cylinder was supported by a support frame and the required hydraulic connections were made as per the circuit diagram presented in Figure 4.15. The drawbar height was manipulated by manually changing the position of DCV to verify the smooth movement of the drawbar in the slot of the new hitch bracket. The drawbar successfully varied within the provided slot of the new hitch bracket.

4.3 Auto Variable Hitch Height

In order to vary the hitch height according to the front axle load, the real-time value of the front axle load had to be collected and analysed to understand the degree of instability concern in the tractor-trailer system under dynamic conditions. The front axle load was continuously monitored by a load cell and the data obtained from the load cell was fed to a microcontroller. The microcontroller was suitably programmed to analyse the load of the front axle and take appropriate action by switching the position of the DCV to vary the drawbar hitch height.

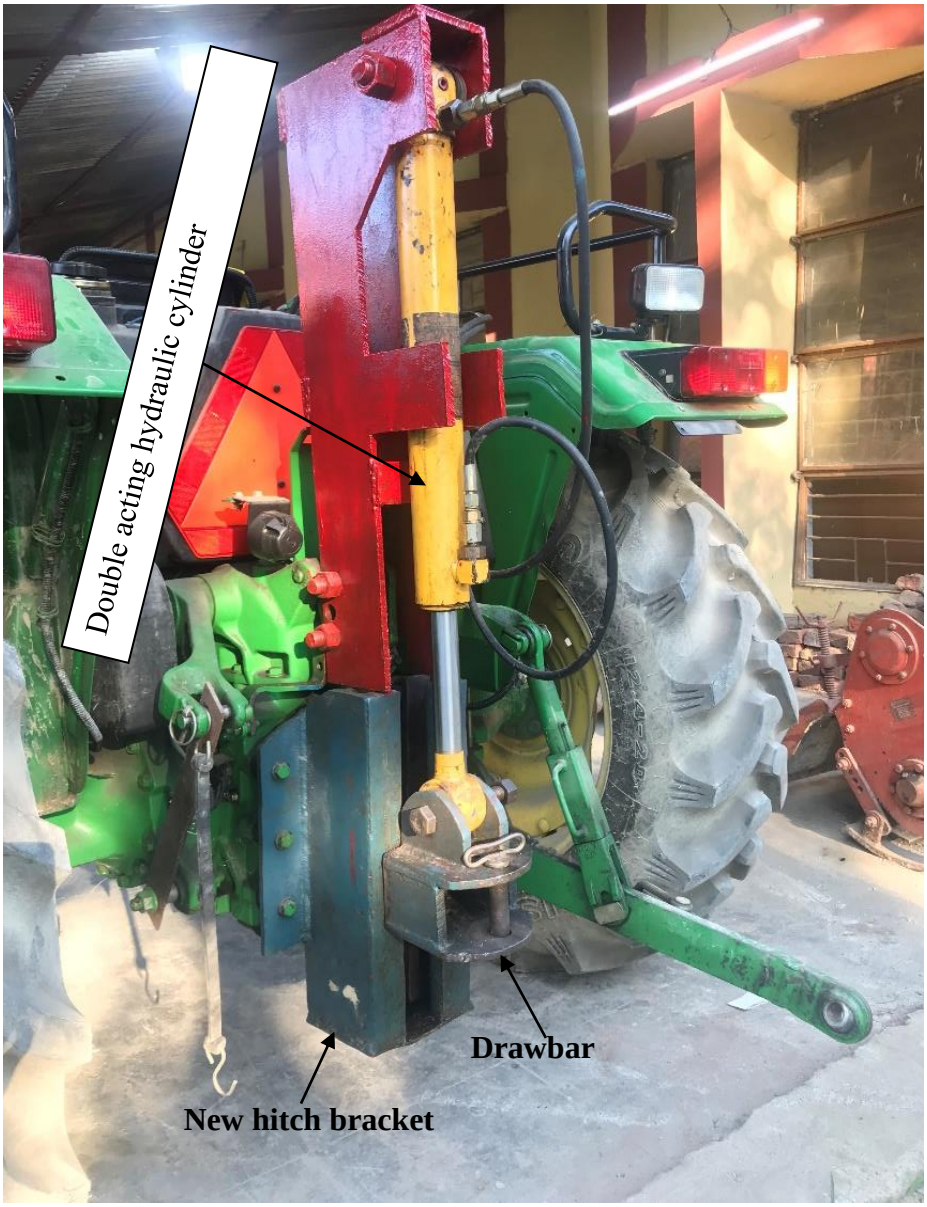

Figure 4.17 Hydraulically operated sliding type drawbar hitch bracket

4.3.1 Microcontroller

A microcontroller is a small integrated circuit that controls one or more functions in an embedded system. On a single chip, a microcontroller contains a CPU, memory, and input/output (I/O) peripherals. The signal from the load cell mounted on the front axle is processed using a 40-pin microcontroller (AT89S52). The signal from the load cell is amplified and delivered to an analogue to digital converter (ADC), which then feeds the transformed signal to the microcontroller port after necessary processing as shown in Figure 4.18. The microcontroller was programmed to assess the input signal and guide the directional control valve (DCV) to raise or reduce the hydraulic piston's position.

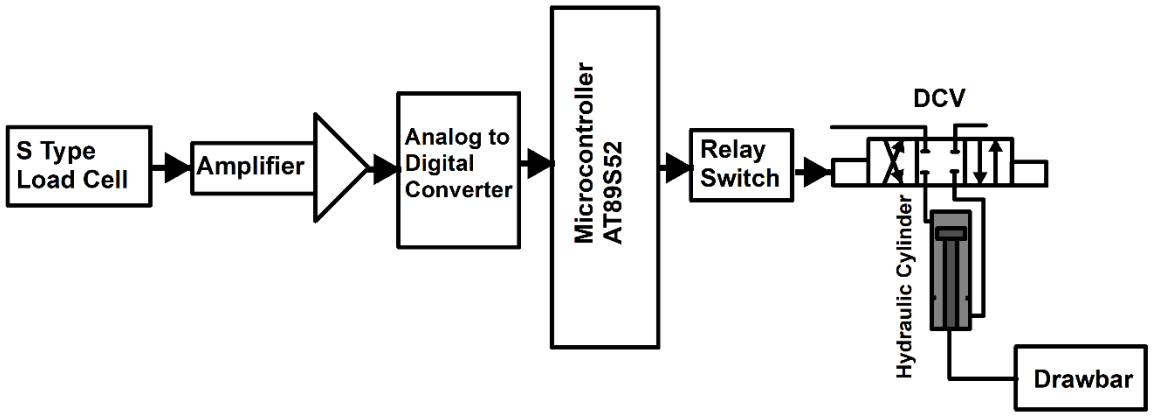

Figure 4.18 Schematic block diagram of the microcontroller-based system

The microcontroller was programmed to regulate the hitch height based on the tractor's traction and stability in dynamic conditions. It was programmed to send a signal to the DCV to lower the hitch height in an attempt to enhance the longitudinal stability of the tractor if the measured front axle load (obtained from the load cell) is below 20% of the total tractor weight. Otherwise, a further weight reduction may increase the likelihood of stability failure due to excess rearward weight transfer. Alternatively, if the measured front axle dynamic load is above 25% of the total tractor weight, indicating sufficient front axle weight and longitudinal stability, the micro-controller was programmed to send a signal to DCV to raise the hitch point, thus enhancing some weight transfer from the front axle and improving the rear wheel traction. The microcontroller was also designed to take no action if the front axle weighed between 20 and 25% of the total tractor static weight, allowing the hitch height to remain in the current position. The process is continuous, and the necessary adjustments are made in response to the front axle load. The process flow chart of the overall functionality of the auto variable hitch height is shown in Figure 4.19.

4.3.2 Measurement of hitch height

An ultrasonic proximity sensor (HC-SR04) as shown in Figure 4.20 coupled with an AT89S52 microcontroller was used to quantify the change in hitch height. This type of sensor is commonly used for object detection and distance measurement ranging from 2 cm to 400 cm. The sensor had a precision of 0.3 cm and operates at a 5V DC supply. The sensor was installed vertically on the lower tip of the hydraulic cylinder positioned just above the drawbar hitch as shown in Figure 4.22 (a). The change in vertical position of the hitch is detected by the sensor and the readings were recorded in a memory chip installed in a microcontroller connected to the sensor. The sensor worked by using the reflected or

transmitted ultrasonic waves to detect the presence or absence of the target. As the distance between the drawbar and the sensor changes, the readings were continuously and automatically recorded in the microcontroller. The sensor and the microcontroller were powered by a USB connected to a computer. The microcontroller was programmed to record the reading every second. Thus, the real-time position of the hitch point was monitored using this proximity sensor connected to the microcontroller.

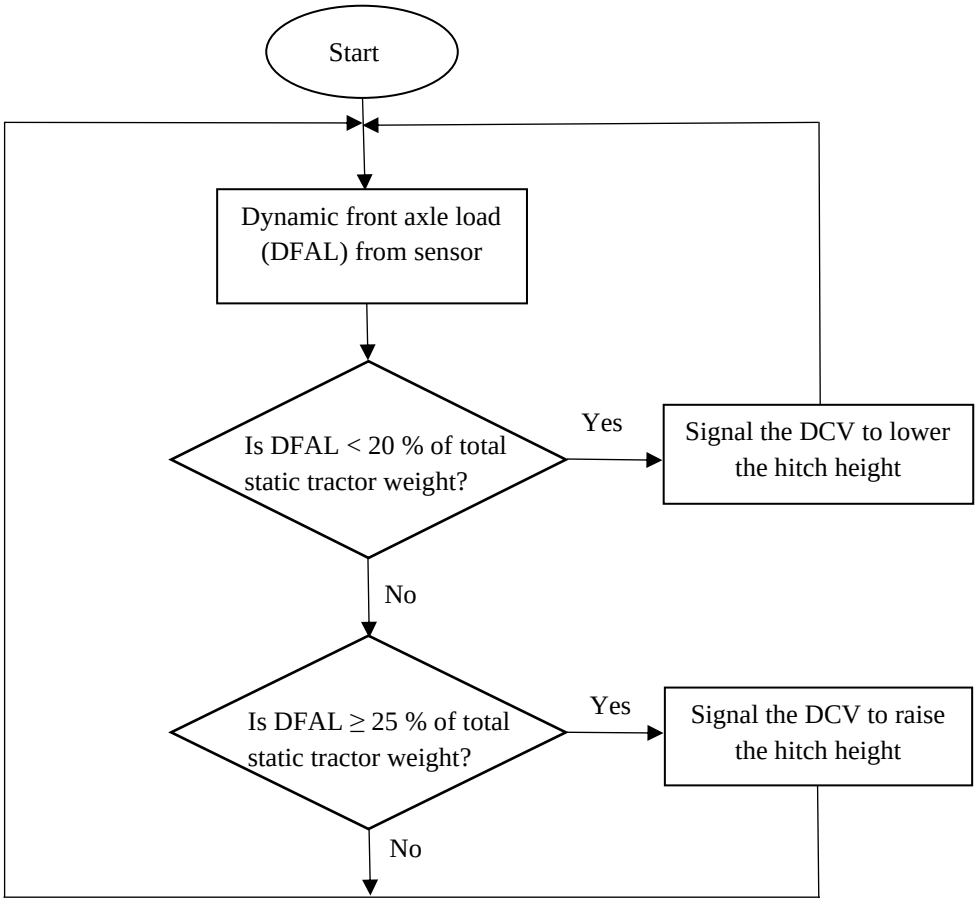

Figure 4.19 Functional diagram of the microcontroller-based system

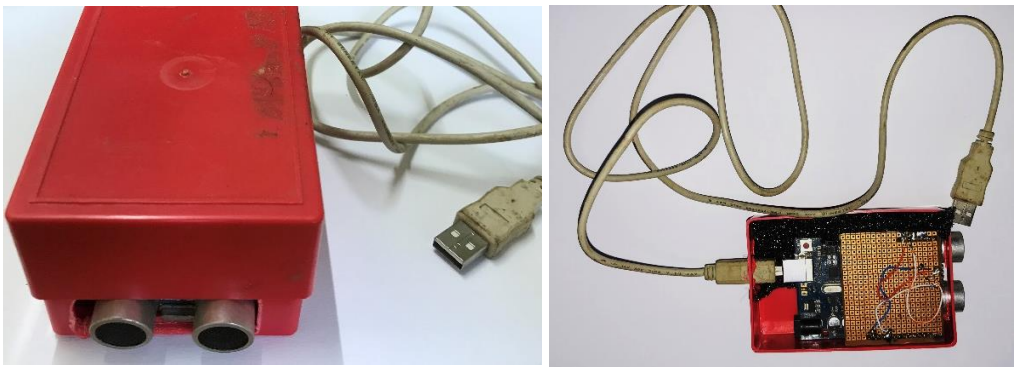

Figure 4.20 Ultrasonic sensor module

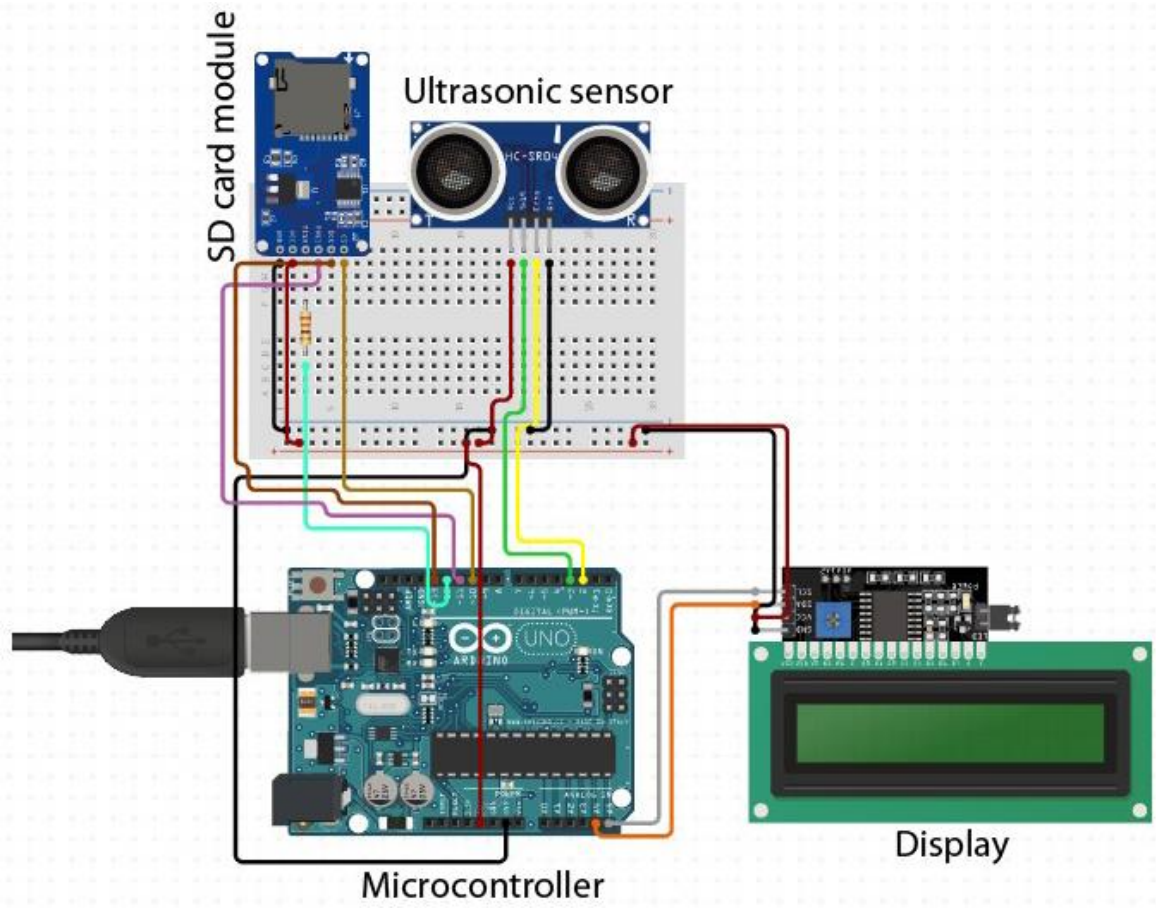

Figure 4.21 Circuit diagram of the ultrasonic sensor for measuring hitch height

4.3.3 Evaluation of the automation system

The developed automatic variable hitch bracket was evaluated under laboratory conditions to validate the proper working of the system. The test tractor with the required accessories was placed on a platform balance. The front axle of the tractor was raised gradually using a lifting jack. The test was carried out to check if the hitch height varied automatically with the change in front axle load. The front end of the tractor was further raised such that its weight reduced beyond 20% of the static tractor weight. As the front weight reduced beyond the 20% value, the microcontroller directed the DCV to lower the hitch height as programmed. On the other hand, while lowering the jack, as the weight on the front axle exceeded 25%, the hitch height was triggered to raise. During this entire test process, the variation in the hitch height was automatically recorded by the ultrasonic proximity sensor connected to a computer. The laboratory test successfully concluded with the expected outcomes.

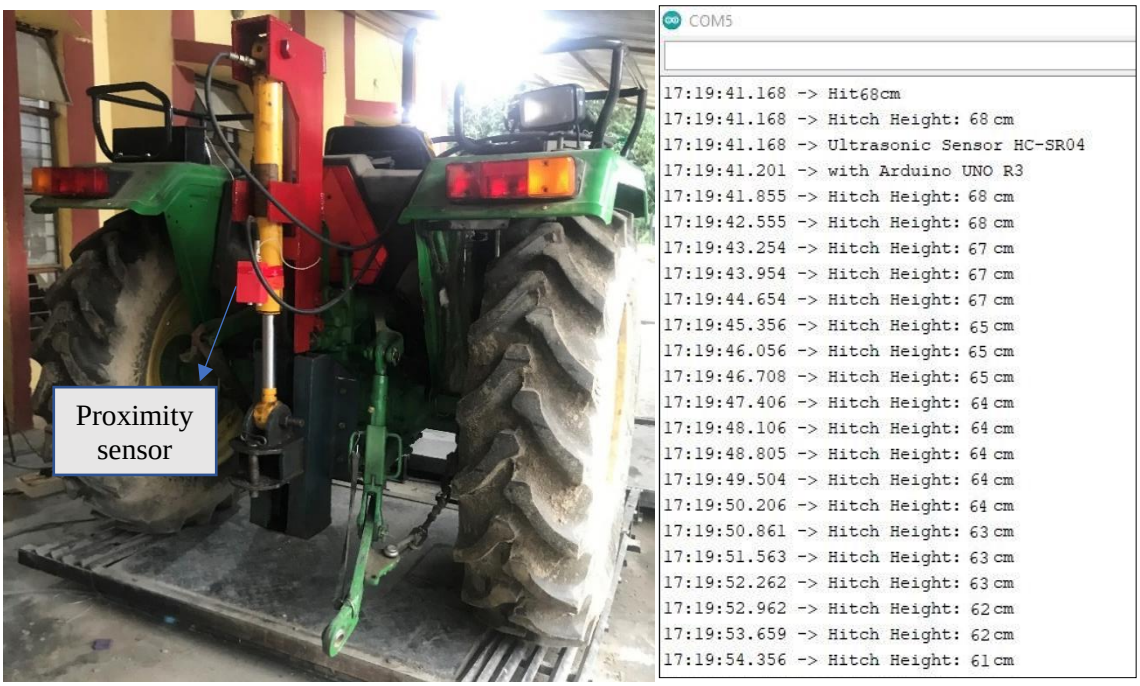

(a) Instrumented proximity sensor (b) sample reading of hitch height

Figure 4.22 Laboratory evaluation of automation system

4.4 Field Evaluation of the Developed System

The instrumented test tractor was taken to the test with different trailer payloads at various surface gradients to understand the effect of different hitch heights on the longitudinal stability of the tractor-trailer system and the tractive performance. The benefits of the automated hitch height system were also examined, especially in the context of the dynamic stability of 2WD tractors. The experiment was carried out with the following research plan:

A. Independent parameters

Parameters	Levels	Description
1. Payload	3	2000, 2500, and 3000 kg
2. Hitch height	5	26, 36, 47, 57, and 68 cm above the ground
3. Types of road surface	2	Unpaved and tarmacadam
4. Gears	3	L3, H1, and H2 for unpaved surfaces and H1, H2 and H3 for tarmacadam surface
5. Engine speed	1	1500 rpm
6. Surface gradient	3	0%, 5% and 9.8% for unpaved surface and 0%, 5.94% and 6.9% for tarmacadam surface
7. Replication	3	

B. Dependent parameters

1. Draft, kg
2. Vertical force, kg
3. Dynamic load on the front axle, kg
4. Theoretical velocity of operation, m/s
5. Actual velocity of operation, m/s

4.4.1 Measurement of soil cone index using a cone penetrometer

A cone penetrometer was used to measure the soil cone index of the unpaved surface. Cone penetrometer is an equipment used to provide a continuous profile of shear strength of soil. The cone index of the tarmacadam surface is considered 10000 kPa. Brixius's model of traction prediction which incorporates the soil cone index parameter was used to determine the tractive performance of the test tractor. The proving ring cone penetrometer consists of a 30° cone, base area measuring 0.98 inch^2, an 18-inch extension rod, a proving ring, a dial indicator, and a handle. When the cone is gradually forced into the ground, the proving ring deforms in proportion to the applied force. The dial inside the ring displays the amount of force needed to progressively push the cone through a given surface. The cone index of the soil refers to this force and is an indicator of the soil's shearing resistance. The cone penetrometer test is shown in Figure 4.23.

(a) Testing of soil strength (b) Cone penetrometer

Figure 4.23 Soil strength test with cone penetrometer on an unpaved surface

4.4.2 Measurement of surface gradient

The experiment was conducted on two types of road surfaces having different gradients. Three sets of surface gradients for each surface type were considered for the experiment. The gradients were measured using dumpy level and level staff. For the tarmacadam surface, the three surface gradients were identified near the PG boys' hostel, within the NERIST campus. While unpaved surfaces were identified outside the NERIST campus within Nirjuli Village 1 circle.

(a) Dumpy level

(b) Levelling with dumpy level and level staff

Figure 4.24 Measurement of surface gradient

4.4.3 Measurement of wheel slip

Wheel slip is the ratio between the actual and theoretical velocities. It was computed by monitoring the actual and theoretical velocities of the instrumented tractor under test during field evaluation. The theoretical and actual velocities of travel were measured using a proximity switch and a ground speed sensor, respectively.

(a) Measurement of theoretical velocity

Theoretical velocity is obtained from the number of revolutions of the rear (drive) wheel in 2WD tractors. An inductive proximity sensor as shown in Figure 4.25 (a) and a pegged wheel ring were used for measuring the theoretical velocity of the test travel during the field test. This type of sensor is used for non-contact detection of metallic objects. Their operating principle is based on a coil and oscillator that creates an electromagnetic field in the close surroundings of the sensing surface. The presence of a metallic object (actuator) in the operating area causes a dampening of the oscillation amplitude and a pulse is generated when the actuator comes close to a proximity switch. Thus, a ring of 69 cm diameter to fit on the rear wheel inner rim was fabricated by bending a 6 mm thick circular

cast iron rod as shown in Figure 4.25 (b). Eighteen pegs were welded on the inner side of this ring at a regular interval of 20º. The proximity switch was mounted close to this pegged ring as shown in Figure 4.27 so that the pegs were approximately within 15 cm sensing distance from the proximity switch and connected to a datalogger DT800. As the ring-mounted wheel revolved and the individual pegs passed by the proximity sensor, a voltage pulse is generated and recorded through the counter channel of the data tracker DT800. The proximity switch was powered by the tractor's battery using suitable arrangements. If the time between the pulse generated and the rolling diameter of the wheel is known, the theoretical velocity can be computed using the given equation:

$$\text{Theoretical velocity} = \frac{\pi D_r}{18\, t} \text{ x no. of pulse generated} \quad \ldots(4.1)$$

where,

D_r = rolling diameter of the wheel, m

t = time, s

(a) Proximity switch (b) Pegged ring

Figure 4.25 Proximity and pegged ring to measure the theoretical velocity

(b) Measurement of actual velocity

The actual velocity of operation was measured by recording the actual amount of ground distance covered by the tractor in a given time. A non-contact type radar-II was used to find the actual velocity of measurement. This sensor works on the principle of the Doppler effect and uses electromagnetic waves to measure the position or motion of an object. Electromagnetic waves propagate in a vacuum with the velocity of light and can be reflected by metallic and non-conducting dielectric objects.

The radar sensor was mounted on the tractor's body as shown in Figure 4.27 (b). A mild steel plate of dimensions 600 x 120 x 6 mm was placed at the rear, right, and the inner side of the tractor mudguard such that it makes an angle of 35º with the horizontal. The sensor

was mounted with its face facing forward in the direction of travel and at a 2 feet height above the ground (recommended) to provide an unobstructed view of the ground. The power to operate the radar sensor was drawn from the tractor's battery, and the output was stored in the DT80 data logger through an analog channel.

Figure 4.26 Radar II Dickey-john ground sensing radar sensor

(a) Theoretical velocity (b) Actual velocity

Figure 4.27 Set up to measure the theoretical and actual velocity of the tractor

The output of the radar sensor was initially calibrated with some known velocities before the experiment. The result of the calibration is shown in Figure 4.28.

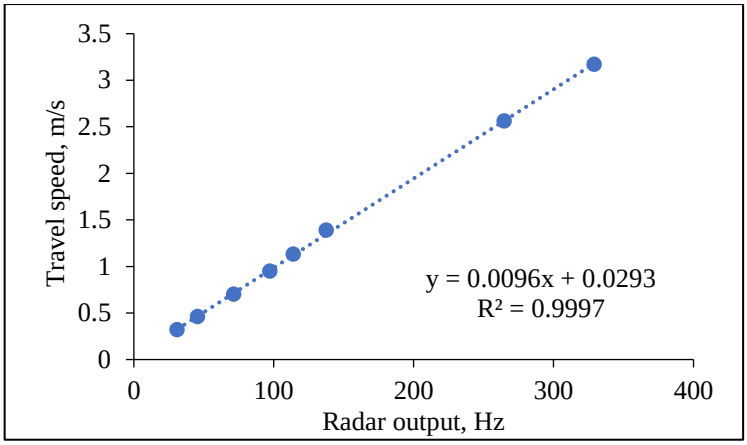

Figure 4.28 Calibration of the ground speed sensor

4.4.4 Draft and vertical force measurements

The force required by a tractor to pull any trailed implement or trailer can be divided into two components: the horizontal component or the draft and the vertical component of the force. Two load cells were used to measure the amount of draft and vertical force required to pull the trailer under field conditions. The load cells were mounted between the tractor drawbar and the trailer as discussed below.

4.4.4.1 Installation of load cells for measuring the draft and vertical force

The draft and the vertical force required to pull the trailer were measured using two S-type load cells. Each load cell had a capacity of 10 kN and was mounted between the tractor and the trailer. For the measurement of the draft, a load cell was mounted horizontally such that the trailer and the drawbar were connected via the load cell. Thus, the horizontal force required to pull the trailer was directly transmitted through the load cell to the tractor drawbar. To measure the vertical force, another load cell was mounted vertically below the trailer eye bolt between two horizontal support plates as shown in Figure 4.29. The lower and the upper support plates measured 11 cm x 36 cm x 8 mm and 11 cm x 14 cm x 10 mm, respectively.

4.4.4.2 Calibration of the load cells

The load cells were calibrated against some known weights (kg) and the readings obtained from the load cells (mV) were plotted against the input loads to determine the relationships between them. The output of the calibration is shown in Figure 4.30.

Figure 4.29 Installation of load cells for the measurements of draft and vertical force

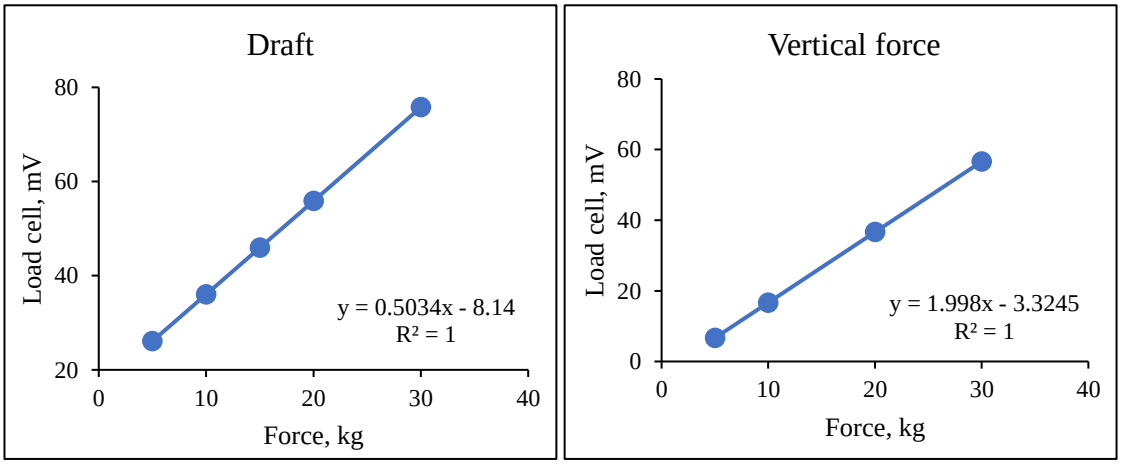

Figure 4.30 Calibration of load cells used for measuring draft and vertical force

From the above calibration relationships, draft (kg) and vertical force (kg) can be calculated using the following formulae:

$$Draft\ (kg) = 0.5034\ x - 8.1418 \quad \ldots(4.2)$$

$$Vertical\ force\ (kg) = 1.998\ x - 3.3245 \quad \ldots(4.3)$$

where,

x, y = load cell readings, mV

4.4.5 Experimental procedure

In order to evaluate the haulage and tractive performances of the tractor-trailer system with the new hitch bracket, the instrumented test tractor along with the unbalanced trailer with the required payloads was hauled to the test sites. The required length of test surfaces was marked, and necessary instructions were given to the tractor operator. The engine was operated at a constant speed of 1500 rpm throughout the experiment. The experiment was carried out in two parts.

The first phase of the trials involved the analysis of the output parameters at five different hitch heights achieved by actuating the cylinder piston. The microcontroller was bypassed during this trial and the hitch height was adjusted at the operator's will. During the second phase, the experiment was conducted with the microcontroller based DCV governing the position of hitch height according to the input received from the front axle load cell. The results obtained from these trials are discussed in the following chapter.

(a) Field test on unpaved surface

(b) Field test on tarmacadam surface

(c) Trailer loaded with a measured quantity of bricks

Figure 4.31 Field test of the instrumented tractor with the loaded trailer

4.4.6 Data acquisition system

The process of obtaining signals that measure actual physical conditions and translating the resulting samples into digital numeric values that can be accessed by a computer is known

as data acquisition. Data loggers are widely adopted data acquisition unit employed in geotechnical monitoring and other instrumentation systems as they can automatically gather real-time data from sensors and show it via mobile devices.

4.4.6.1 Data logger

A data logger is a small, battery-operated device with a CPU, data storage, and one or more sensors or sensor ports. Two data loggers, namely data tracker DT80 and data tracker DT800 were used in the experiment as shown in Figure 4.32. The specifications of these data loggers are given in Appendices – III and IV, respectively. The output from the three load cells and the proximity switch used in the study were recorded via data logger DT800, while data logger DT80 was used to store data obtained from the ground speed sensor. The load cells were connected to the data logger in bridge connection through analog channels, while the proximity switch was connected through a digital channel. The ground speed sensor was connected in frequency connection to the analog channel of DT80 and powered by the tractor battery.

(a) Data taker DT80 (b) Data taker DT800

Figure 4.32 Data loggers used in the study

The data loggers recorded the readings obtained from the three load cells, the proximity switch, and the ground speed sensor. The data loggers collected data every second which was later downloaded into a computer for further analysis. The sample of the data collected is shown in Figure 4.33.

The data obtained from the various instrumentation mounted on the test tractors are analysed in this test. It includes the monitoring of weight transfer from the front axle, measurement of theoretical and actual travel velocities to obtain the wheel slip, measurement of draft and vertical component of pull, and prediction of tractive efficiency with these data.

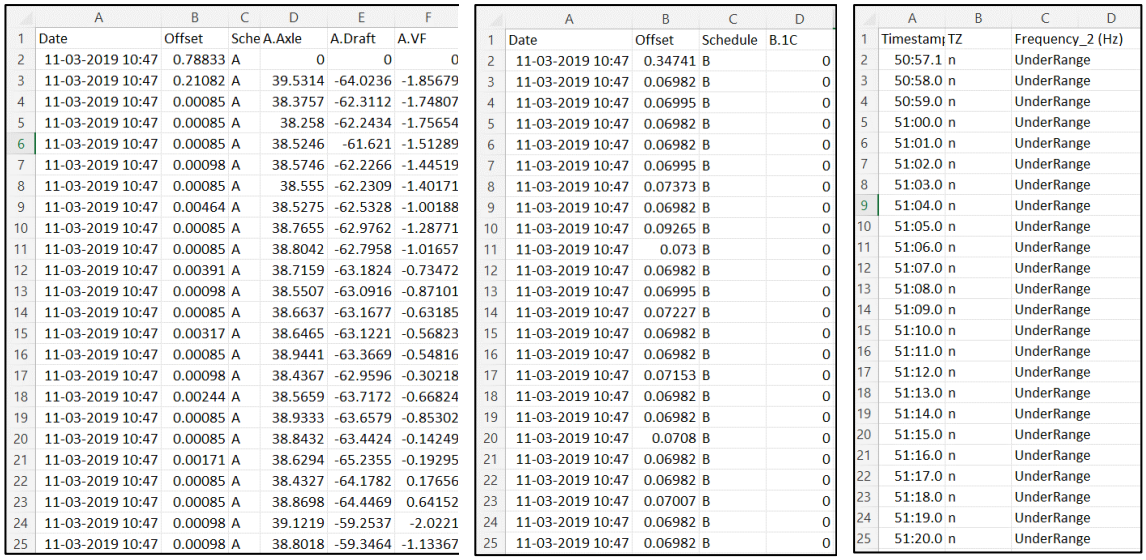

	A	B	C	D	E	F
1	Date	Offset	Sche	A.Axle	A.Draft	A.VF
2	11-03-2019 10:47	0.78833	A	0	0	0
3	11-03-2019 10:47	0.21082	A	39.5314	-64.0236	-1.85679
4	11-03-2019 10:47	0.00085	A	38.3757	-62.3112	-1.74807
5	11-03-2019 10:47	0.00085	A	38.258	-62.2434	-1.75654
6	11-03-2019 10:47	0.00085	A	38.5246	-61.621	-1.51289
7	11-03-2019 10:47	0.00098	A	38.5746	-62.2266	-1.44519
8	11-03-2019 10:47	0.00085	A	38.555	-62.2309	-1.40171
9	11-03-2019 10:47	0.00464	A	38.5275	-62.5328	-1.00188
10	11-03-2019 10:47	0.00085	A	38.7655	-62.9762	-1.28771
11	11-03-2019 10:47	0.00085	A	38.8042	-62.7958	-1.01657
12	11-03-2019 10:47	0.00391	A	38.7159	-63.1824	-0.73472
13	11-03-2019 10:47	0.00098	A	38.5507	-63.0916	-0.87101
14	11-03-2019 10:47	0.00085	A	38.6637	-63.1677	-0.63185
15	11-03-2019 10:47	0.00317	A	38.6465	-63.1221	-0.56823
16	11-03-2019 10:47	0.00085	A	38.9441	-63.3669	-0.54816
17	11-03-2019 10:47	0.00098	A	38.4367	-62.9596	-0.30218
18	11-03-2019 10:47	0.00244	A	38.5659	-63.7172	-0.66824
19	11-03-2019 10:47	0.00085	A	38.9333	-63.6579	-0.85302
20	11-03-2019 10:47	0.00085	A	38.8432	-63.4424	-0.14249
21	11-03-2019 10:47	0.00171	A	38.6294	-65.2355	-0.19295
22	11-03-2019 10:47	0.00085	A	38.4327	-64.1782	0.17656
23	11-03-2019 10:47	0.00085	A	38.8698	-64.4469	0.64152
24	11-03-2019 10:47	0.00098	A	39.1219	-59.2537	-2.0221
25	11-03-2019 10:47	0.00098	A	38.8018	-59.3464	-1.13367

	A	B	C	D
1	Date	Offset	Schedule	B.1C
2	11-03-2019 10:47	0.34741	B	0
3	11-03-2019 10:47	0.06982	B	0
4	11-03-2019 10:47	0.06995	B	0
5	11-03-2019 10:47	0.06982	B	0
6	11-03-2019 10:47	0.06982	B	0
7	11-03-2019 10:47	0.06995	B	0
8	11-03-2019 10:47	0.07373	B	0
9	11-03-2019 10:47	0.06982	B	0
10	11-03-2019 10:47	0.09265	B	0
11	11-03-2019 10:47	0.073	B	0
12	11-03-2019 10:47	0.06982	B	0
13	11-03-2019 10:47	0.06995	B	0
14	11-03-2019 10:47	0.07227	B	0
15	11-03-2019 10:47	0.06982	B	0
16	11-03-2019 10:47	0.06982	B	0
17	11-03-2019 10:47	0.07153	B	0
18	11-03-2019 10:47	0.06982	B	0
19	11-03-2019 10:47	0.06982	B	0
20	11-03-2019 10:47	0.0708	B	0
21	11-03-2019 10:47	0.06982	B	0
22	11-03-2019 10:47	0.06982	B	0
23	11-03-2019 10:47	0.07007	B	0
24	11-03-2019 10:47	0.06982	B	0
25	11-03-2019 10:47	0.06982	B	0

	A	B	C	D
1	Timestam	TZ	Frequency_2 (Hz)	
2	50:57.1	n	UnderRange	
3	50:58.0	n	UnderRange	
4	50:59.0	n	UnderRange	
5	51:00.0	n	UnderRange	
6	51:01.0	n	UnderRange	
7	51:02.0	n	UnderRange	
8	51:03.0	n	UnderRange	
9	51:04.0	n	UnderRange	
10	51:05.0	n	UnderRange	
11	51:06.0	n	UnderRange	
12	51:07.0	n	UnderRange	
13	51:08.0	n	UnderRange	
14	51:09.0	n	UnderRange	
15	51:10.0	n	UnderRange	
16	51:11.0	n	UnderRange	
17	51:12.0	n	UnderRange	
18	51:13.0	n	UnderRange	
19	51:14.0	n	UnderRange	
20	51:15.0	n	UnderRange	
21	51:16.0	n	UnderRange	
22	51:17.0	n	UnderRange	
23	51:18.0	n	UnderRange	
24	51:19.0	n	UnderRange	
25	51:20.0	n	UnderRange	

(a) Load cells (b) Proximity switch (c) Radar sensor

Figure 4.33 Samples of data collected through data loggers

4.4.7 Prediction of tractive efficiency

Tractive efficiency is the product of the pull ratio and velocity ratio as represented by equation 3.20. The pull ratio is the ratio between the net traction ratio and the gross traction ratio while the velocity ratio is the ratio between actual and theoretical velocities. Since the gross traction cannot be measured directly, Brixius (1987) traction equations were used to calculate the tractive efficiency of the test tractor.

4.4.7.1 Development of computer program

A computer program was developed in Visual Basic 6.0 to calculate the tractive efficiency based on the following input parameters:

Input parameters

1. Draft, kg
2. Vertical force, kg
3. Actual and theoretical velocities, m/s
4. Static weight on the front and rear axles, kg
5. Dynamic weight on the front axle, kg
6. Cone index, kPa
7. Payload, kg
8. Dimensions of the front and rear wheels (width x rim diameter), inch
9. Aspect ratio of the tyres, %

A window in the developed software program allows users to enter different input parameters. The developed software contains a window where a user can provide various input parameters. The actual and theoretical velocities, draft, vertical load, front axle load, and cone index were provided from the experimental values. The window also contains an 'OK' tab. The program calculates and displays the tractive efficiency in the same window as we click the "OK" button, as illustrated in Figure 4.34.

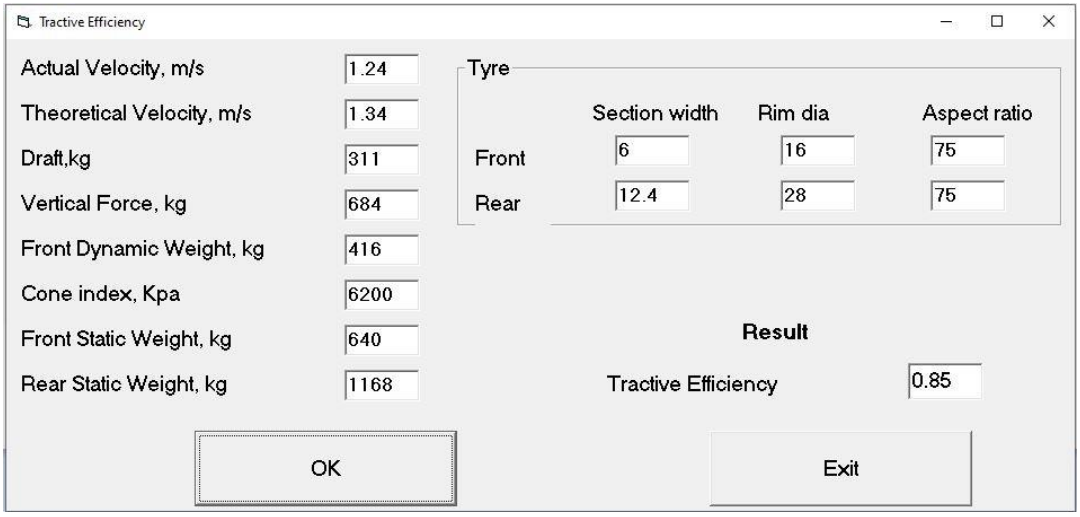

Figure 4.34 Window of the developed computer program

4.5 Field Evaluation of the Developed Automation System

The instrumented test tractor was evaluated under different field conditions to analyse the effect of the developed auto-adjustable hitch height mechanism. The tractor was operated with a given trailer payload on three different surface grades on unpaved and tarmacadam surfaces. The dynamic front axle load was recorded along with the corresponding position of the hitch height. The procedure was repeated by varying the payloads as per the given research plan:

Research plan

A. Independent parameters		
Parameters	**Levels**	**Description**
1. Payload	3	2000, 2500, and 3000 kg
2. Types of road surface	2	Unpaved and tarmacadam
3. Gears	2	H1 and H2
4. Engine speed	1	1500 rpm
5. Surface gradient	3	0%, 5% and 9.8% for unpaved surface and 0%, 5.94% and 6.9% for tarmacadam surface
6. Replication	3	

B. Dependent parameters	
1.	Dynamic load on the front axle, kg
2.	Position of hitch height, cm

The data collected through the above experiment were analysed to examine the change in hitch height location with respect to the front axle load as programmed in the microcontroller. The result of this exercise is presented in Chapter 5.2.

Chapter 5
Results and Discussion

This chapter deals with the outcomes of the experiment carried out in this study. The effect of different hitch heights on tractor performance is thoroughly discussed in this chapter. It also deals with the effect of automating the hitch height on the dynamic stability of the tractor-trailer combination. The chapter is broadly divided into the following subheadings:

5.1 Haulage Test at Various Hitch Heights

The haulage test of the developed system was conducted on two types of road surfaces, viz. unpaved surface (US) and tarmacadam surface (TS). The trials were conducted at gear settings Low 3 (L3), High 1 (H1), and High 2 (H2) for the unpaved surface while at gears H1, H2, and High 3 (H3) for tarmacadam surface. Three different trailer payloads: 2000, 2500, and 3000 kg were considered for both the road surfaces, operating at 0% gradient (G1), 5% gradient (G2) and 9.8% gradient (G3) for unpaved surfaces and 0% gradient (G1), 5.94% gradient (G2) and 6.9% gradient (G3) for tarmacadam surface. The trailer was hitched to the new hitch bracket and varied hydraulically between 26 to 68 cm height, above the ground surface. The engine speed was maintained at 1500 rpm throughout the experiment. Three replications were carried out for each set to obtain the required parameters.

The various tractor performance and haulage parameters that were studied include draft, vertical load, theoretical and actual travel speeds, and dynamic weight on the front axle. Further, wheel slip and tractive efficiency were calculated from the above-mentioned parameters through the developed computer program. A one-way analysis of variance (ANOVA) was conducted to observe the effect of hitch height on various haulage parameters.

5.1.1 Effect of hitch height on draft and vertical load

Effect of hitch height on draft and vertical load at different conditions on three surface grades are shown through Figures 5.1 to 5.3.

5.1.1.1 On surface gradient 1

The relationships between draft and vertical load against hitch height of the trailer drawbar operating on gradient 1 (G1) with a payload of 2000 kg, 2500 kg and 3000 kg are shown in Figure 5.1. It was found that the draft requirement was almost constant at all hitch heights

for the given payload in all three gear selections for both road surfaces.The draft requirement for a 2000 kg payload on the unpaved surface at gear L3 was observed to vary between 241 to 271 kg, 281 to 317 kg at gear H1, and 286 to 306 kg at gear H2 as shown in Figure 5.1 (a). Similarly, it varied between 269 to 289 kg at gear H1, 287 to 298 kg at gear H2, and 306 to 327 kg at gear H3 on the tarmacadam surface while operating between 26 to 68 cm hitch height on both the surfaces. The vertical load acting on the drawbar showed a declining trend in all three operating speeds for both road surfaces for the given payload on increasing the hitch height. The vertical load reduced from 756 to 561 kg (L3), 688 to 514 kg (H1) and 658 to 488 kg (H2) on the unpaved surface, and 644 to 504 kg (H1), 593 to 468 kg (H2), and 580 to 445 kg (H3) on tarmacadam surface while raising the hitch height from 26 to 68 cm, respectively.

For a 2500 kg payload, the experiment showed similar trends as observed with a payload of 2000 kg. Figure 5.1 (b) represents the relationships between draft and vertical load with the varying hitch height. The draft requirements did not vary much on varying the hitch height for both the surfaces. However, the vertical load decreased with the increase in hitch height. The draft was found to lie between 289 to 314 kg, 327 to 340 kg, and 355 to 367 kg for the unpaved surface at gear L3, H1, and H2, respectively, and 317 to 325 kg, 334 to 351 kg, and 366 to 381 kg for tarmacadam surface at gear H1, H2, and H3, respectively. The vertical load on the drawbar decreased from 872 to 684 kg, 792 to 620 kg, and 728 to 601 kg while raising the hitch height from 26 to 68 cm on the unpaved surface, and 813 to 668 kg, 748 to 621 kg, and 697 to 586 kg for tarmacadam surface at gear H1, H2 and H3 respectively.

Figure 5.1 (c) shows the relationships between draft and vertical load with the hitch height while operating the tractor with a 3000 kg payload. Similar trends in the draft and vertical load were observed for both the road surfaces with a negligible effect of hitch height on draft and inverse relation between vertical load and hitch height in all gear settings. The draft for unpaved surface lay between 370 to 383 kg (L3), 409 to 418 kg (H1) and 408 to 443 kg (H2); and between 387 to 397 kg (H1), 412 to 422 kg (H2) and 438 to 451 kg (H3) for tarmacadam surface. The vertical load decreased from 1056 to 850 kg (L3), 975 to 818 kg (H1) and 917 to 771 kg (H2) on the unpaved surface, and 934 to 814 kg (H1), 899 to 790 kg (H2) and 869 to 760 kg (H3) on tarmacadam surface.

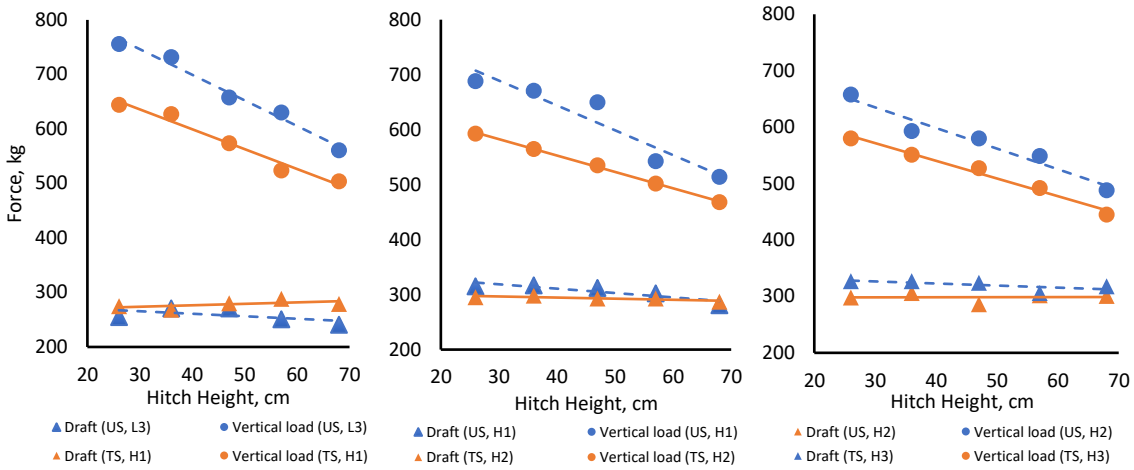

(a) 2000 kg payload

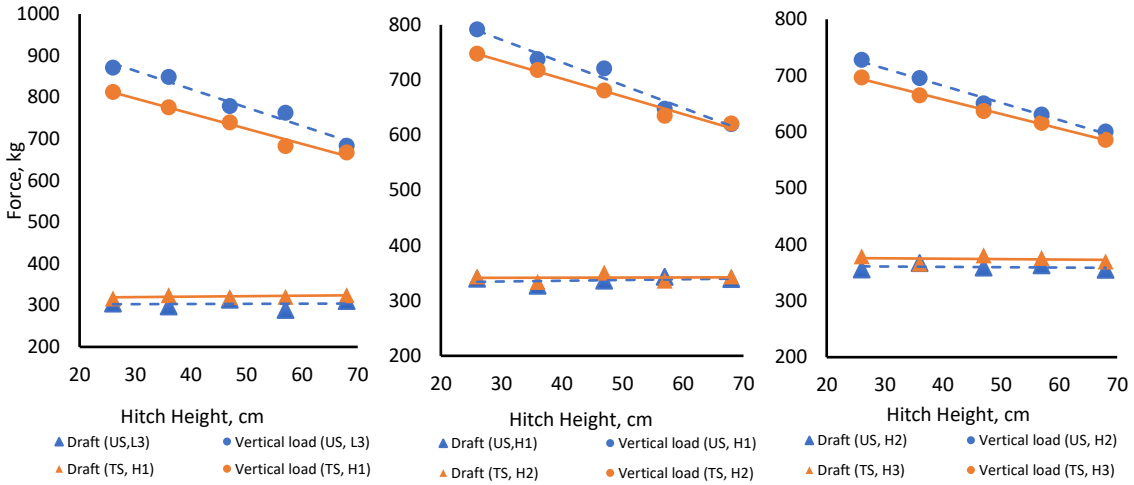

(b) 2500 kg payload

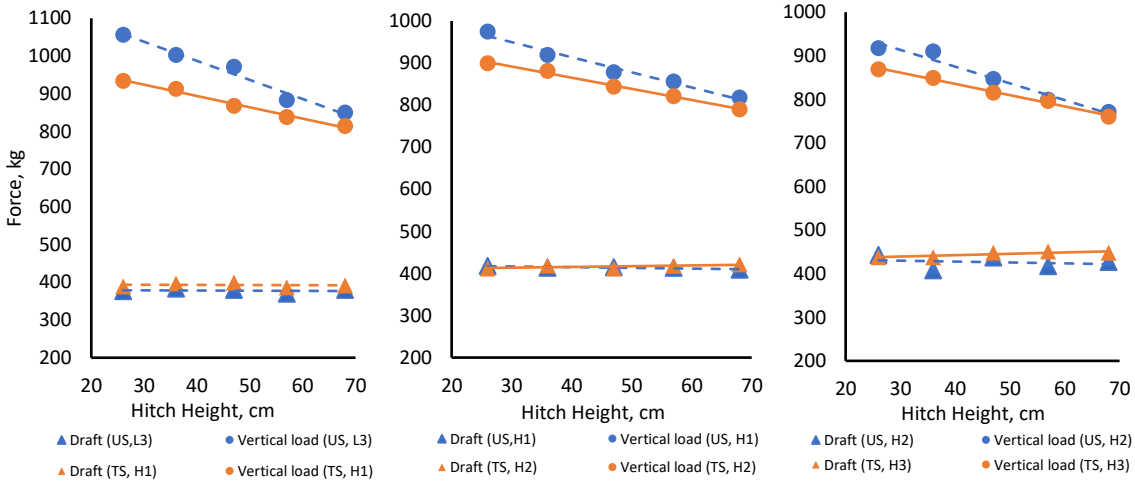

(c) 3000 kg payload

Figure 5.1 Hitch height vs draft and vertical force on surface gradient 1

5.1.1.2 On surface gradient 2

The relationships between draft and vertical load against hitch height of the trailer drawbar operating at gradient 2 with a payload of 2000, 2500 and 3000 kg are shown in Figure 5.2. The results obtained indicated similar trends as found in gradient 1 for both the road surfaces in all gear selections.

As indicated in Figure 5.2 (a), the draft for the unpaved surface was found to vary between 294 to 312 kg (L3), 310 to 330 kg (H1) and 339 to 349 kg (H2) and 314 to 325 kg (H1), 333 to 341 kg (H2) and 348 to 351 kg (H3) for the tarmacadam when operating with a 2000 kg payload. In the mean-time, the vertical load decreased from 669 to 498 kg (L3), 597 to 441 kg (H1) and 542 to 384 kg (H2) on the unpaved surface, and 591 to 432 kg (H1), 560 to 404 kg (H2) and 484 to 353 kg (H3) on tarmacadam surface while increasing the hitch height from 26 to 68 cm, respectively.

With a 2500 kg payload, the draft for unpaved surface remained between 371 to 390 kg, 393 to 409 kg, and 411 to 433 kg at gears L3, H1 and H2 respectively, and 362 to 385 kg, 384 to 408 kg, and 426 to 442 kg at gears H1, H2 and H3, respectively for tarmacadam surface. While the vertical load decreased from 779 to 629 kg, 753 to 581 kg, and 675 to 539 kg on raising the hitch height from 26 to 68 cm at gear L3, H1 and H2, respectively for unpaved surface and 712 to 554 kg, 635 to 508 kg and 578 to 471 kg for tarmacadam surface while operating at gear H1, H2 and H3, respectively as shown in Figure 5.2 (b).

With a 3000 kg payload, the draft was observed to lie between 397 to 411 kg (L3), 419 to 430 kg (H1), and 444 to 455 kg (H2) for unpaved surface and 413 to 427 kg (H1), 438 to 449 kg (H2), and 463 to 479 kg (H3) for tarmacadam surface on varying the hitch height between 26 to 68 cm. Whereas, the vertical load reduced from 849 to 709 kg (L3), 764 to 621 kg (H1), and 725 to 562 kg (H2) on unpaved surface and 736 to 634 kg (H1), 659 to 560 kg (H2), and 618 to 507 kg (H3) on tarmacadam surface on increasing the hitch height from 26 to 68 cm for both road types as represented by Figure 5.2 (c).

5.1.1.3 On surface gradient 3

Likewise, the results obtained from the experiment showed similar trends as found in gradient 1 and 2 for both the road surfaces and payloads at all gear selections. The relationships between draft and vertical load against hitch height of the trailer drawbar operating at gradient 3 with a payload of 2000 kg, 2500 kg and 3000 kg are shown in Figures 5.3.

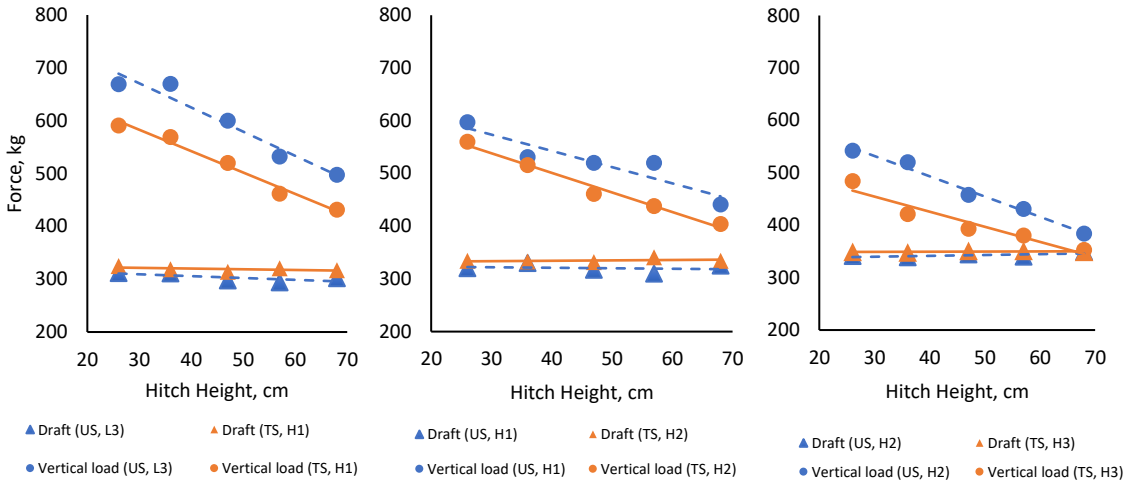

(a) 2000 kg payload

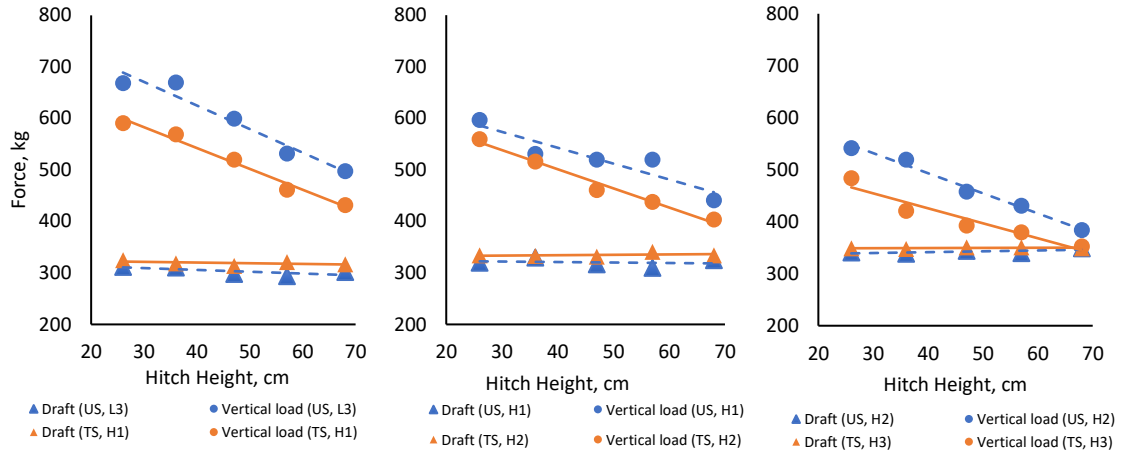

(b) 2500 kg payload

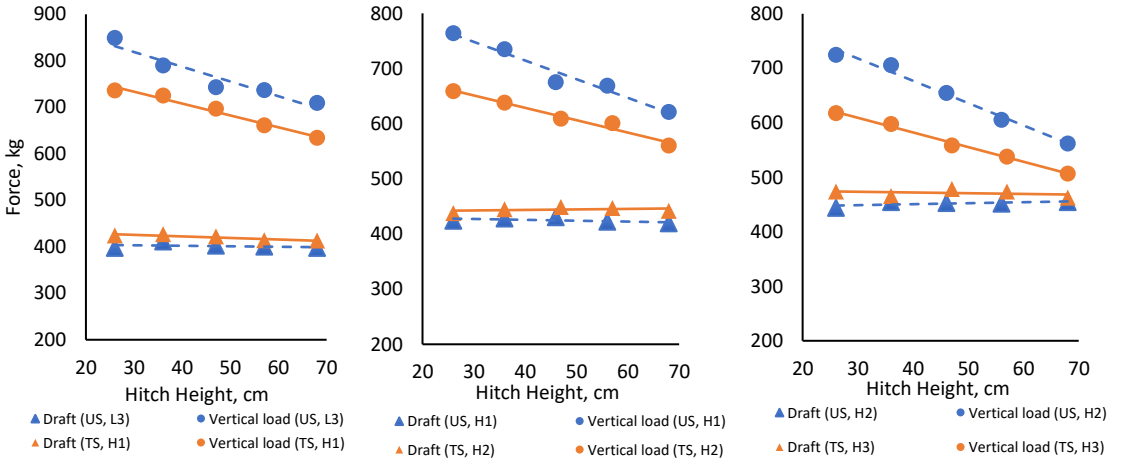

(c) 3000 kg payload

Figure 5.2 Hitch height vs draft and vertical force on surface gradient 2

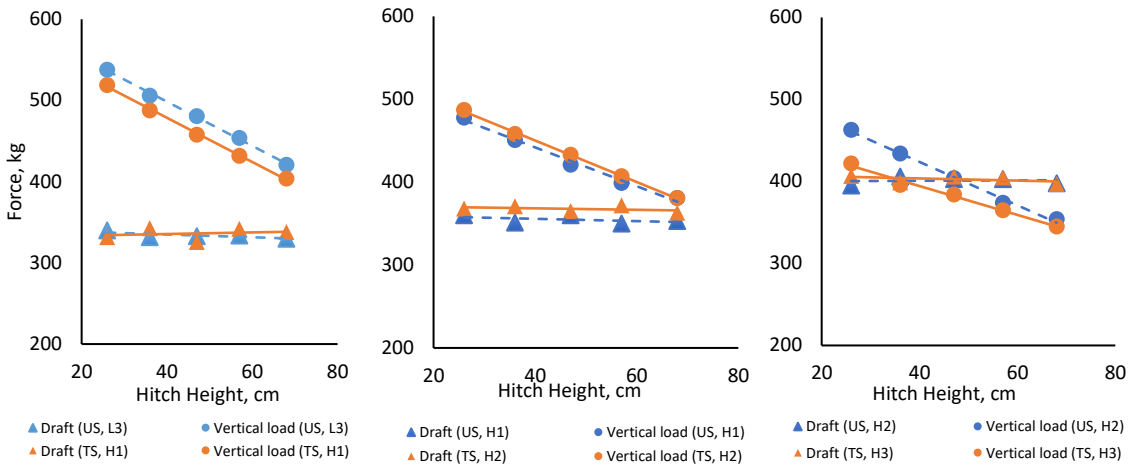

(a) 2000 kg payload

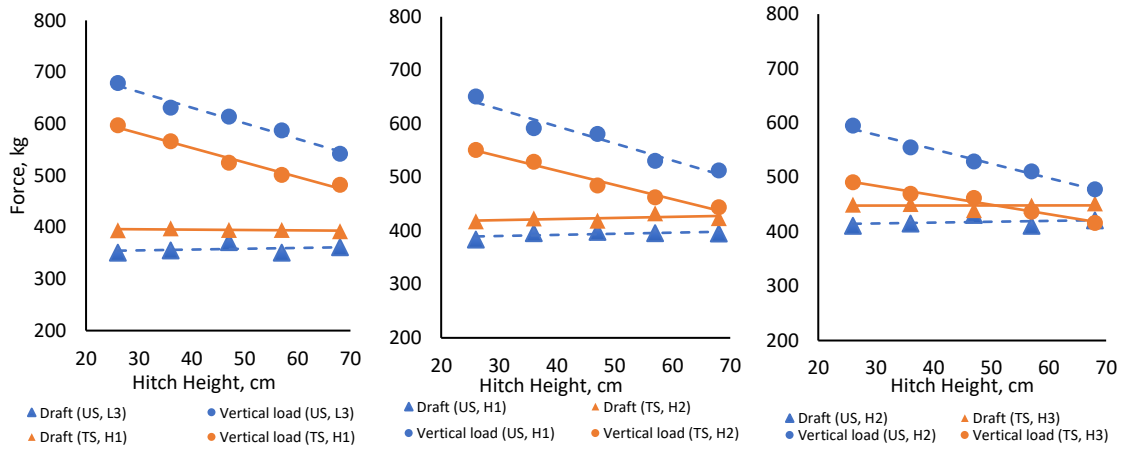

(b) 2500 kg payload

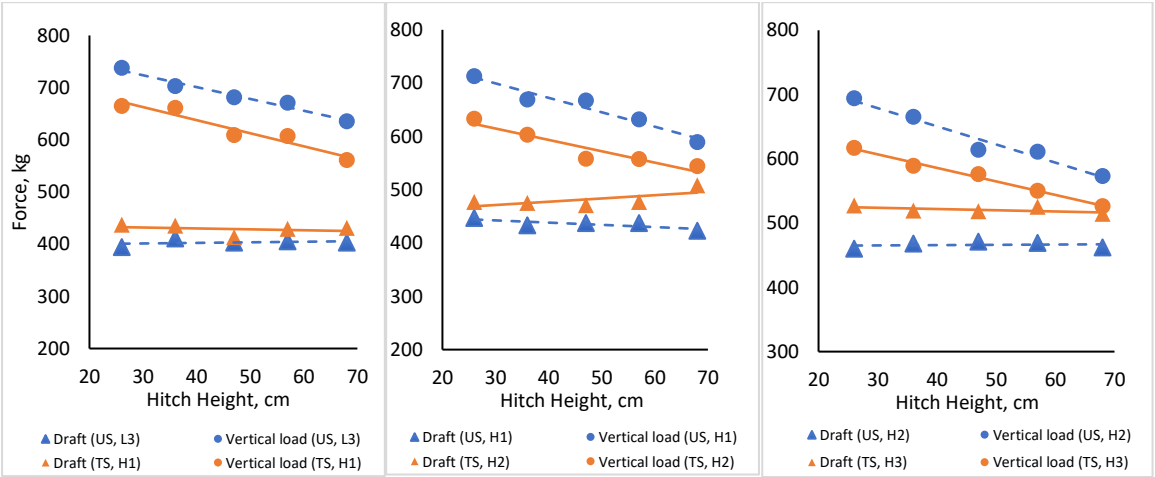

(c) 3000 kg payload

Figure 5.3 Hitch height vs draft and vertical force on surface gradient 3

For 2000 kg payload, the draft requirement ranged between 330 to 340 kg (L3), 350 to 360 kg (H1), and 398 to 406 kg (H2) for unpaved surface and 326 to 343 kg (H1), 363 to 372 kg (H2), and 397 to 407 kg (H3) for tarmacadam surface on varying the hitch between 26 to 68 cm above the ground surface as shown in Figure 5.3 (a). For 2500 kg payload, the value lied between 351 to 371 kg (L3), 384 to 398 kg (H1), and 411 to 431 kg (H2) for unpaved surface and 392 to 398 kg (H1), 418 to 433 kg (H2) and, 440 to 452 kg (H3) for tarmacadam surface as shown in Figure 5.3 (b). For 3000 kg payload, it was found to be 394 to 411 kg (L3), 423 to 447 kg (H1), and 460 to 471 kg (H2) for unpaved surface, and 413 to 437 kg (H1), 471 to 508 kg (H2), and 514 to 527 kg (H3) for tarmacadam surface as shown in Figure 5.3 (c).

Correspondingly, the vertical load on drawbar reduced from 538 to 421 kg (L3), 478 to 381 kg (H1), and 463 to 354 kg (H2) on raising the hitch height from 26 to 68 cm, respectively on unpaved surface, and 519 to 404 kg (H1), 487 to 381 kg (H2), and 422 to 345 kg (H3) on tarmacadam surface when towing a 2000 kg payload. Similarly, for a 2500 kg payload, it was found to reduce from 679 to 542 kg (L3), 651 to 513 kg (H1), and 595 to 478 kg (H2) on unpaved surface, and 597 to 482 kg (H1), 551 to 444 kg (H2), and 491 to 416 kg (H3) on tarmacadam surface on increasing the hitch height from 26 to 68 cm, respectively for both road surfaces. Also, load reduction from 738 to 635 kg (L3), 713 to 589 kg (H1), and 694 to 573 kg (H2) on unpaved surface, and 665 to 561 kg (H1), 633 to 544 kg (H2), and 617 to 526 kg (H3) on tarmacadam surface were observed when operating with a 3000 kg payload. The one-way ANOVA test revealed that the hitch height has no significant effect on the draft with *p*-value at 0.994 (non-significant), whereas there was a significant effect of hitch height on the vertical force with *p*-value at 0.015 (significant) as shown in Appendix VI.

In a nutshell it can be concluded that the change in hitch height did not have any considerable effect on the draft requirement irrespective of test surfaces, speed of operation, payloads, and surface gradients. This result is theoretically validated by the fact that the horizontal force requirement remains independent of the height of hitch. Hence, draft requirement is not affected by location of hitch height. However, the vertical load on the drawbar showed an inverse relationship with the hitch height, i.e., as the hitch height increased, the drawbar vertical load decreased. This is obvious, because, as the hitch height increases, the centre gravity of the loaded trailer moves behind, resulting in lower vertical load.

5.1.2 Effect of hitch height on per cent front axle load and tractive efficiency

Effect of hitch height on per cent front axle load and tractive efficiency at different load conditions on three surface grades are shown through Figures 5.4 to 5.6.

5.1.2.1 On surface gradient 1

The effect of hitch height on the logitudinal stability and tractive efficeincy of the test tractor carrying a payload of 2000, 2500 and 3000 kg payloads are shown in Figure 5.4. While the per cent front axle and longitudinal stability decreased with the increase in hitch height, tractive efficiency increased with the increased hitch height in all load conditions.

During haulage of 2000 kg payload, the load on the front axle reduced from 31.75 to 27.67% (L3), 29.87 to 25.11% (H1), and 27.99 to 21.9% (H2) on the unpaved surface, and 28.87 to 25.44% (H1), 26.77 to 22.29% (H2), and 24.23 to 20.46% (H3) on tarmacadam surface on raising the hitch height from 26 to 68 cm, respectively, as shown in Figure 5.4 (a). On the other hand, tractive efficiency increased from 48.16 to 69.77% (L3), 57.54 to 76.29% (H1), and 53.52 to 81.17% (H2) on the unpaved surface and 46.15 to 57.95% (H1), 47.54 to 68.44% (H2), and 48.86 to 65.61% (H3) on tarmacadam surface when the hitch height was raised from 26 to 68 cm, respectively.

While trailing a 2500 kg payload, similar trends were observed in the per cent front axle load and tractive efficeiny as obtained with a 2000 kg payload. The front axle load reduced from 28.21 to 23.01 (L3), 27.71 to 21.57 (H1), and 26.33 to 20.30 (H2) on unpaved surface on increasing the hitch height from 26 to 68 cm as represented by Figure 5.4 (b). Likewise, the load reduced from 27.65 to 22.79% (H1), 26.05 to 20.58% (H2), and 25.17 to 20.08% (H3) on tarmacadam surface. Meanwhile, the tractive efficiency increased from 54.09 to 84.74% (L3), 59.8 to 82.92% (H1) and 61.84 to 82.35% (H2) on the unpaved surface, and 45.6 to 56.83% (H1), 44.69 to 58.35 % (H2), 50.81 to 59.59% (H3) on tarmacadam surface when the hitch height was raised from 26 to 68 cm, respectively.

As represented in Figure 5.4 (c), the front axle load decreased from 27.77 to 21.52% (L3), 26.99 to 20.13% (H1), and 25.83 to 18.53% (H2) on the unpaved surface, and 27.88 to 21.68% (H1), 26.99 to 20.69% (H2), and 25.83% to 19.69% (H3) on tarmacadam surface while shifting the hitch height from 26 to 68 cm, respectively on pulling a 3000 kg payload. For both the surfaces, it was observed that the load on the front axle decreased below the recommended 20% value, viz. 18.53% (H2) and 19.69% (H3) for unpaved and tarmacadam surfaces, respectively, while operating at a hitch height of 68 cm. This reduction of the

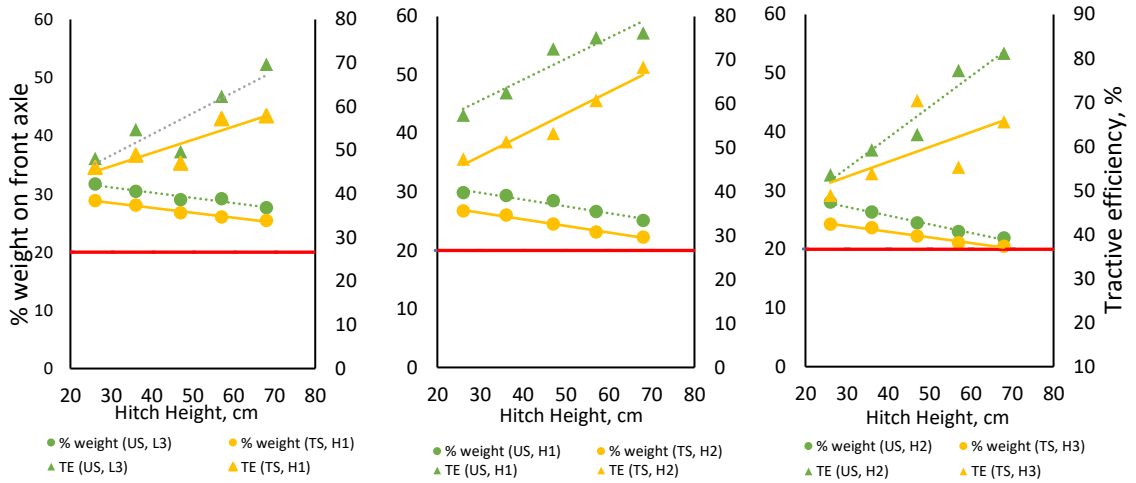

(a) 2000 kg payload

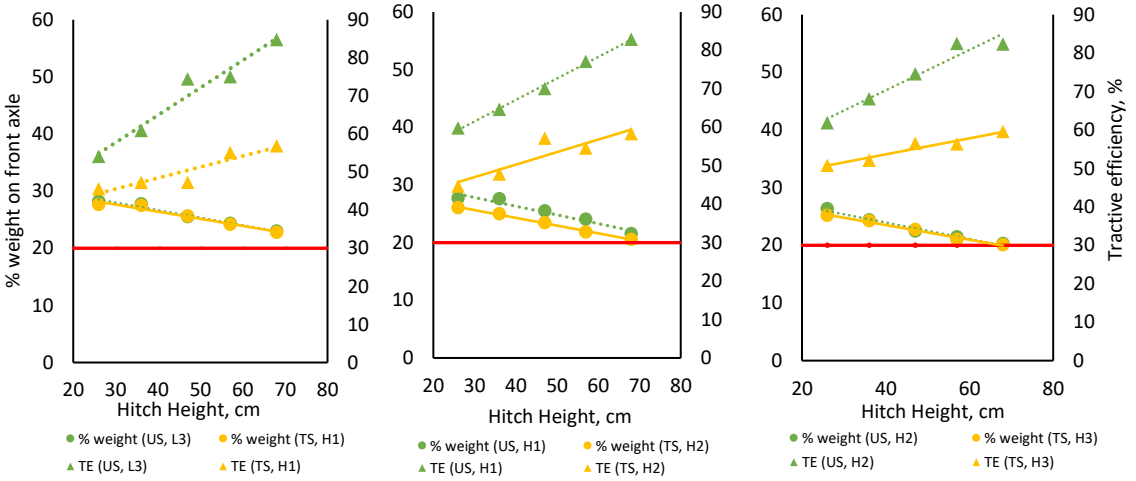

(b) 2500 kg payload

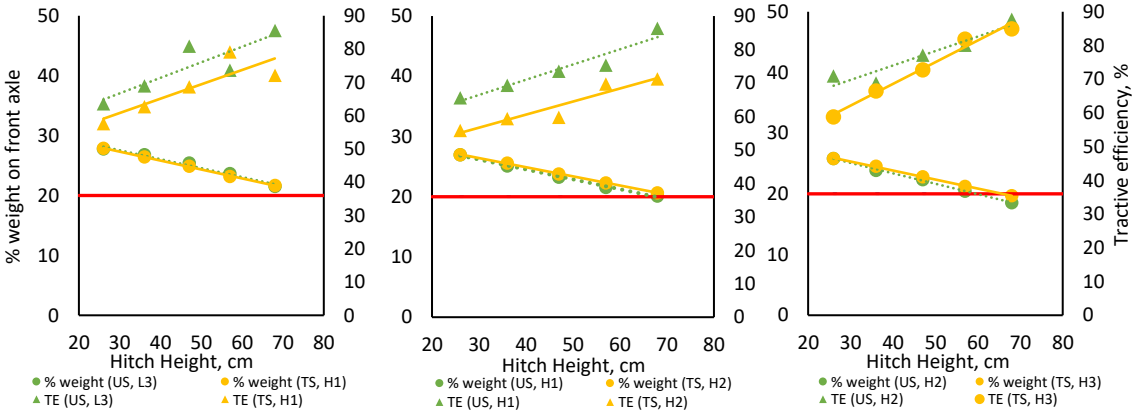

(c) 3000 kg payload

Figure 5.4 Hitch height vs per cent front axle load vs tractive efficiency on gradient 1

front axle load below the safe zone calls for required intervention and necessary corrective measure in order to avoid any untoward mishap during haulage operation. While at the same time, the tractive efficiency increased from 63.57 to 85.6% (L3), 65.63 to 86.4% (H1), and 71.01 to 87.78% (H2) on the unpaved surface, and 57.56 to 72.09% (H1), 55.89 to 71.27% (H2), and 58.79 to 84.96% (H3) on tarmacadam surface.

5.1.2.2 On surface gradient 2

The effect of hitch height on the logitudinal stability and tractive efficeincy of the test tractor operating on gradient 2 carrying a payload of 2000, 2500 and 3000 kg payloads are shown in Figure 5.5. Similar trends in the per cent load and tractive efficiency were observed as found in gradient 1.

While towing a 2000 kg payload, the front axle load decreased from 28.71 to 23.45% (L3), 28.21 to 22.29% (H1), and 27.93 to 21.46% (H2) on unpaved surface and 27.1 to 22.79% (H1), 27.71 to 21.63% (H2), and 25.61 to 18.2% (H3) on tarmacadam surface when the hitch height was increased from 26 to 68 cm as shown in Figure 5.5 (a). It is worth mentioning here that the load on the front axle, when operating on H3 gear setting, was recorded below 20% i.e., 19.52 and 18.2% while hitched at 57 and 68 cm, respectively, on the tarmacadam surface. While the tractive efficiency increased from 56.6 to 79.18% (L3), 57.06 to 81.08 (H1), 56.79 to 85.3% (H2), and 55.93 to 64.11% (H1), 49.16 to 65.38% (H2) and 48.82 to 66.02% (H3) on tarmacadam surface on increasing the hitch height from 26 to 68 cm, respectively.

As shown in Figure 5.5 (b), with the increase in hitch height from 26 to 68 cm, the front axle load decreased from 27.88 to 21.13% (L3), 26.94 to 20.02% (H1), and 26.6 to 18.81% (H2) on unpaved surface and 24.67 to 20.69% (H1), 25.5 to 19.8% (H2), and 24.94 to 18.36% (H3) on tarmacadam surface when pulling a 2500 kg payload. The per cent front axle load dropped to unsafe zone at several instances: 19.75 (H1) and 18.81 (H2) at hitch height of 57 and 68 cm, respectively, on unpaved surface, and 19.63 (H3) and 18.36 (H3) at hitch height of 57 and 68 cm, respectively, on tarmacadam surface. Whereas the tractive efficiency improved from 62.43 to 82.16% (L3), 66.4 to 89.48% (H1), 66.85 to 91.97% (H2) on the unpaved surface, and 51.56 to 71.49% (H1), 55.6 to 74.76% (H2), 60.97 to 78.62% (H3) on the tarmacadam surface.

While working with a 3000 kg payload, as indicated in Figure 5.5 (c), increasing the hitch height from 26 to 68 cm lead to the decrease in the front axle load from 26.38 to 19.41%

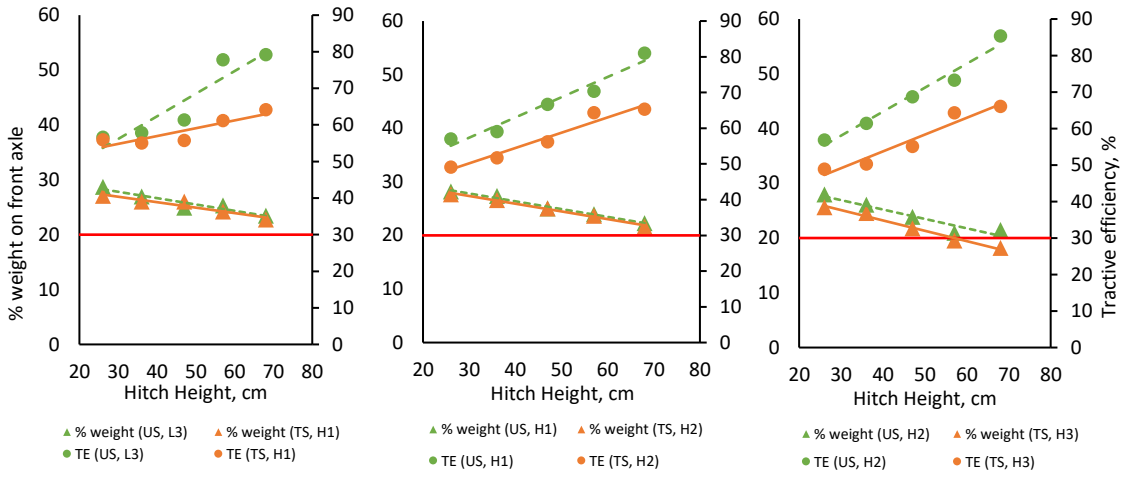

(a) 2000 kg payload

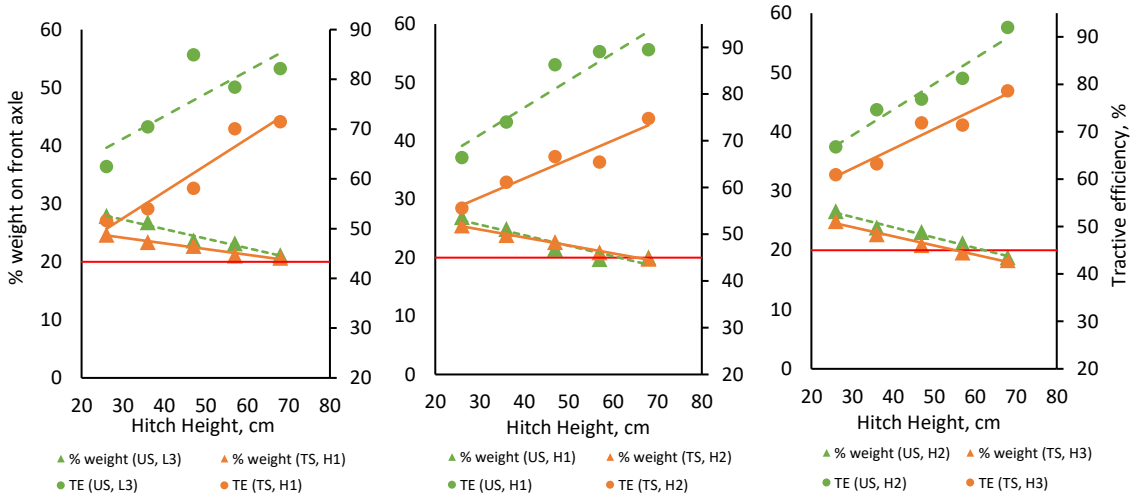

(b) 2500 kg payload

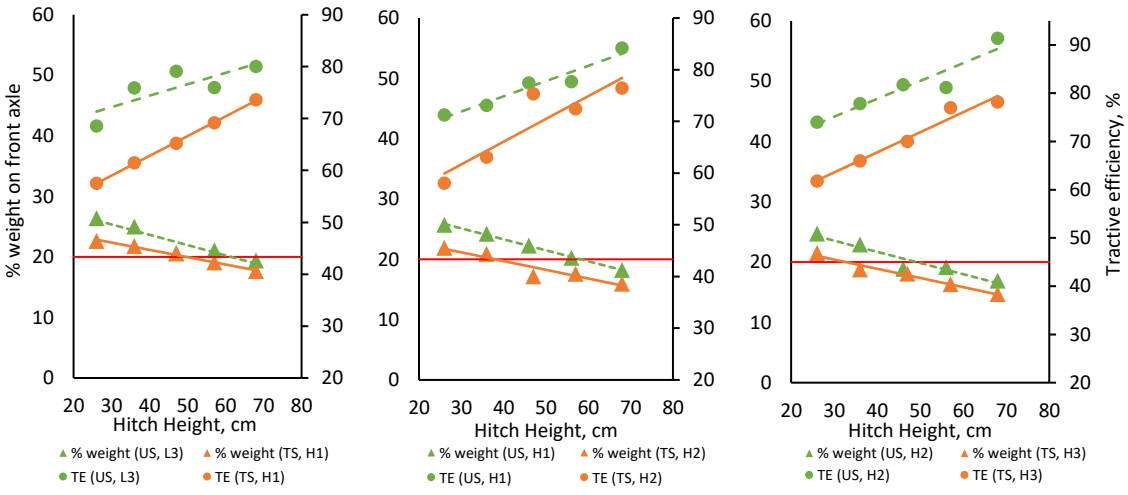

(c) 3000 kg payload

Figure 5.5 Hitch height vs percent front axle load vs tractive efficiency on gradient 2

(L3), 25.72 to 18.25% (H1), and 24.72 to 16.92% (H2) on the unpaved surface, and, 22.62 to 17.64% (H1), 21.9 to 15.98% (H2), and 21.46 to 14.66% (H3) on tarmacadam surface. In all gear settings, a hitch height of 68 cm was found to be unsuitable as the front axle load was found to be below the recommended 20% weight for both the test surface. Also, while operating in H2 gear on the unpaved surface, the front axle load fell below 20% as we increased the hitch height beyond 36 cm. A similar observation was revealed while increasing the hitch height above 47, 36 and 26 cm in gear H1, H2 and H3, respectively, on the tarmacadam surface. The corresponding values of tractive efficiencies gained from 68.51 to 80.02%, 71.25 to 84.19% and 73.96 to 91.35% on the unpaved surface and 57.51 to 73.63%, 58.05 to 76.43% and 61.79 to 78.17% and tarmacadam surface, respectively.

5.1.2.3 On surface gradient 3

Identically, the per cent front axle load and tractive efficiency of the test tractor operating on gradient 3 revealed similar behaviour on lifting the hitch height from 26 to 68 cm above the ground. The relationships between per cent front axle load and tractive efficiency at various hitch heights are shown in Figure 5.6 for 2000, 2500, and 3000 kg payloads. On increasing 24.39 to 17.26%, and 23.89 to 16.21% with 2500 kg payload [Figure 5.6 (b)], and 24.56 to 17.53%, 24.39 to 6.48%, and 22.95 to 14.21% with 3000 kg payload [Figure 5.6 (c)], while operating in gear L3, H1 and H2, respectively, on the unpaved surface. Similarly, the axle load decreased from 26.38 to 21.4%, 26.16 to 19.8%, 26 to 18.14% with 2000 kg payload, 26.71 to 20.46%, 25.88 to 18.86%, 24.67 to 17.04% with 2500 kg payload, and 25.61 to 19.63%, 23.95 to 17.04%, and 23.62 to 16.26% with a payload of 3000 kg, while operating in gears H1, H2, and H3, respectively, on tarmacadam surface. Thus, it was observed that operating the trailer with the given payloads on gradient 3 at higher hitch heights was causing an alarming situation on the longitudinal stability of the test tractor.

The corresponding gain in tractive efficiency was found to increase from 49.57 to 74.25% (L3), 52.09 to 71.28% (H1), and 53.74 to 73.58% (H2) on unpaved surface, and 54.81 to 74.38% (H1), 56.3 to 74.04% (H2), and 58.27 to 72.36% (H3) with payload of 2000 kg. Similarly, the tractive efficiency improved from 47.14 to 75.16% (L3), 48.05 to 79.03% (H1), and 52.94 to 83.62% (H2) on unpaved surface, and 46.95 to 62.43% (H1), 48.46 to 69.1% (H2), and 50.49 to 69.02% (H3) on tarmacadam surface with 2500 kg of payload. And 46.42 to 66.74% (L3), 49.48 to 63.27% (H1), and 51.49 to 72.2% (H2) on unpaved surface, and 47.88 to 62.83% (H1), 48.51 to 61.34% (H2), and 51.47 to 64.91% (H3) on

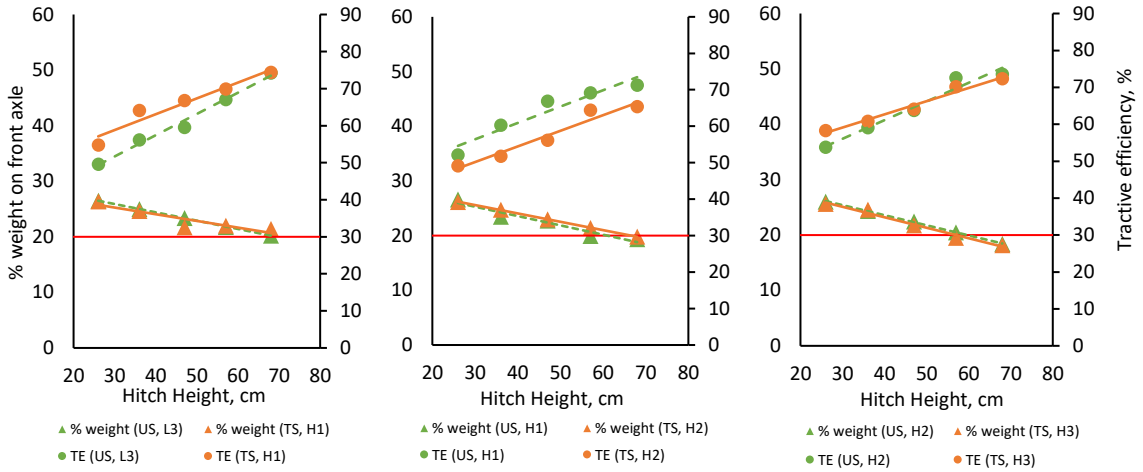

(a) 2000 kg payload

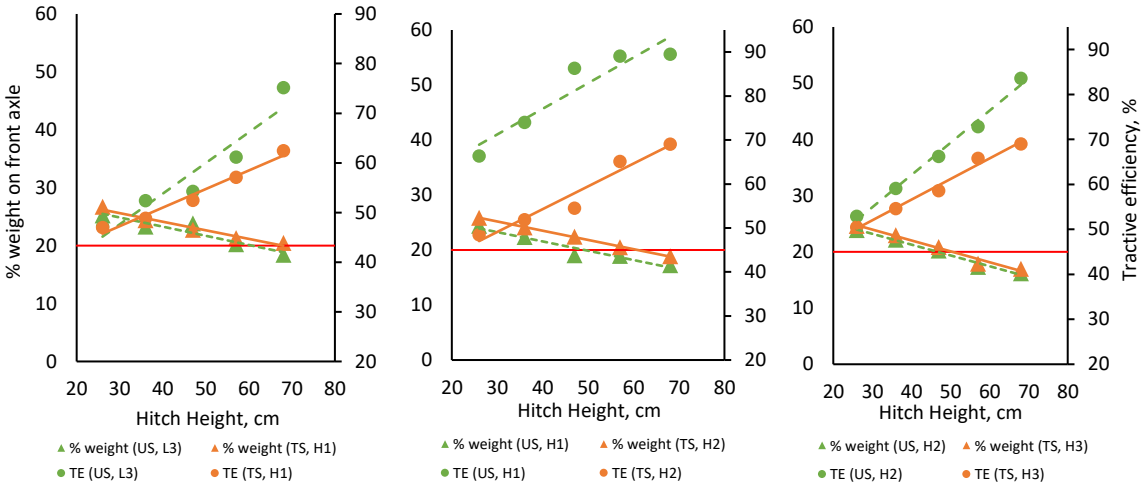

(b) 2500 kg payload

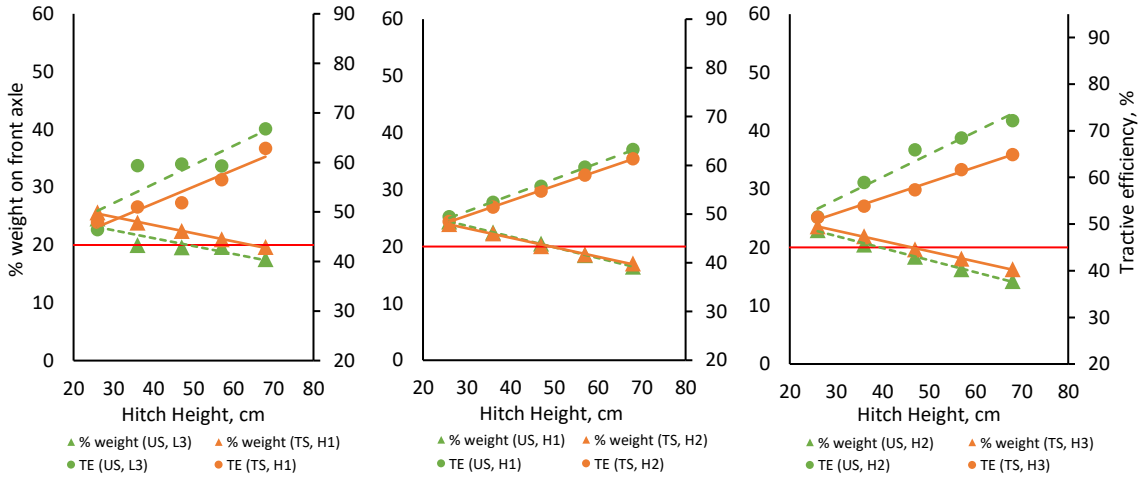

(c) 3000 kg payload

Figure 5.6 Hitch height vs percent front axle load vs tractive efficiency on gradient 3

tarmacadam surface with a 3000 kg payload. The one-way ANOVA test indicated that the hitch height has significant effects on both per cent front axle load and tractive efficiency with *p*-values of 0.000 (significant) and 0.005 (significant), respectively, as shown in Appendix VI.

Thus, we can infer that sufficient load on the front axle permits longitudinal stability of 2WD tractor operation. Increasing the hitch height resulted in the reduction of front axle load which due to excess weight transfer caused by the additional moment generated about the drive (rear) wheel due to higher hitching. This reduction in front axle load triggers a concern for longitudinal instability in tractor. Conversely, more weight transfer from the front to the rear axle led to the increase in the rear axle weight. This additional weight on the rear axle enables the drive wheels to generate more traction and encourages tractive efficiency. The tractive efficeincy was calculated from the developed computer program with the inputs obtained from the field experimental values. Thus, though increasing the height may tend to compromise the longitudinal stability, it encourages tractive efficiency of such 2WD tractors. This phenomenon was evident in all conditions of operation.

5.1.3 Effect of hitch height on wheel slip and tractive efficiency

Effect of hitch height on wheel slip and tractive efficiency at different load conditions on three surface grades are shown through Figures 5.7 to 5.9.

5.1.3.1 On surface gradient 1

The relationships between slip and tractive efficiency against hitch height of the trailer drawbar with a 2000, 2500 and 3000 kg payloads at gradient 1 are shown in Figure 5.7. The wheel slip had inverse relation with the hitch height, while the tractive efficiency increased with the increase in the hitch height.

While trailing a 2000 kg payload, the wheel slip decreased from 15.42 to 7.21% (L3), 16.77 to 8% (H1), and 16.94 to 7.93% (H2) on the unpaved surface and 9.52 to 6.94% (H1), 11.49 to 6.13% (H2), and 12.29 to 7.32% (H3) on tarmacadam surface while increasing the hitch height from 26 to 68 cm, respectively, as shown in Figure 5.7 (a). The tractive efficiency increased on increasing the hitch height as discussed above in Chapter 5.1.2.1.

As shown in Figure 5.7 (b), it was observed that the wheel slip on the unpaved surface decreased from 16.67 to 7.46% (L3), 17.37 to 9.09% (H1) and 17.65 to 9.87% (H2), and 12.12 to 8.79% (H1), 13.81 to 8.66% (H2), and 13.01 to 9.41% (H3) on tarmacadam surface on elevating the hitch point from 26 to 68 cm above the ground, respectively when

operating with a 2500 kg payload. While, the tractive efficeicy increased on increasing the hitch height as discussed above in Chapter 5.1.2.2.

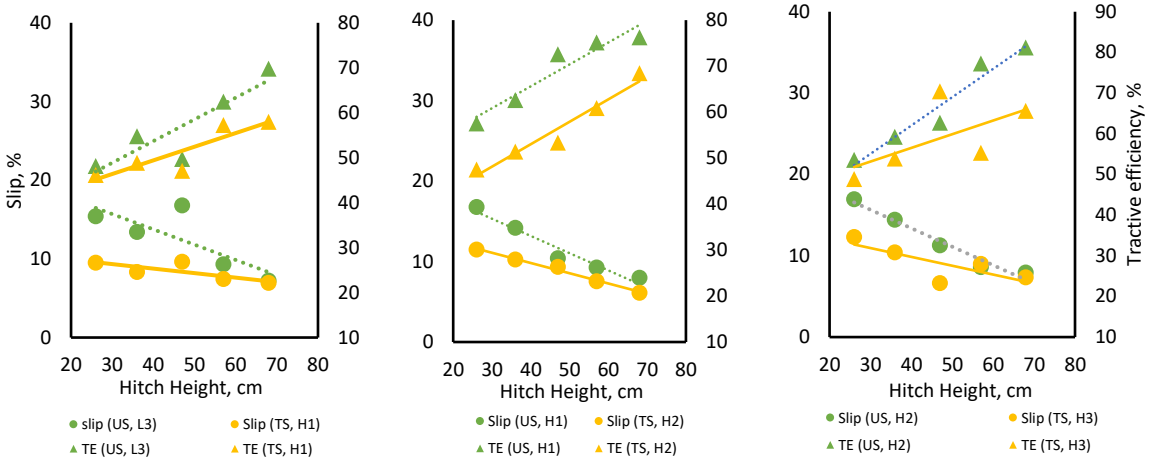

(a) 2000 kg payload

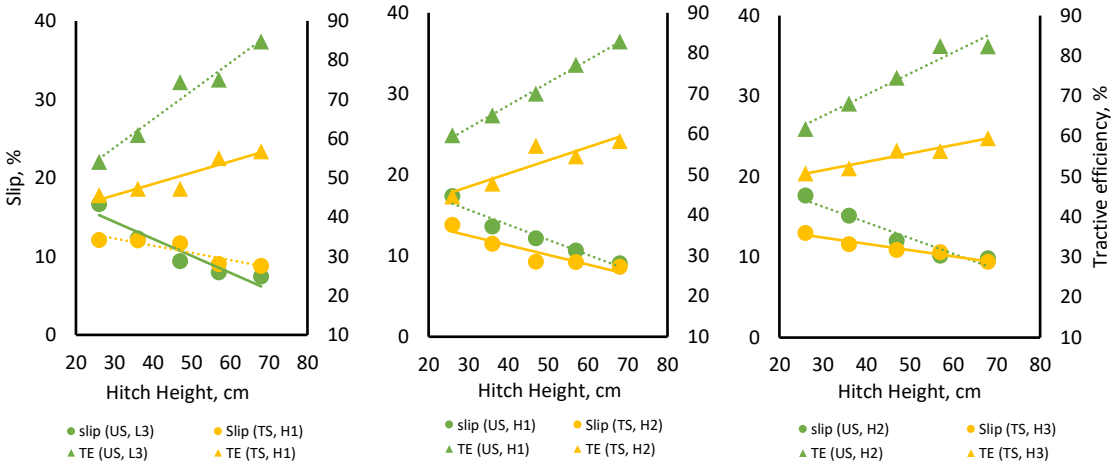

(b) 2500 kg payload

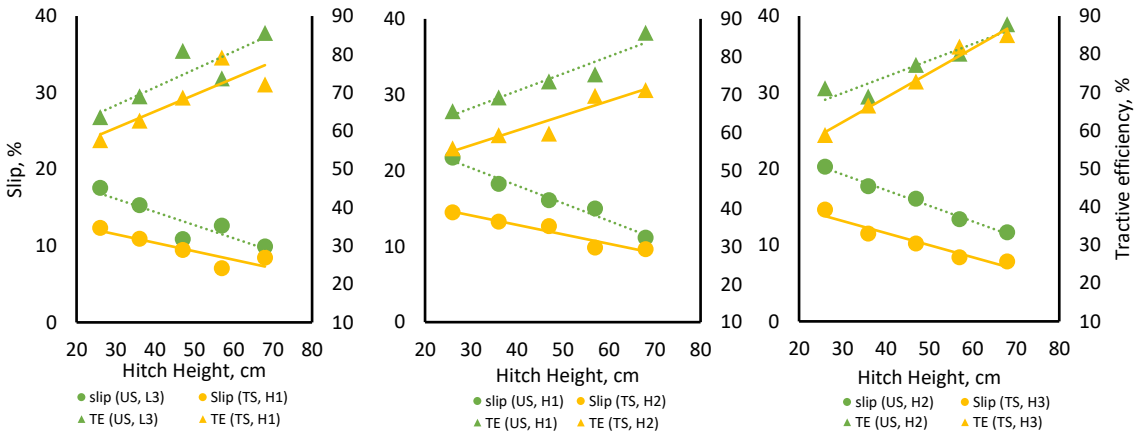

(c) 3000 kg payload

Figure 5.7 Hitch height vs slip vs tractive efficiency on surface gradient 1

Similarly, when towing a 3000 kg payload, as shown in Figure 5.7 (c), the wheel slip decreased from 17.55 to 9.92% (L3), 21.7 to 11.14% (H1) and 20.27 to 11.65% (H2) on the unpaved surface, and 12.34 to 8.42% (H1), 14.5 to 9.64% (H2) and 14.61 to 7.83% (H3) on tarmacadam surface when raising the hitch height from 26 to 68 cm, respectively. While at the same time, the tractive efficiency increased on increasing the hitch height on both the surface types.

5.1.3.2 On surface gradient 2

The relationships between slip and tractive efficiency against hitch height of the trailer drawbar with a 2000, 2500 and 3000 kg payloads at gradient 2 are shown in Figure 5.8. The experiment yielded similar results for both surface types as slip and tractive efficiency indicated an inverse relationship in the same way, as in the case of gradient 1. The tractive efficiency showed a positive correlation with the hitch height at all settings and payloads as discussed in Chapter 5.1.2.2.

As shown in Figure 5.8 (a), the wheel slip decreased from 17.19 to 8.53% (L3), 18.18 to 9.34 (H1) and 21.85 to 9.77 (H2) on the unpaved surface, and 10.53 to 8.29% (H1), 14.17 to 8.66% (H2), and 15.66 to 8.99% (H3) on the tarmacadam surface while raising the hitch point from 26 to 68 cm, respectively while trailing a 2000 kg payload.

While towing a 2500 kg payload, the wheel slip improved from 20.71 to 10.94% (L3), 21.39 to 10.67% (H1), 21.68 to 11.18% (H2) when operating on the unpaved surface, and 14.92 to 8.99 % (H1), 13.91 to 9.02% (H2), 14.99 to 9.24% (H3) on the tarmacadam surface while increasing the hitch height from 26 to 68 cm, respectively as shown in Figure 5.8 (b).

Similarly, when pulling a 3000 kg payload, the wheel slip decreased from 17.83 to 12.7% (L3), 19.41 to 12.94% (H1), and 19.67 to 12.9% (H2) on the unpaved surface, and 15.25 to 9.2% (H1), 16.15 to 9.69% (H2), and 16.58 to 10% (H3) on tarmacadam surface when elevating the hitch height from 26 to 68 cm, respectively on both surfaces as shown in Figure 5.8 (c).

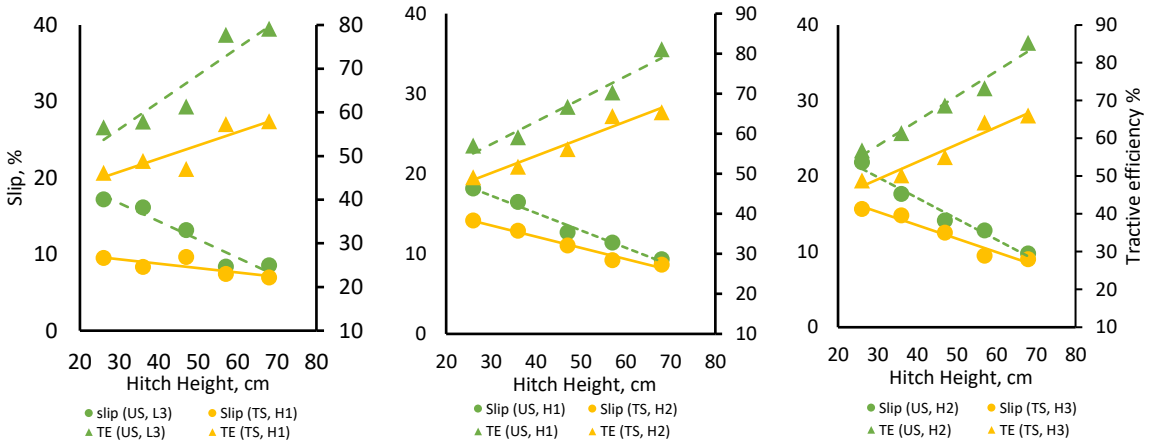

(a) 2000 kg payload

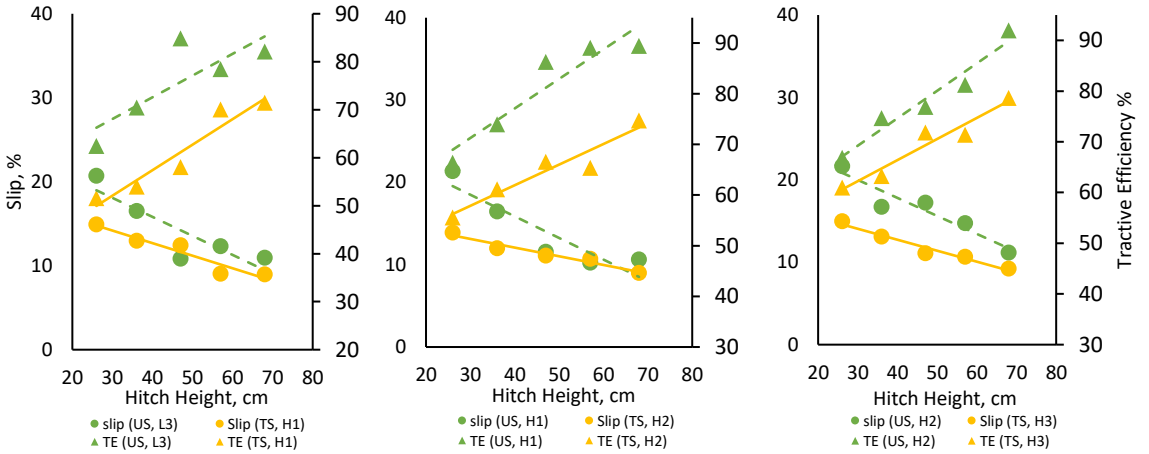

(b) 2500 kg payload

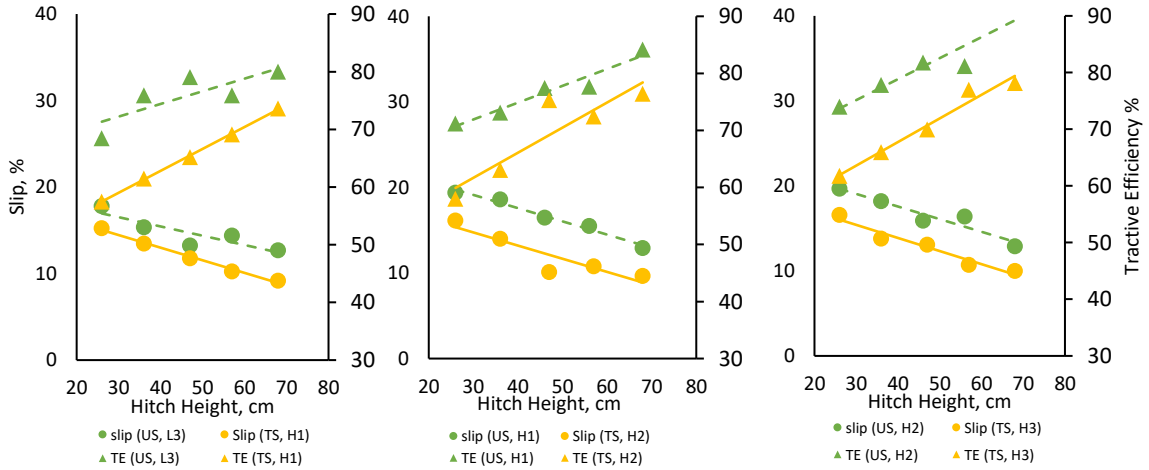

(c) 3000 kg payload

Figure 5.8 Hitch height vs slip vs tractive efficiency on surface gradient 2

5.1.3.3 On surface gradient 3

Likewise, the wheel slip and tractive efficiency of the test tractor operating on gradient 3 revealed similar behaviour on lifting the hitch height from 26 to 68 cm above the ground. The relationships between slip and tractive efficiency at various hitch heights are shown in Figure 5.9.

While operating with a payload of 2000 kg [Figure 5.9 (a)], the wheel slip decreased from 18.52 to 9.63% (L3), 19.44 to 11.43% (H1), and 21.48 to 13.13% (H2) on unpaved surface and 13.55 to 8.64% (H1), 15.98 to 9.96% (H2), and 17.42 to 11.42% (H3) on tarmacadam surface on increasing the hitch height. Likewise, it reduced from 20.61 to 10.37% (L3), 23.16 to 11.05% (H1), and 22.38 to 11.22% (H2) on unpaved surface, and 15.82 to 10.27% (H1), 16.67 to 9.96% (H2), and 17.76 to 10.93% (H3) on tarmacadam surface with 2500 kg payload each [Figure 5.9 (b)] and 25 to 14.39% (L3), 27.71 to 17.04% (H1), and 27.2 to 15.79% (H2) on unpaved surface, and 17.51 to 11.35% (H1), 19.69 to 13.57% (H2) and 21.04 to 13.96% (H3) on tarmacadam surface when operating with 3000 kg payloads [Figure 5.9 (c)].

The corresponding gain in tractive efficiency due to the increase in hitch height is discussed in Chapter 5.1.2.3. The one-way ANOVA test showed that the hitch height has significant effect on wheel slip with *p*-value at 0.001 (significant), as shown in Appendix VI.

Increasing the hitch height had a positive effect on the wheel slip and tractive efficiency of the tractor. Increasing the hitch height resulted in more weight transfer to the rear axle from the front axle. Due to this increase in rear axle weight, the wheel slip decreased and the tractive efficiency increased. The experiment revealed that slip and tractive efficiency had an inverse relationship with each other. This phenomenon was evident in all conditions of operation. While the wheel slip decreased with the increase in hitch height, tractive efficiency increased with the increased hitch height.

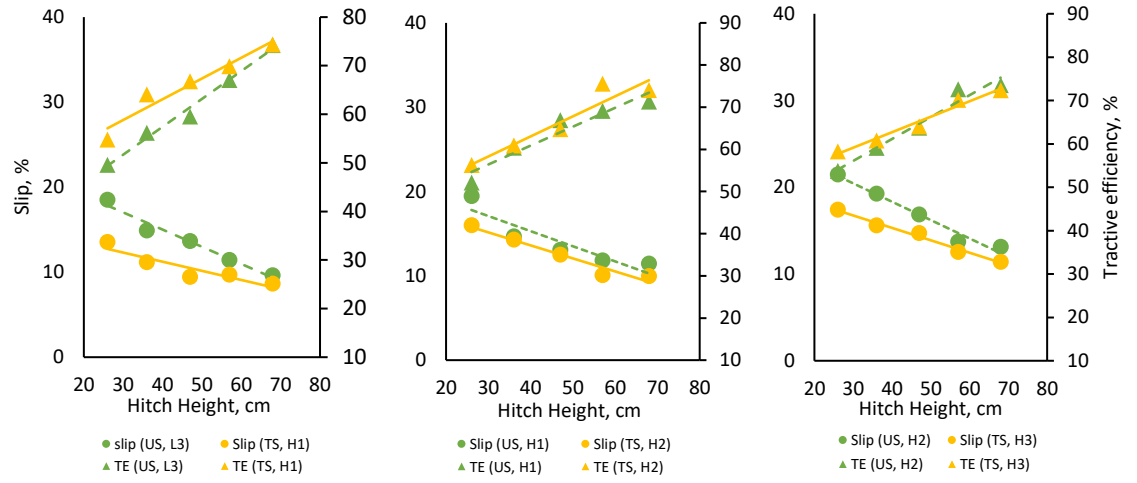

(a) 2000 kg payload

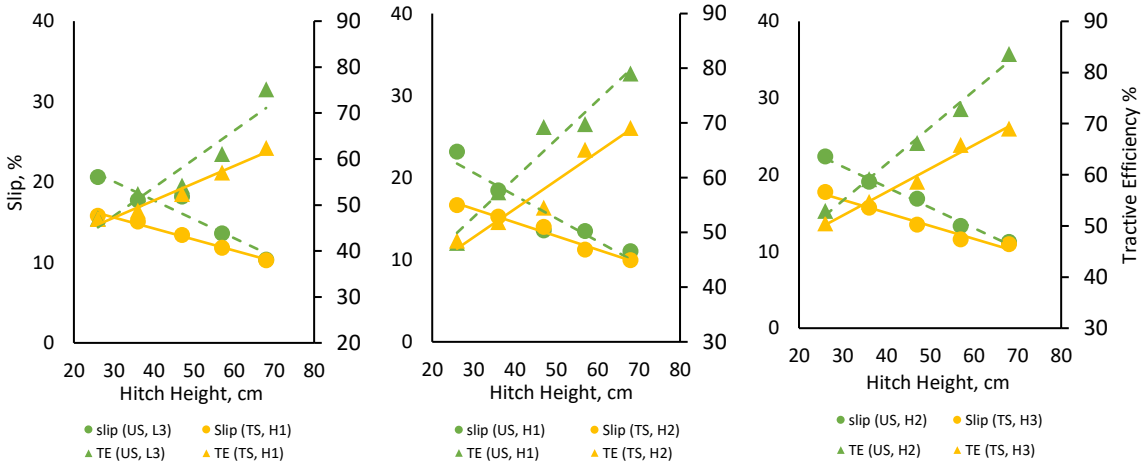

(b) 2500 kg payload

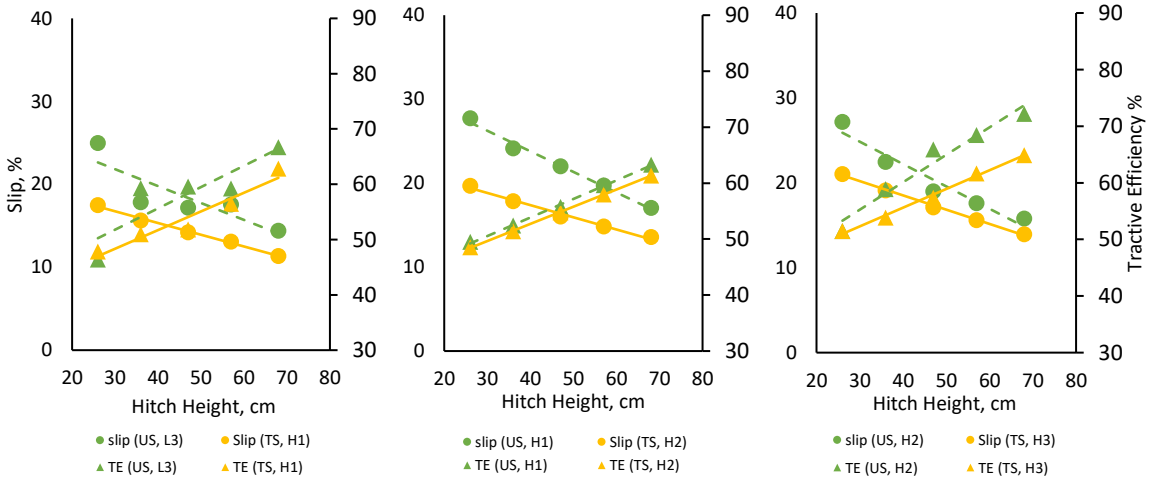

(c) 3000 kg payload

Figure 5.9 Hitch height vs slip vs tractive efficiency on surface gradient 3

5.2 Evaluation of the Developed Automation System

The instrumented test tractor was operated on unpaved and tarmacadam surfaces. The experiment was carried out to evaluate the position of auto variable hitch height under dynamic conditions on varying surface gradients and payloads (as discussed in the research plan under Chapter 4.5). The effect of different payloads and surface gradients on the hitch height was thoroughly investigated.

5.2.1 Effect of payload on the hitch height

The test tractor with the trailer was operated with different payloads to detect the real time front axle load and accordingly optimise the position of the drawbar hitch height. The test was carried out on both road surface types, in gears H1 and H2, at three surface gradients with payloads of 2000, 2500, and 3000 kg as represented through Figures 5.10 to 5.12.

5.2.1.1 On surface gradient 1

The effect of different payloads on the hitch height while operating on surface gradient 1 in gears H1 and H2 are shown in Figure 5.10. The hitch height tends to decrease as the payload increased from 2000 to 3000 kg in all test conditions while also attempting to maintain the front axle load within the design range of 20 to 25% of the total static tractor weight.

While operating with a 2000 kg payload on unpaved surface in gear H1, the hitch height was recorded to be at the highest position (i.e., 68 cm above the ground) and the corresponding front axle load being recorded at 27.93% as shown in Figure 5.10 (a). The hitch height reduced to 51 and 41 cm when towing a 2500 and 3000 kg payload, respectively, with the corresponding front axle load being 24.45 and 24.34%. Likewise, while operating with similar payloads on tarmacadam surface, the hitch height was recorded at 68, 53 and 42 cm above the ground surface, respectively, with the corresponding front axle load being 25.66, 24.83 and 25.66%.

The effect of three different payloads on the hitch height while operating on surface gradient 1 in gear H2 is shown in Figure 5.10 (b). While pulling a 2000 kg payload on an unpaved surface, the hitch height was recorded at 68 cm above the ground i.e., the highest design position with the corresponding value of front axle being 22.18%. When the payload was increased to 2500 kg, the front axle load measured 20.07% (> 20%) and thus the hitch was also retained at the same maximum height. Finally, when the payload was increased to 3000 kg, the front axle load dipped below 20% and thus the hitch was auto guided to a

lower height. The drawbar was recorded to be 62 cm height and the corresponding front axle load was found to be 19.47%. While operating on a tarmacadam surface, the hitch was recorded at 68 cm height at all payloads as the front axle load never decreased below 20%. The percentage front axle load was found to be 22.29, 21.07 and 20.43% at 2000, 2500, and 3000 kg payloads, respectively.

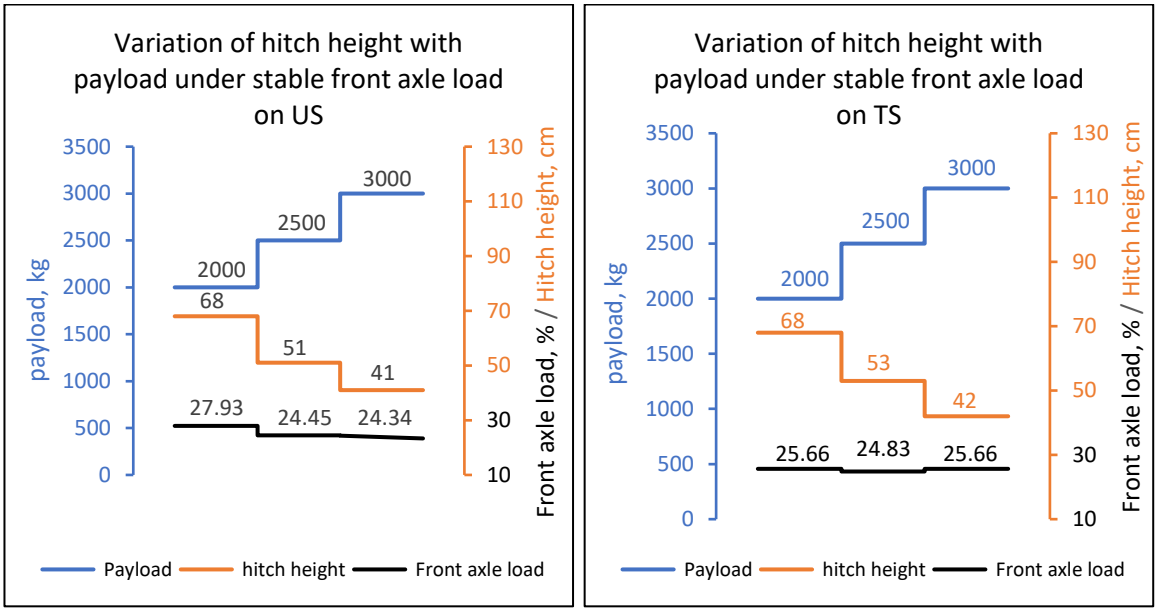

(a) Operating in gear H1

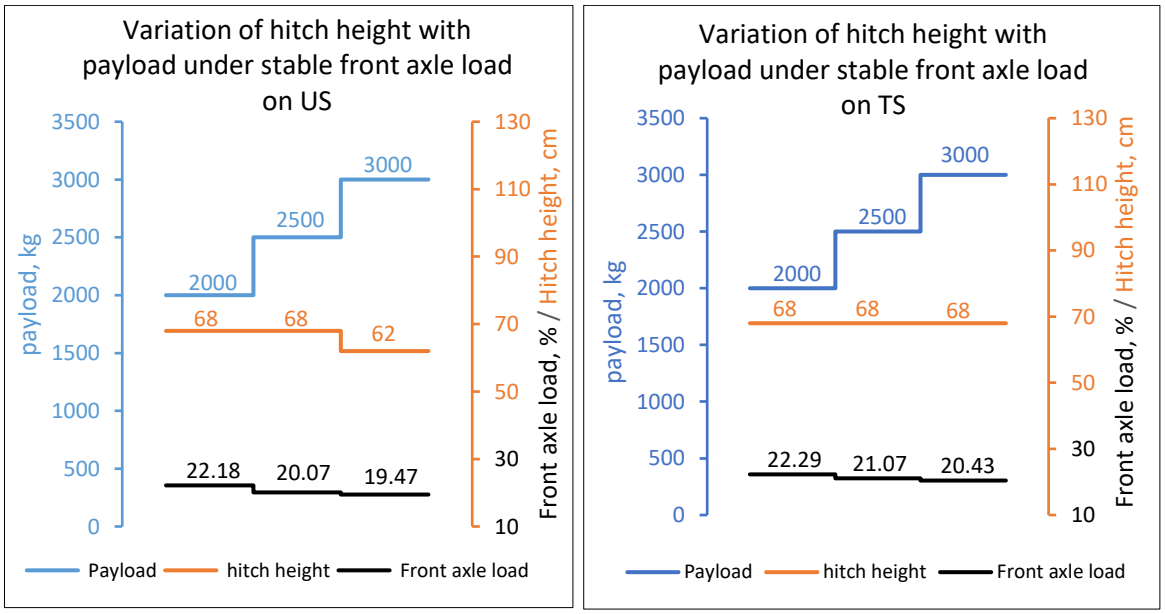

(b) Operating in gear H2

Figure 5.10 Payload vs hitch height on gradient 1

5.2.1.2 On surface gradient 2

The effect of different payloads on the hitch height while operating on surface gradient 2 in gears H1 and H2 are shown in Figure 5.11.

While towing a 2000, 2500 and 3000 kg payload in gear H1 on unpaved surface, the hitch was recorded at 49, 35 and 38 cm height and the corresponding front axle load was found to be 25.73, 24.17 and 24.86%, respectively, as shown in Figure 5.11 (a).

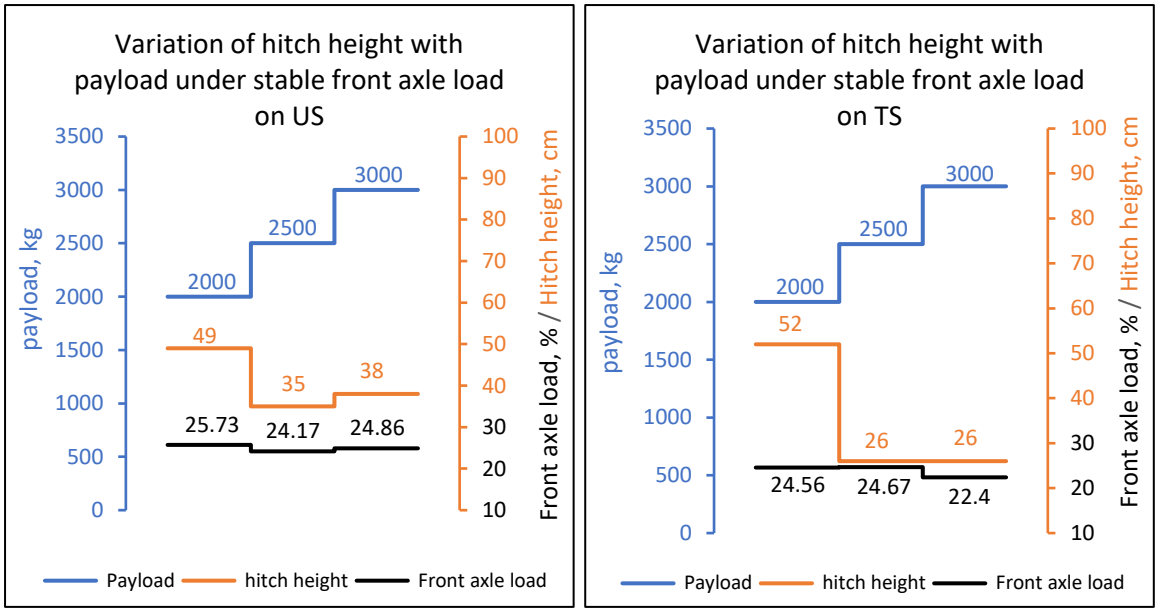

(a) Operating in gear H1

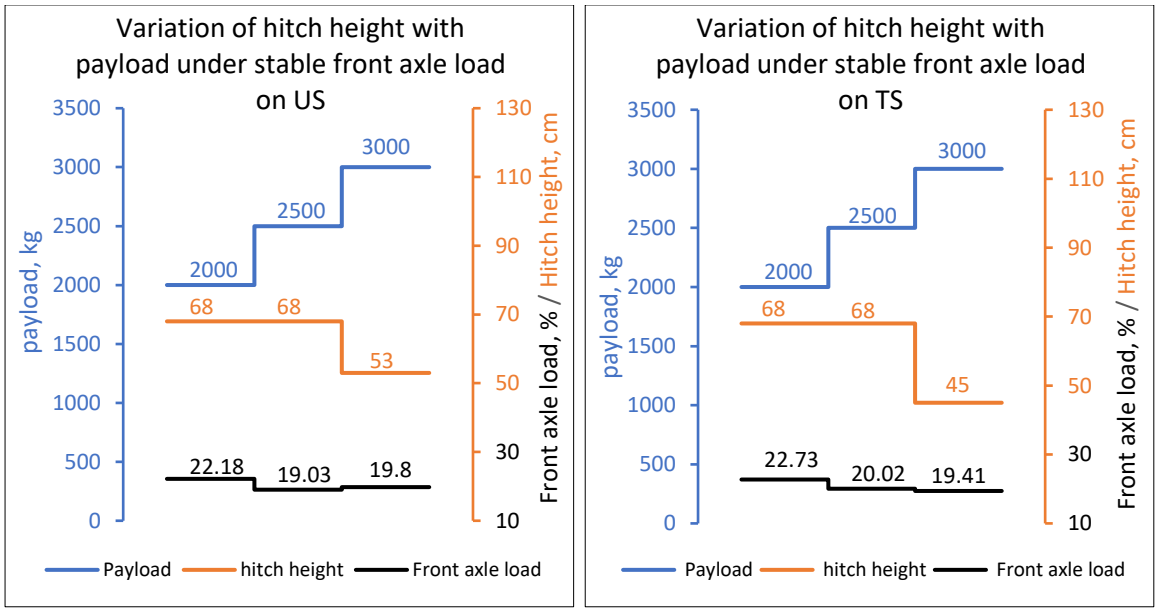

(b) Operating in gear H2

Figure 5.11 Payload vs hitch height on gradient 2

Similarly, while operating with the same payloads on tarmacadam surface, the hitch height was recorded at 52, 26 and 26 cm above the ground surface with the corresponding front axle loads being 24.56, 24.67 and 22.4%, respectively.

The effect of payload on hitch height while operating in gear H2 on surface gradient 2 is shown in Figure 5.11 (b). The drawbar hitch was recorded at 68 cm height while pulling payloads of 2000 and 2500 kg on the unpaved surface with the respective front axle loads being recorded at 22.18 and 19.03%. As the payload increased to 3000 kg, the hitch height was auto optimised to 53 cm such that the front axle load measured 19.8%. Similarly, while operating on the tarmacadam surface, the hitch was recorded at 68 cm height while towing 2000 and 2500 kg payloads with the corresponding load on the front axle being 22.73 and 20.02%, respectively. However, while towing a 3000 kg payload, the hitch height automatically dropped to 45 cm height and the front axle load measured 19.41%.

5.2.1.3 On surface gradient 3

The effect of different payloads on the hitch height while operating on surface gradient 3 in gears H1 and H2 are shown in Figure 5.12.

While pulling payloads of 2000, 2500 and 3000 kg on unpaved surface in gear H1, the hitch was recorded at 41, 26 and 26 cm heights with the corresponding load on the front axle found to be 24.12, 23.84 and 24.51%, respectively, as represented by Figure 5.12 (a). When these payloads were operated on tarmacadam surface, the hitch height was recorded at 31, 26 and 26 cm, respectively, with the corresponding values of front axle load being 25.5, 25.17 and 24.56%.

The effect of payload on the hitch height while operating in gear H2 on surface gradient 3 is shown in Figure 5.12 (b). The drawbar hitch height dropped from 58 to 46 cm, and further to 34 cm when the payload was increased from 2000 to 3000 kg with an increment of 500 kg while operating on unpaved surface. The corresponding front axle load was recorded as 20.46, 19.19 and 19.41%, respectively. Also, the hitch height dropped from 68 to 63 cm, and 63 to 55 cm as the load increased from 2000 to 2500 kg and 2500 to 3000 kg on the tarmacadam surface. The corresponding front axle load was recorded as 19.69, 19.63 and 19.58%, respectively.

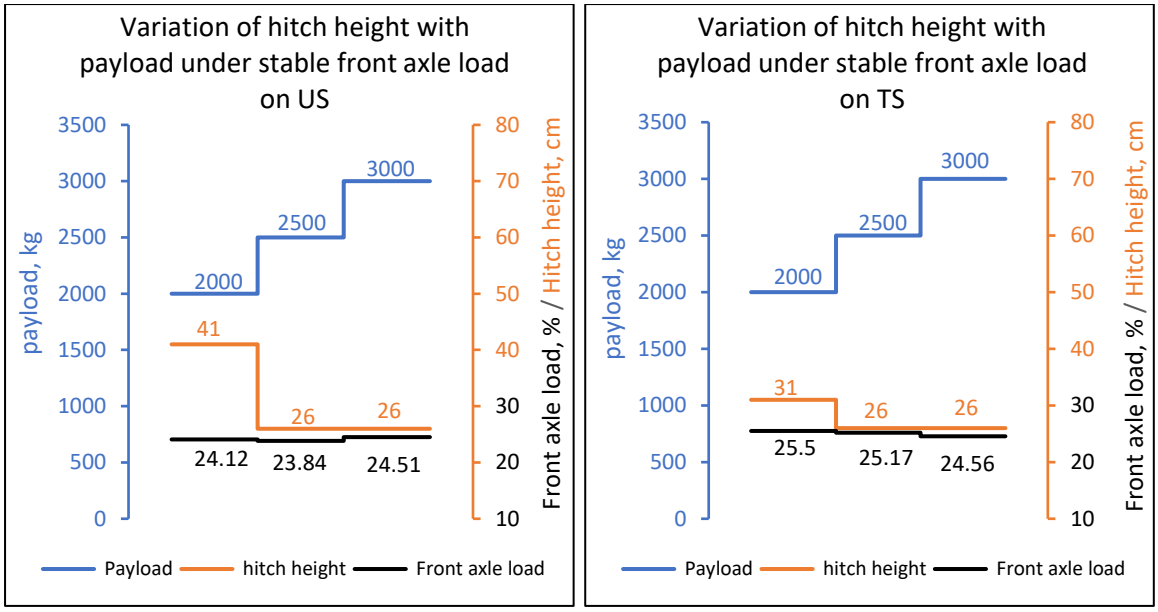

(a) Operating in gear H1

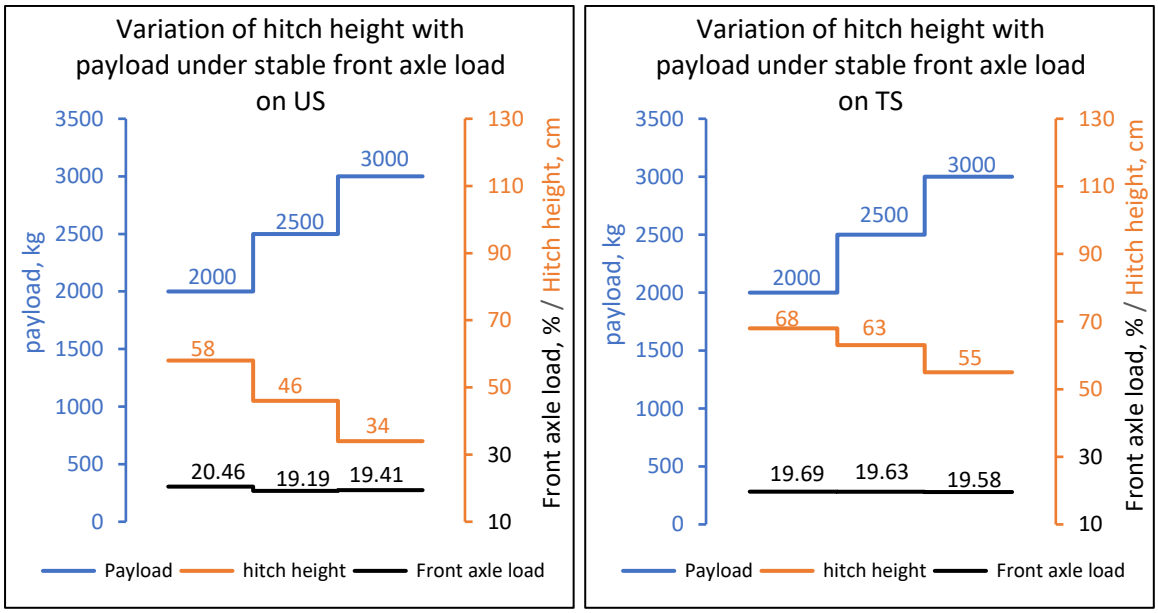

(b) Operating in gear H2

Figure 5.12 Payload vs hitch height on gradient 3

It can be concluded from the trials that, whenever the load on the front axle was more than 25% of the static tractor weight, the hitch height automatically optimised itself, in order to lower the front axle load to a maximum value of 25% tractor weight within the limit of the hitch range. On the other hand, if the front axle load was detected below 20%, the hitch adjusted itself to achieve at least the minimum recommended 20% tractor weight.

5.2.2 Effect of surface gradient on the hitch height

The instrumented test tractor along with the trailer was operated with different payloads on varying surface gradients to analyse the effect of surface gradient on the drawbar hitch height as shown through Figures 5.13 to 5.15.

5.2.2.1 With 2000 kg payload

The effect of surface gradient on the hitch height while trailing a 2000 kg payload in gears H1 and H2 is shown in Figure 5.13.

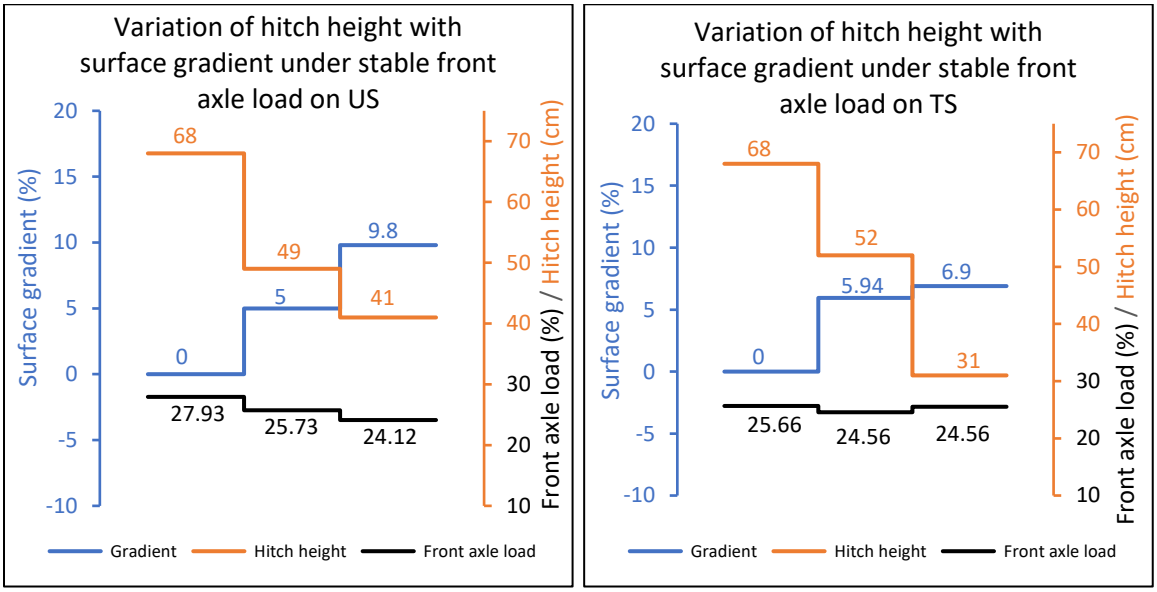

(a) Operating in gear H1

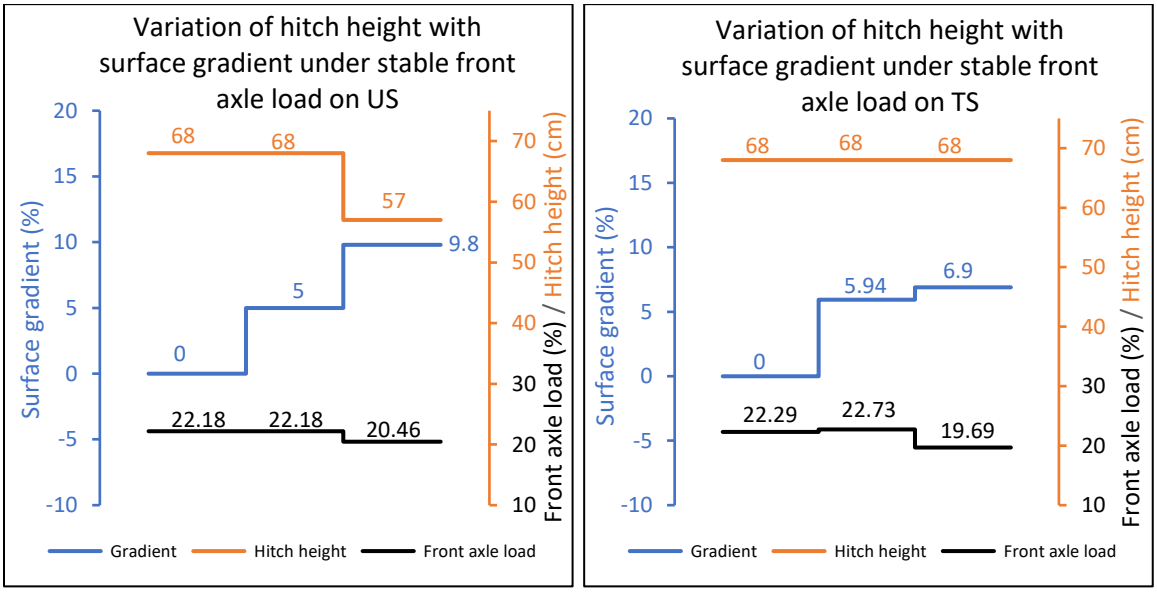

(b) Operating in gear H2

Figure 5.13 Surface gradients vs hitch height with 2000 kg payload

While operating on unpaved surface in gear H1, as shown in Figure 5.13 (a), the hitch height was measured at 68, 49 and 41 cm when towing on gradient 1, 2 and 3, respectively. Whereas the corresponding values of front axle load were recorded at 27.93, 25.73 and 24.12%. When operating on tarmacadam surface, the hitch was recorded at 68, 52 and 31 cm height while travelling on gradient 1, 2 and 3 respectively, with the corresponding values of front axle load being recorded as 25.66, 24.56 and 25.5%.

The effect of surface gradient on the hitch height while pulling a 2000 kg payload in gear H2 is shown in Figure 5.13 (b). The hitch height was recorded at 68 cm while operating on all unpaved surface gradients 1 and 2 as the front axle load was recorded at 22.18 and 22.18, respectively. However, the hitch height dropped to 57 cm when pulling the load on gradient 3 to optimise front axle load at 20.46%. Similarly, the hitch height was recorded at 68 cm when operating on tarmacadam surface on all three gradients as the front axle load measured 22.29, 22.73 and 19.69%, respectively.

5.2.2.2 With 2500 kg payload

The effect of surface gradient on the hitch height while pulling a 2500 kg payload in gears H1 and H2 is shown in Figure 5.14.

While operating on unpaved surface in gear H1, the hitch height was recorded at 51, 35 and 26 cm when towing on gradient 1, 2 and 3, respectively, with the corresponding values of front axle load recorded at 24.45, 24.17 and 23.84% as shown in Figure 5.14 (a). Similarly, while operating on tarmacadam surface, the hitch was recorded at 53, 26 and 26 cm height when travelling on gradient 1, 2 and 3 respectively, with the corresponding values of front axle load being recorded as 24.83, 24.67 and 25.17%.

The effect of surface gradient on the hitch height while towing a 2500 kg payload in gear H2 is shown in Figure 5.14 (b). The hitch height was recorded at 68 cm when operating on unpaved surface gradients 1 and 2 as the front axle load measured 20.07 and 19.03%, respectively. The hitch height reduced to 47 cm when operating on gradient 3 to optimise the front axle load to 19.19%. Similarly, the hitch height of the drawbar was recorded at 68 cm when operating on tarmacadam surface gradients 1 and 2 as the front axle load measured 21.07 and 20.02%, respectively. However, the hitch was automatically reduced to 63 cm height when operating on gradient 3 to optimise the front axle load to 19.63%.

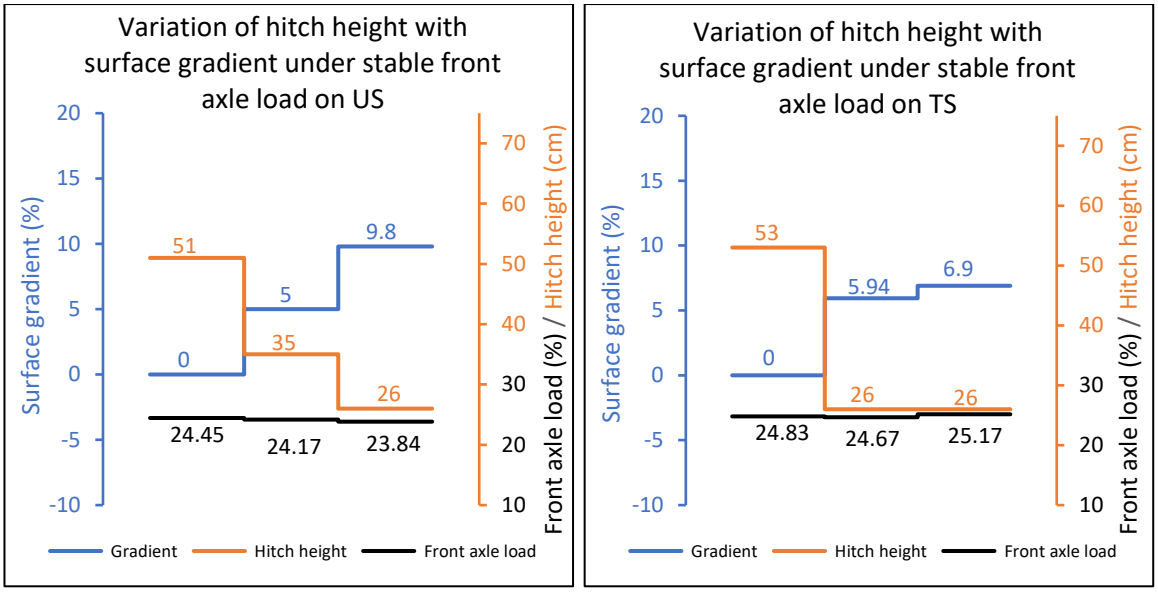

(a) Operating in gear H1

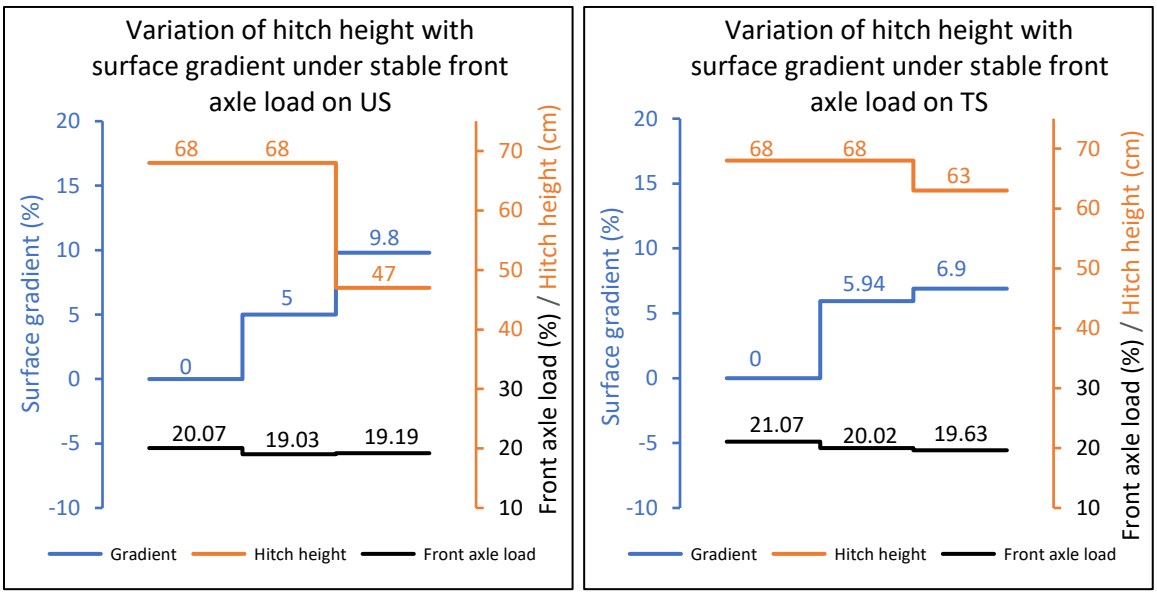

(b) Operating in gear H2

Figure 5.14 Surface gradients vs hitch height with 2500 kg payload

5.2.2.3 With 3000 kg payload

The effect of surface gradient on the hitch height while towing a 3000 kg payload in gears H1 and H2 is shown in Figure 5.15.

While operating on unpaved surface in gear H1, the hitch height was recorded at 41, 38 and 26 cm when pulling on gradient 1, 2 and 3, respectively, with the corresponding values of front axle load recorded at 24.34, 24.86 and 24.51%, as shown in Figure 5.15 (a). Similarly, while operating on tarmacadam surface, the hitch was recorded at 42, 26 and 26 cm height

when travelling on gradient 1, 2 and 3 respectively, with the corresponding values of front axle load being recorded as 25.66, 22.4 and 24.56%.

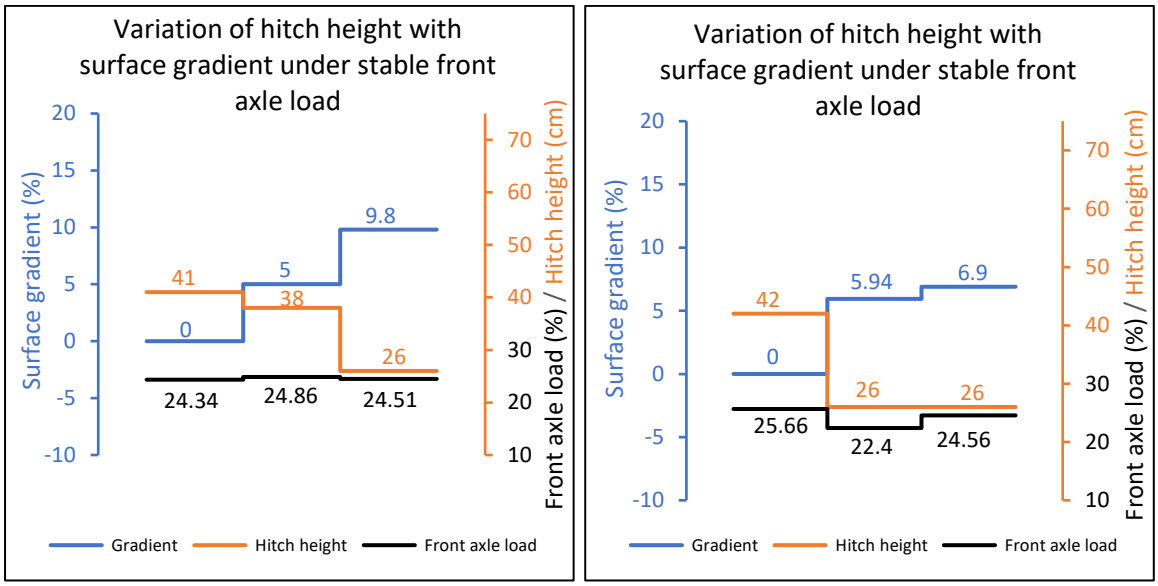

(a) Operating in gear H1

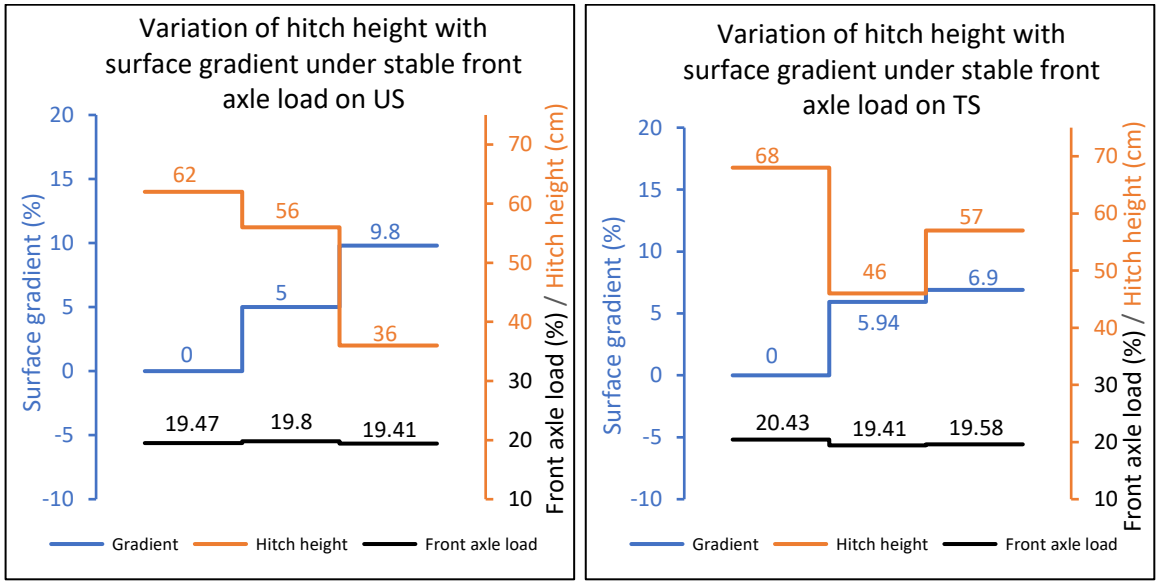

(b) Operating in gear H2

Figure 5.15 Surface gradients vs hitch height with 3000 kg payload

The effect of surface gradient on the hitch height while trailing a 3000 kg payload in gear H2 is shown in Figure 5.15 (b). The hitch was recorded at 62, 56 and 36 cm height when operating on unpaved surface gradient 1, 2 and 3 to optimise the front axle load at 19.47, 19.8 and 19.41%, respectively. The hitch height never achieved the highest position as the corresponding front axle load fell below 20%. However, the hitch height was maintained

at 68 cm when operating on tarmacadam surface gradient 1 as the front axle load recorded 20.43%. The drawbar hitch dropped to 46 and 57 cm height when operating on gradients 2 and 3, respectively to optimise the front axle load to 19.41 and 19.58%, respectively.

Thus, on all the surface gradients, provided that the front axle load is greater than 25% tractor weight, the hitch optimised its height to obtain a corresponding maximum front axle load of 25%. On the other hand, when the surface grade steepens and the front axle reduced below 20%, the hitch optimised itself to a lower height in an attempt to increase the front axle load to at least 20% of the static tractor weight. It may be noted that the optimization of hitch height is limited by its designed hitch range i.e., between 26 to 68 cm above a level ground surface. Therefore, varying the hitch height to maintain the tractor's front axle weight between 20 to 25% of the total tractor weight is possible within the hitch bracket's design range.

References

Abbaspour-Gilandeh, Y., and Rashidi-Mohammadabad, F. (2013). Evaluation of Dynamic Load Equations Through Continuous Measurement of Some Tractor Tractive Performance Parameters. *International Journal of Heavy Vehicle Systems* (Vol. 20, Issue 3).

Abu-Hamdeh, N. H., and Al-Jalil, H. F. (2004). Computer Simulation of Stability and Control of Tractor-Trailed Implement Combinations Under Different Operating Conditions. *Simulação Computacional Da Estabilidade E Controle De Combinações Trator-Carreta Sob Difer*. *63*(1), 149–162.

Antunes, S. M., Cordeiro, C., and Teixeira, H. M. (2018). Analysis of Fatal Accidents with Tractors in the Centre of Portugal: Ten Years Analysis. *Forensic Science International*. https://doi.org/10.1016/j.forsciint.2018.03.048

Ashok Kumar, A., Tewari, V. K., Nare, B., Chetan, C. R., Srivastava, P., and Prakash Kumar, S. (2017). Embedded Digital Drive Wheel Torque Indicator for Agricultural 2WD Tractors. *Computers and Electronics in Agriculture*, *139*, 91–102. https://doi.org/10.1016/j.compag.2017.05.007

Battiato, A., and Diserens, E. (2013). Influence of Tyre Inflation Pressure and Wheel Load on the Traction Performance of a 65 kW MFWD Tractor on a Cohesive Soil. *Journal of Agricultural Science*, *5*(8), 197–215. https://doi.org/10.5539/jas.v5n8p197

Bhattarai, M., Singh, G., Takeshima, H., and Shekhawat, R. S. (2020). Farm Machinery Use and the Agricultural Machinery Industries in India: Status, Evolution, Implications. https://doi.org/10.2499/9780896293809_03

Bhondave, B., Ganesan, T., Varma, N., Renu, R., and Sabarinath, N. (2017). Design and Development of Electro Hydraulics Hitch Control for Agricultural Tractor. *SAE International Journal of Commercial Vehicles*, *10*(1), 405–410. https://doi.org/10.4271/2017-26-0227

Bietresato, M., Friso, D., and Sartori, L. (2012). Assessment of the Efficiency of Tractor Transmissions Using Acceleration Tests. *Biosystems Engineering*, *112*(3), 171–180. https://doi.org/10.1016/j.biosystemseng.2012.03.009

Bietresato, M., and Mazzetto, F. (2019). Definition of the Layout for a New Facility to Test the Static and Dynamic Stability of Agricultural Vehicles Operating on Sloping Grounds. *Applied Sciences (Switzerland)*, *9*(19). https://doi.org/10.3390/app9194135

Boye, T. E., Olabisi, A. I. and Emagbetere, E. E. (2017). Design and Finite Element Analysis of Double-Acting, Double Ends Hydraulic Cylinder for Industrial Automation System. *American journal of engineering research*, *6*(3): 131-138.

Bulgakov, V., Adamchuk, V., Arak, M., Nadykto, V., Kyurchev, V. and Olt, J. (2016).

Theory of Vertical Oscillations and Dynamic Stability of Combined Tractor-Implement Unit. *Agronomy Research, 14* (3), 689-710.

C. I. Nichol, H. J. Sommer III, and D. J. Murphy. (2005). Simplified Overturn Stability Monitoring of Agricultural Tractors. *Journal of Agricultural Safety and Health*, *11*(1), 99–108. https://doi.org/10.13031/2013.17900

Catalán, H., Linares, P., and Méndez, V. (2008). Tractor_PT: A Traction Prediction Software for Agricultural Tractors. *Computers and Electronics in Agriculture*, *60*(2), 289–295. https://doi.org/10.1016/J.COMPAG.2007.07.009

Demsar et al. (2012). A Mathematical Model and Numerical Simulation of the Static Stability of a Tractor. *Agriculturae Conspectus Scientificus, 77* (3) 143-150. https://hrcak.srce.hr/89912

Farm Safety Association (1999). A Guide to Safe Farm Tractor Operation. *National Ag Safety Database.* https://nasdonline.org/static_content/documents/1650/d001534.pdf

Fedorenko, V. F., and Tarkivskij, V. E. (2019). Digital Filtration Method for Determining Traction Power of Agricultural Tractors. *Machinery and Equipment for Rural Area*, (1) 8-12.

Gilfillan, G. (1970). Tractor Behaviour during Motion Uphill I. Factors Affecting Behaviour. *Journal of Agriculture Engineering Research, 15*(3) 221-235. https://doi.org/10.1016/0021-8634(70)90118-6

Gonzalez, O. D., Martin-Gorriz, B., Berrocal, I. I., Hernandez, B. M., Garcia, C. F., and Sanchez, P. M. (2016). Development of an Automatically Deployable Roll Over Protective Structure for Agricultural Tractors Based on Hydraulic Power: Prototype and First Tests. *Computers and Electronics in Agriculture*, *124*, 46–54. https://doi.org/10.1016/j.compag.2016.03.027

Habarta, F. (1971). Determination in Relation to Safety of Operation of the Minimal Load on the Front Steering Axle of a Tractor with Implements Attached. *Journal of Agricultural Engineering Research*, *16*(2), 126–140. https://doi.org/10.1016/S0021-8634(71)80027-6

Hard, D. L., Myers, J. R., Snyder, K. A., Casini, V. J., Morton, L. L., Cianfrocco, R., and Fields, J. (1999). Identifying Work-related Fatalities in the Agricultural Production Sector Using Two National Occupational Fatality Surveillance Systems, 1990-1995. *Journal of Agricultural Safety and Health*, *5*(2), 155-. https://doi.org/10.13031/2013.5676

Havasi et al. (2009). Design, Fabrication and Evaluating on the Instrument for Digital Measurement of Tractor Wheel Slip. *The Scientific Journal of Agriculture (SJA)*, *31*(2), 177–185. https://www.sid.ir/en/Journal/ ViewPaper.aspx?ID=181447

Indian Standard, Agricuctural Tractor Trailer - Specification. *Bureau of Indian Standards* December (2000). (Third Revision).

Janulevičius, A., and Damanauskas, V. (2022). Prediction of Tractor Drive Tire Slippage Under Different Inflation Pressures. *Journal of Terramechanics*, *101*, 23–31. https://doi.org/10.1016/J.JTERRA.2022.03.001

Kheti Gaadi. (2018). Evolution of Tractors in India and Its Current Scenario. https://khetigaadi.com/blog/evolution-of-tractors/

Kim, W. S., Kim, Y. J., Baek, S. Y., Baek, S. M., Kim, Y. S., and Park, S. U. (2020). Development of a Prediction Model for Tractor Axle Torque During Tillage Operation. *Applied Sciences 2020, Vol. 10, Page 4195*, *10*(12), 4195. https://doi.org/10.3390/APP10124195

Kumar, V. M. (1994). Drawbar Performance of a Tractor for Haulage Operation. *Unpublished Thesis of Agricultural and Food Engineering Department, IIT Kharagpur.*

Kumar, A. A., Pandey, K. P., and Kumar, R. (2013). Longitudinal Stability Indication for 2WD Tractors Working in Different Field Operations. *International Journal of Advance Agricultural Research*, *1*(1), 1–6. http://www.bluepenjournals.org/ijaar/abstract/ 2013/March/Kumar et al.html

Kumar, A., Mohan, D., and Mahajan, P. (1998). Studies on Tractor Related Injuries in Northern India. *Accident Analysis and Prevention*, *30*(1), 53–60. https://doi.org/10.1016/S0001-4575(97)00061-4

Kumar, A., and Pandey, K. P. (2012). A Device to Measure Dynamic Front Wheel Reaction to Safeguard Rearward Overturning of Agricultural Tractors. *Computers and Electronics in Agriculture*, *87*, 152–158. https://doi.org/10.1016/j.compag.2012.06.003

Kumar, A. A., Pandey, K. P., and Srinivasarao, A. (2012). Design of Digital Weight Transfer Display for Agricultural Tractors. *African Journal of Agricultural Reseearch*, *7*(36), 5160-5169. https://doi.org/10.5897/ajar12.951

Kumar, N., Kumar, S., Kumar, R., and Pandey, K. P. (2020b). Dynamic Behaviour of High-Powered Agricultural Tractor for Haulage Operation. *Pantnagar Journal of Research 69*, *18*(1), 69–75.

Kumar, R. and Pandey, K. P. (2009). A program in Visual Basic for Predicting Haulage and Field Performance of 2WD Tractors. *Computer and Electronics in Agriculture, 67*: 18-26.

Kumar, N. and Pandey, K. P. (2015). A Visual Basic Program for Predicting Optimum Gear and Throttle Position for Best Fuel Economy for 32 kW Tractor. *Computers and*

Electronics in Agriculture, *119*, 217–227. https://doi.org/10.1016/j.compag.2015.10.024

Kumar, R. and Raheman, H. (2015). Design and Development of a Variable Hitching System for Improving Stability of Tractor Trailer Combination. *Engineering in Agriculture, Environment and Food*, *8*(3), 187–194. https://doi.org/10.1016/j.eaef.2014.12.003

Kumar, S., Pranav, P. K., and Pal, A. (2020a). Effect of Hitch Distance on Haulage Performance for 2WD Tractors: A Theoretical Analysis. *Spanish Journal of Agricultural Research*, *18*(2), 1–10. https://doi.org/10.5424/sjar/2020182-15296

Lankenau, D. G. F., and Winter, A. G. (2018). An Engineering Review of the Farm Tractor's Evolution to a Dominant Design. *Proceedings of the ASME 2018 International Design Engineering*. https://doi.org/10.1115/detc2018-86285

Lee, J. W., Kim, J. S., and Kim, K. U. (2016). Computer Simulations to Maximise Fuel Efficiency and Work Performance of Agricultural Tractors in Rotovating and Ploughing Operations. *Biosystems Engineering*, *142*, 1–11. https://doi.org/10.1016/j.biosystemseng.2015.11.012

Liu, J. Y., Tan, J. Q., Mao, E. R., Song, Z. H., and Zhu, Z. X. (2016). Proportional Directional Valve Based Automatic Steering System for Tractors. *Frontiers of Information Technology and Electronic Engineering*, *17*(5), 458–464. https://doi.org/10.1631/FITEE.1500172

Malik, A., and Kohli, S. (2020). Materials Today : Proceedings Electric tractors : Survey of Challenges and Opportunities in India. *Materials Today: Proceedings*, *28*(4), 2318-2324. https://doi.org/10.1016/j.matpr.2020.04.585

Mondal, P., and Rao, P. N. (2005). Digital Throttle Gear Optimizer for Better Fuel Economy of Tractors. *SAE Technical Papers*, *2005*(January). https://doi.org/10.4271/2005-26-066

Murphy, D. J. Beppler, D. C., and Sommer, H. J. (1985). Tractor Stability Indicator. *Applied Ergonomics, 16*(3): 187-191.

Murphy, D. (2014). Tractor Stability and Instability. *Agricultural Safety and Health*. PennState Extension. https://extension.psu.edu/tractor-stability-and-instability

Myers, J. R., and Hendricks, K. J. (2010). Agricultural Tractor Overturn Deaths: Assessment of Trends and Risk Factors. *American Journal of Industrial Medicine, 53:* 662-672.

Naderi, M., Alimardani, R., Abbaszadeh, R., and Ahmadi, H. (2008). Assessment of Dynamic Load Equations Through Drive Wheel Slip Measurement. *Journal of Agriculture and Environment Science, 3*(5), 778–784.

Nichol, C. I., Sommer, H. J., Murphy, D. J. (2005). Simplified Overturn Stability Monitoring of Agricultural Trcators. *Journal of Agricultural Safety and Health, 11*(1): 99-108.

Nguyen, V. N., and Inaba, S. (2011). Effects of Tire Inflation Pressure and Tractor Velocity on Dynamic Wheel Load and Rear Axle Vibrations. *Journal of Terramechanics*, *48*(1), 3–16. https://doi.org/10.1016/j.jterra.2010.09.001

Okoko, P., Ajay, E. A., and Olosunde, W. A. (2018). Draft and Power Requirements for some Tillage Implements Operating in a Clay Loam Soil. *Agricultural Engineering International: CIGR Journal, 20*(1): 95-102.

Park, W.-Y., and Lee, S.-S. (2012). Development of a Tractive Performance Prediction Program of Tractors. *Journal of Biosystems Engineering*, *37*(3), 131–139. https://doi.org/10.5307/jbe.2012.37.3.131

Patel, T., Chakravorty, A., and Karmakar, S. (2012). Software for Performance Prediction and Matching of Tractor-Implement System. *Proceedings - 2012 3rd National Conference on Emerging Trends and Applications in Computer Science, NCETACS-2012*, 262–269. https://doi.org/10.1109/NCETACS.2012.6203271

Patil, M. R. (2015). Measurement of Weight Transfer in Two-Wheel Drive Tractor by Developed Ring Transducer. *International Journal of Agricultural Engineering*, *8*(2)*:* 181-189.

Peeters, M., Kloster, V., Fedde, T., and Frerichs, L. (2018). Integrated Wheel Load Measurement for Tractors. *Landtechnik*, *73*(4), 116–128. https://doi.org/10.15150/lt.2018.3188

Petrovic, D. V., Cerovic, V. B., Radojevic, R. L., and Mileusnic, Z. I. (2021). An Approach to Characterization of the Agricultural Self-Propelled Machines Stability. In *Journals of Terramechanics, 93* (February), 51-63. https://doi.org/10.1016/j.jterra.2020.11.001

Pinches, M. J. and Ashby, J. G. (1988). Power Hydraulics. *Prentice Hall International Hemel Hemstead, UK.*

Pranav, P. K., and Pandey, K. P. (2008). Computer Simulation of Ballast Management for Agricultural Tractors. *Journal of Terramechanics, 45:* 185-192.

Pranav, P. K., Pandey, K. P., and Tewari, V. K. (2010). Digital Wheel Slipmeter for Agricultural 2WD Tractors. *Computers and Electronics in Agriculture*, *73*(2), 188–193. https://doi.org/10.1016/j.compag.2010.05.003

Pranav, P. K., Tapang, T., Pal, A., and Deb, S. K. (2015). Importance of Automatic Variable Single Hitch Point for 2WD Tractors - A Theoretical Analysis. *Engineering in Agriculture, Environment and Food*, *8*(4), 298–306. https://doi.org/10.1016/j.eaef.2015.03.005

Pranav, P. K., Tewari, V. K., Pandey, K. P., and Jha, K. R. (2012). Automatic Wheel Slip Control System in Field Operations for 2WD Tractors. *Computers and Electronics in Agriculture*, *84*, 1–6. https://doi.org/10.1016/j.compag.2012.02.002

Raheman, H., and Jha, S. K. (2007). Wheel Slip Measurement in 2WD Tractor. *Journal of Terramechanics*, *44*(1), 89–94. https://doi.org/10.1016/j.jterra.2006.03.001

Rondelli, V., Casazza, C., and Martelli, R. (2018). Tractor Rollover Fatalities, Analyzing Accident Scenario. *Journal of Safety Research*, *67*(December), 99–106. https://doi.org/10.1016/j.jsr.2018.09.015

Roşca, R., Cârlescu, P., and Ţenu, I. (2014). A Semi-Empirical Traction Prediction Model for an Agricultural Tyre, Based on the Super Ellipse Shape of the Contact Surface. *Soil and Tillage Research*, *141*, 10–18. https://doi.org/10.1016/j.still.2014.03.007

Sahay, C.S. and Tewari, V.K. (2004). Computer Simulation of Tractor Single-point Drawbar Performance. *Biosystems Engineering* *88*(4), 419–428. doi:10.1016/j.biosystemseng.2004.05.005

Sahu, R. K. (2001). Computer Simulation of Haulage Performance of Agricultural Tractors in Visual Basic. *Unpublished M. Tech Thesis, Agricultural and Food Engineering Department, IIT, Kharagpur.*

Sahu, R. K., and Pandey, K. P. (2005). Effect of Operating Parameters on Haulage Performance of 2WD Tractor-Trailer Systems. *Journal of Agricultural Engineering* *42*(2), 21-28.

Sahu, R., and Pandey, K. P. (2007). A Simulation Program for Predicting Haulage Performance of 2WD Tractor and Balanced Trailer System. *Ama, Agricultural Mechanization in Asia, Africa and Latin America, 38*(4), 31-36.

Sakno, O., Moysya, D. L., and Kolesnikova, T. (2018). Dyanamic Stability of a Model of a Tractor-Lorry-Trailer Combination. *Scientific Journal of Silesian University of Technology Series Transport*, *99*, 163–175. doi.org/10.20858/sjsutst.2018.99.15

Shafaei, S. M., Loghavi, M., and Kamgar, S. (2019). Feasibility of Implementation of Intelligent Simulation Configurations Based on Data Mining Methodologies for Prediction of Tractor Wheel Slip. *Information Processing in Agriculture*, *6*(2), 183–199. https://doi.org/10.1016/j.inpa.2018.10.004

Shafaei, S. M., Loghavi, M., and Kamgar, S. (2020). Ascertainment of Driving Lead of Tractor Front Wheels as Loaded by Draft Force. *Measurement: Journal of the International Measurement Confederation* (Vol. 165). Elsevier Ltd. https://doi.org/10.1016/j.measurement.2020.108134

Sharifzadeh, M., Farman, A., Senatore, Adolfo., Timpone, F. and Akbari, A. (2017). Delay-Dependent Criteria for Robust Dynamic Stability Control of Articulated Vehicles.

International Conference on Robotics in Alpe-Adria Danube Region, Advances in Service and Industrial Robotics, 424-432. DOI: 10.1007/978-3-319-61276-8_46

Singh, N., and Pandey, K. P. (2017). Design, Development and Laboratory Testing of a Front Mounted Three Point Linkages for Higher Power Tractors. *International Journal of Science, Environment and Technology*, *6*(3), 2087–2099. www.ijset.net

Spencer, H. B. (1978). Stability and Control of Two Wheel Drive Tractors and Machinery on Sloping Ground. *Journal of Agricultural Engineering Research, London, 23:* 169-188. https://doi.org/10.1016/0021-8634(78)90047-1

Springfeldt, B. (1996). Rollover of Tractors – International Experiences. *Safety science, 24*(2), 95-110. https://doi.org/10.1016/S0925-7535(96)00069-0

Szakács, T. (2010). Developing Stability Control Theories for Agricultural Transport Systems. *Acta Polytechnica Hungaria, 7*(2), 25-37.

Tarighi, J., Mohtasebi, S. S. and Alimardani, R. (2011). Static and Dynamic Analysis of Front Axle Housing of Tractor Using Finite Element Methods. *Australian Journal of Agricultural Engineering*, *2*(2), 45-49.

Van, N. N., Matuso, T., Koumoto, T. and Inaba, S. (2009). Transducers for Measuring Dynamic Axle Load of Farm Tractor. *Bull. Fac. Agr., Saga Univ. No*. 9*4*, 23–25.

Wu, X., Shen, W., Lou, P., Wu, B., Wang, L., and Tang, D. (2016). An Automated Guided Mechatronic Tractor for Path Tracking of Heavy-Duty Robotic Vehicles. *Mechatronics*, *35*, 23–31. https://doi.org/10.1016/J.MECHATRONICS.2015.10.011

Xie, L. (1984). Simulation of Trailer System Stability. *Iowa State University Capstones, Retrospective Theses and Dissertations. Paper 16351*. https://lib.dr.iastate.edu/rtd

Yin, X., and Lu, B. (2010). Development of Tractor Slippage Virtual Test System. *IFAC Proceedings Volumes (IFAC-PapersOnline)*, *3*(Part 1). https://doi.org/10.3182/20101206-3-jp-3009.00055

Yisa, M, Terao, H., Noguchi, N., and Kubota, M. (1995). Dynamics of Tractor – Implements Combinations on Slopes (Part II) – Computer Simulation of Directional Dynamics. *Journal of Faculty of Agriculture Hokkaido University*, *66*(2), 263-275. http://hdl.handle.net/2115/13139

Yisa, M, Terao, H., Noguchi, N., and Kubota, M. (1998). Stability Criteria for Tractor-Implement Operation on Slopes. *Journal of Terramechanics, 35,* 1-19. https://doi.org/10.1016/S0022-4898(98)00008-1

Zoz, F.M. (1972). Predicting Tractor Field Performance. *Transaction of the ASAE 15*(2), 249-255. doi: 10.13031/2013.37878.

Appendix - I

Technical specifications of John Deere 5038D

Sl. No.	Particulars	Specification
1.	Total weight, kg	1760
2.	Wheelbase, mm	1910
3.	Minimum ground clearance, mm	390
4.	Overall width, mm	1780
5.	Front wheel size, inch	6 x 16
6.	Rear wheel size, inch	13.6 x 28
7.	Static weight on front wheels, kg	639
8.	Static weight on rear wheels, kg	1156
9.	Engine power	38 hp
10.	Nominal working pressure of pump, kg/cm^2	150
11.	Maximum allowable pressure of pump, kg/cm^2	180
12.	Rated pump pressure, kg/cm^2	214
13.	Maximum operating speed, rpm	3000
14.	Minimum pump discharge rate @2000 rpm, lpm	21.4
15.	Hydraulic lift capacity	1400

Appendix – II

Technical specifications of the load cells

Sl. No.	Particulars	Specification
1.	Load cell	S-Type
2.	Capacity	10 kN
3.	Dimensions	100×75×24 mm
4.	Rated output	2.0394 mV/V±5%
5.	Safe load limit	200% of rated output
6.	Recommended excitation Voltage	DC 5 to 12 V
7.	Input terminal resistance	Approx. 400Ω
8.	Output terminal resistance	350±3.5Ω
9.	Temperature range	-10° to 60°C
10.	Cable length and diameter	3 m and 6 mm

Appendix – III

Technical specifications of datalogger DT80

Sl. No.	Particulars	Specification
1.	Data logger	dataTaker DT80
2.	Analog channels	5 Input channels (Expandable to 100)
3.	Fundamental input ranges	Voltage, frequency, current resistance
4.	Sample speed	40Hz
5.	Sensor excitation	12V/5V
6.	Analog output	0-10V or 0-24mA
7.	Analog sensors	Thermocouples, RTDS, Thermistors, Strain Gauge and bridge sensors, Monolithic temp. sensor
8.	Digital Input/ Output	8 bi-directional channels
9.	Communication interfaces	Ethernet port, USB port, Host RS232 Port
10.	Display and keypad	LCD, 2 line by 16 character, backlight.
11.	Power supply	10-30Vdc
12.	Physical and Environment	Dimensions: 180×137×65 mm
		Weight: 1.5 kg
		Temperature range: -45 to 70^{o}C
		Humidity: 85%RH

Appendix – IV

Technical specifications of datalogger DT800

Sl. No.	Particulars	Specification
1.	Data logger	dataTaker DT800
2.	Analog channels	24 (2 wire), 12 (3 wire), 12 (4 wire), and 6 (6 wire)
3.	Fundamental input ranges	Voltage, current, resistance, temperature
4.	Sample speed	1kHz to 100kHz
5.	Sensor excitation	12V/5V
6.	Analog output	0-10V or 0-24mA
7.	Analog sensors	Thermocouples, RTDS, Thermistors, Bridge sensors, Monolithic temp. sensor
8.	Digital Output	8 shared with bi-directional channels
9.	Counter channels	16, size: 32 bit
10.	Communication interfaces	Ethernet, RS232
11.	Power supply	11 to 28 V dc (external)
12.	Real time clock	200 µs (normal resolution)
13.	Physical and Environment	Dimensions: 260×110×90 mm
		Weight: 3.1 kg
		Temperature range: -45 to 70^{o}C
		Humidity: 85%RH

Appendix – V

Technical specifications of ground speed senor

Sl. No.	Particulars	Specification
1.	Ground speed sensor	Radar-II
2.	Mounting face	Forward or backward from vehicle
3.	Velocity range	0.53-96.6 km/h
4.	Mounting angle	35±5°
5.	Mounting height range	610 mm to 2440 mm
6.	Sleek design	10×10×31.1 mm
7.	Weight	2.05 kg
8.	Velocity error (in field calibration)	±1-3%
9.	Temperature range	-40°C to +85°C

Appendix – VI

One-way ANOVA test of various haulage parameters at different hitch heights

Analysis of variance

Source	DF	Sum of squares	Mean squares	F	Pr > F
(a) Effect of hitch height on draft (surface gradient 3)					
Draft	4	141.733	35.433	0.035	0.997
Error	10	10258.000	1025.800		
Corrected Total	14	10399.733			
(b) Effect of hitch height on vertical load (surface gradient 3)					
Vertical load	4	22746.000	5686.500	6.876	0.006
Error	10	8270.000	827.000		
Corrected Total	14	31016.000			
(c) Effect of hitch height on per cent front axle load (surface gradient 3)					
Per cent front axle load	4	106.640	26.660	14.044	0.000
Error	10	18.983	1.898		
Corrected Total	14	125.623			
(d) Effect of hitch height on tractive efficiency (surface gradient 3)					
Tractive efficiency	4	558.298	139.574	7.312	0.005
Error	10	190.891	19.089		
Corrected Total	14	749.189			
(e) Effect of hitch height on wheel slip (surface gradient 3)					
Wheel slip	4	201.507	50.377	11.477	0.001
Error	10	43.894	4.389		
Corrected Total	14	245.400			

Chapter 6

Summary and Conclusions

This chapter presents the summary of the research work carried out in the present study. The present study deals with one of the most common causes of fatal farm accidents – tractor rollover, factors affecting such rollover and the engineering intervention to minimise or prevent such accidents. Tractor rollovers, more specifically, the longitudinal rollover is reported to be very prominent reason leading to fatalities of tractor operators and damage to the tractor that occurs due to sudden reduction in the front axle during operation such that the front end of the tractor lifts off the ground and the tractor tips backward. This problem is typical to 2WD tractors. Today, tractors are being widely used in India for various agricultural activities as well as rural transportation purposes. According to a study, 70 per cent of the use of tractors is related to haulage operations (Kumar, 1994). Owing to the poor road conditions, especially across rural parts of the country, transportation by tractor-trailer is very popular. However, the basic design of a tractor is for off-road tasks i.e., field operations rather than haulage work. This often leads to its poor performance during haulage and also causes many fatal and non-fatal accidents. Around 50 per cent of the annual overall fatalities in agricultural accidents are related to tractors (Hard et al., 1999). More importantly, approximately 70 per cent of these accidents are caused due to tractor rollovers which may be either sideways or rearward. According to National Safety Council (1968), rearward rollovers which occur when the dynamic front wheel reaction is reduced to zero, are more fatal than sideways rollovers. Rearward rollovers are caused due to weight transfer from the front axle to the rear due to the moment generated by the position of applied pull about the ground contact point of the rear wheel. The safety and tractive ability of wheeled tractors depend largely on the values of the normal to ground components of the wheel/ground reactions (Gilfillan, 1970). Tractor turnovers are the primary cause of fatal injuries on US farms and lead to about 130 deaths annually which is more than 50% of all tractor related deaths (NASD - National Agricultural Tractor Safety Initiative, 2004). This type of rollover is more prominent when pulling a loaded trailer in hilly areas with sloppy surfaces and occurs due to obstruction in the rear wheel(s). For safe tractor-implement operation, the dynamic weight on the front axle should not be less than 20 per cent of the weight of the tractor (Habarta, 1971).

Drawbar hitch plays an important role in tractor rollovers as its location directly relates to the weight transfer from the front. Modern day tractors are provided with variable hitch height points to suit the various operating conditions for the safe operation of such tractor-trailer systems. However, the frequency of rollover accidents could not be reduced by a considerable amount by adjusting the hitch height. This is because, in the present system, the hitch height cannot be varied in dynamic conditions. The inability of the operator to adjust the hitch height according to the demand of the field and operating conditions like uneven terrain, sudden and unseen obstructions in the driving wheels, sloppy surfaces, etc. restricts the profitable use of such a variable hitching system.

There are three limiting factors for maximum drawbar pull (i) longitudinal stability (ii) traction developed and (iii) power of the engine. Longitudinal stability and traction significantly depend upon hitch height during haulage operation. Lower hitch height increases the maximum payload capacity and greater slope traversing ability (Pranav et al., 2015). It is worth mentioning here that maximum payload is limited by the vehicle stability which implies, that varying the hitch height affects the stability of tractor-trailer operation. Kumar and Raheman, (2015) also found that the lowering of hitch height improved the front wheel utilization factor, thereby ensuring better longitudinal stability. Nevertheless, higher hitch height also has some favourable effects on the system. The dynamic load on the rear axle increases on raising the hitch height. Due to this, there is a reduction in wheel slip and improvement in tractive performance. Thus, the benefits of variable hitch height can be realised by adjusting the hitch height according to the given circumstances. To avail this advantage, tractor manufacturers have provided variable drawbar hitch height which can be selected by the user as per need. Practically, instability is caused due to higher road slopes and obstruction on rear wheels while operating, which however does not occur throughout the entire travel period. If the user selects lower hitch height to eliminate instability, which occurs only occasionally, it will result in a decrease in traction performance. Therefore, the user must select a lower hitch height only if the dynamic load on the front wheel is less than 20 per cent of total static weight, else, operate at a higher hitch point to ensure efficient traction. During operation, field conditions vary frequently, and varying the hitch height manually by an operator according to such variation is not possible. In absence of auto variable hitch height, most of the time, the tractor runs either by compromising stability or traction. Auto adjustable hitch point can solve the problem which will adjust the height according to the requirement of stability or traction.

Keeping these points in mind, a study had been planned to develop an auto variable hitch height adjustment system during haulage operation in a 2WD tractor with the following specific objectives:

i) To develop an instrumentation system to measure the front axle dynamic load of 2WD tractors.
ii) To design and develop a variable single-point hydraulic hitch bracket.
iii) To develop a microcontroller-based system for automatic hitch height variation based on the front axle dynamic load.
iv) To evaluate the developed variable hitch system under various operating conditions.

6.1 Measurement of the Dynamic Front Axle Load

A two-wheel drive tractor was used as the test tractor in the present study. An S-type load cell having a capacity of 5 kN was mounted (under initial tension) horizontally below the front axle of the tractor to estimate the dynamic front axle load using suitable clamps. The load cell takes the readings based on the stress (compressive or tensile) it experiences. Initially, during the static condition, when the tyres are resting on the ground surface, the load cell experiences tension. As soon as the tractor comes into the dynamic condition, the load on the front axle changes and the corresponding change in stress on the axle is recorded by the load cell. The mounted load cell was then calibrated by observing the weight of the front axle using a platform weighing balance against the readings obtained in the load cell. Thus, a relationship was achieved between these readings using regression analysis. The readings obtained from the load cell were further validated in laboratory conditions. The load cell mounted test tractor was placed on a platform balance and given a horizontal pull by another tractor from the rear end under static conditions. The amount of pull applied was recorded using a spring dynamometer. Due to this pull, some load transfer is expected from the front axle towards the rear. The consequent change in the front axle load is recorded from the load cell and compared with the readings obtained in the spring dynamometer to validate the developed setup.

6.2 Design and Development of a Variable Single Hitch Point

The design was conceptualized and fabricated to ensure a minimum change in the existing hitch system. It was mounted at the existing hitch location with the major difference being the presence of slots for facilitating the sliding movement of the hitch point rather than the current bolt-pin system. A double acting hydraulic cylinder powered by the inbuilt hydraulic system of the test tractor was mounted suitably to vary the hitch point. This

enabled the hitch height to be adjusted in the range of 26 to 68 cm above a level ground surface. The proposed design was analysed for stress and deformation using ANSYS and Solidworks software.

6.3 Microcontroller-based Auto Variable Hitch Height

An Arduino Uno microcontroller having 40 pins was used to compute and process the readings obtained from the front axle load cell. A microcontroller is a small computer on a single integrated circuit containing a processor core, memory, and programmable input/output peripherals. The signal obtained from the load cell was amplified and fed to the microcontroller as the input signal. The microcontroller evaluates the input signal such as the front axle dynamic load is either lower than 20% or more than 25% of total static weight of tractor or lies between the specified range and accordingly directs the directional control valve to lower, raise or unchanged hitch height, respectively.

6.4 Field Evaluation of the Developed System

The developed system was tested in two phases on unpaved and tarmacadam surfaces. In the first phase, the effect of variable hitch height on the haulage and tractor performance parameters was analysed under various field conditions. In the second phase, the automation system was evaluated by operating the tractor-trailer system with different payloads and surface gradients. The experiment was conducted at three different surface grades, payloads, and gear settings. The tractor engine speed was maintained at 1500 rpm throughout the study.

6.5 Prediction of Tractive Efficiency

A computer program was developed in Visual Basic 6.0 to calculate the tractive efficiency based on various input parameters such as draft, vertical force, actual and theoretical velocity, payload, dynamic weight on the front axle, static weight on the front axle, static weight on the rear axle, cone index, wheel size, aspect ratio of front and rear tyres. Brixius' (1987) traction equations were used to calculate the tractive efficiency of the test tractor.

6.6 Results and Discussion

6.6.1 Effect of hitch height on draft and vertical load

The effect of hitch height on the draft for a 2000 kg payload was minimal on surface gradient (G1) in gears L3, H1 and H2 on unpaved, and H1, H2 and H3 on tarmacadam surface as it varied in the range of 241 to 271 kg, 281 to 317 kg at gear H1, and 286 to 306

kg at gear H2 on the unpaved surface and between 269 to 289 kg at gear H1, 287 to 298 kg at gear H2, and 306 to 327 kg at gear H3 on the tarmacadam surface while operating between 26 to 68 cm hitch height on both the surfaces. Whereas the vertical load acting on the drawbar showed a declining trend in all three operating speeds for both road surfaces for the given payload on increasing the hitch height. The vertical load reduced from 756 to 561 kg (L3), 688 to 514 kg (H1) and 658 to 488 kg (H2) on the unpaved surface, and 644 to 504 kg (H1), 593 to 468 kg (H2), and 580 to 445 kg (H3) on tarmacadam surface while raising the hitch height from 26 to 68 cm, respectively. Similar trends were observed for both draft and vertical load while experimenting with 2500 and 3000 kg payloads on all surface gradients.

Hence, it can be concluded that on both the test surfaces, in all gear sear selections, payloads, and surface gradients, the change in hitch height did not have any considerable effect on the draft requirement throughout the experiment. However, the vertical load on the drawbar showed an inverse relationship with the hitch height, i.e., as the hitch height increased, the drawbar vertical load decreased under all operating conditions.

6.6.2 Effect of hitch height on per cent front axle load and tractive efficiency

While operating with a 3000 kg payload at gradient 3, increasing the hitch height resulted in the reduction of front axle load thereby triggering concern for longitudinal instability of the tractor. This reduction in front axle load means more weight transfer from the front to the rear axle and thus increasing the rear axle weight. The additional weight on the rear axle translates to better tractive efficiency. Therefore, though increasing the hitch height compromises the longitudinal stability, it encourages the tractive efficiency of 2WD tractors.

On increasing the hitch height from 26 to 68 cm, the front axle load decreased from 24.56 to 17.53%, 24.39 to 16.48%, and 22.95 to 14.21% with 3000 kg payload, while operating in gear L3, H1 and H2 on the unpaved surface, respectively. Similarly, the axle load decreased from 25.61 to 19.63%, 23.95 to 17.04%, and 23.62 to 16.26% with a payload of 3000 kg, while operating in gears H1, H2, and H3, respectively, on tarmacadam surface. Thus, it was observed that operating the trailer with the given payloads on gradient 3 at higher hitch heights caused an alarming situation on the longitudinal stability of the test tractor. Likewise, similar behaviour were found for front axle load and tractive efficiency when operating with 2000 and 2500 kg payloads on all surface gradients and gear settings.

6.6.3 Effect of hitch height on slip and tractive efficiency

The relationships between slip and tractive efficiency against hitch height of the trailer with a 2500 kg payload at gradient 2 indicate that the wheel slip decreased with the increase in hitch height while the tractive efficiency increased with the increase in hitch height. The wheel slip improved from 20.71 to 10.94% (L3), 21.39 to 10.67% (H1), 21.68 to 11.18% (H2) when operating on the unpaved surface, and 14.92 to 8.99 % (H1), 13.91 to 9.02% (H2), 14.99 to 9.24% (H3) on the tarmacadam surface while increasing the hitch height from 26 to 68 cm, respectively. Correspondingly, tractive efficiency improved from 62.43 to 82.16% (L3), 66.4 to 89.48% (H1), 66.85 to 91.97% (H2) on the unpaved surface, and 51.56 to 71.49% (H1), 55.6 to 74.76% (H2), 60.97 to 78.62% (H3) on the tarmacadam surface.

Increasing the hitch height had a positive effect on the wheel slip and tractive efficiency of the tractor. Tractive efficiency was calculated from the developed computer program with the inputs obtained from the field experimental values. The experiment revealed that slip and tractive efficiency had an inverse relationship with each other. These phenomena were evident in all conditions of operation.

6.7 Evaluation of the Developed Automation System

The instrumented test tractor was operated on unpaved and tarmacadam surfaces to evaluate the position of auto variable hitch height under dynamic conditions on varying surface gradients and payloads.

6.7.1 Effect of payload on the hitch height

The test revealed that, whenever the load on the front axle was more than 25% of the total static weight of tractor, the hitch height automatically raised, in order to lower the front axle load. On the other hand, if the front axle load was detected below 20%, the hitch lowered to recommended 20% of total tractor weight.

While pulling payloads of 2000, 2500 and 3000 kg on unpaved surfaces in gear H1, the hitch was found at 41, 26 and 26 cm heights with the corresponding load on the front axle as to be 24.12, 23.84 and 24.51% of total static weight of tractor, respectively, on surface gradient 3. However, when these payloads were trailed on tarmacadam surface, the hitch height was recorded at 31, 26 and 26 cm, respectively, with the corresponding values of front axle load being 25.5, 25.17 and 24.56%. Similarly, the drawbar hitch height dropped from 57 to 46 cm, and further to 34 cm when the payload was increased from 2000 to 2500

kg, and further to 3000 kg, respectively, while operating on an unpaved surface in gear H2. The corresponding front axle load was recorded as 20.46, 19.19 and 19.41%, respectively. Likewise, the hitch height dropped from 68 to 63 cm, and 63 to 55 cm as the load increased from 2000 to 2500 kg and 2500 to 3000 kg on the tarmacadam surface in gear H2. The corresponding front axle load was recorded as 19.69, 19.63 and 19.58%, respectively. Thus, the developed automation system managed to position the hitch height corresponding to the design and safe range of front axle load by automatically varying the hitch height under dynamic conditions. This phenomenon was evident under all test conditions.

6.7.2 Effect of surface gradient on the hitch height

The instrumented test tractor along with the trailer was operated with different payloads on varying surface gradients to analyse the effect of surface gradient on the drawbar hitch height. As the surface gradient steepens, the test showed that, for any given payload, the hitch height was generally lowered to a value corresponding to about 20% of the front axle load. The test was carried out on both road surfaces in gears H1 and H2.

While operating with a 2500 kg payload on unpaved surface in gear H1, the hitch height was recorded at 51, 35 and 26 cm when towing on gradients 1, 2 and 3, respectively, with the corresponding values of front axle load recorded as 24.45, 24.17 and 23.84%. Similarly, while operating on tarmacadam surface, the hitch was recorded at 53, 26 and 26 cm height when travelling on gradients 1, 2 and 3 respectively, with the corresponding values of front axle load being recorded as 24.83, 24.67 and 25.17%.

Likewise, while towing a 2500 kg payload on unpaved surface gradient 1 in gear H2, the hitch height was recorded at 68 cm each while operating on surface gradients 1 and 2 as the front axle load measured 20.07 and 19.03%, respectively. The hitch height was reduced to 47 cm when operating on gradient 3 to optimise the front axle load to 19.19%. Similarly, the hitch height of the drawbar was recorded at 68 cm when operating on tarmacadam surface gradients 1 and 2 as the front axle load measured 21.07 and 20.02%, respectively. However, the hitch was automatically reduced to 63 cm height when operating on gradients 3 to optimise the front axle load to 19.63%. Thus, the developed auto variable hitch system managed to optimise the front axle load to the required safe limit by varying the hitch height within its limit under different surface gradients. This process was evident throughout the study under all test conditions.

6.8 Conclusions

The major conclusions of the study are enlisted as follows:

1. A system was developed to measure the front axle dynamic load using a load cell mounted below the front axle.
2. A hydraulically operated variable hitch point that can vary from 26 to 68 cm above the ground surface was developed.
3. The hitch height had no considerable effect on the draft requirement; however, the vertical component of the drawbar pull had an inverse relationship in all operating conditions.
4. Lowering the hitch height reduced the weight transfer and consequently enhanced the longitudinal stability.
5. The increase in hitch height decreased the wheel slip due to higher weight transfer from the front axle and enhanced the tractive performance.
6. An automation system was successfully developed to optimise the front axle load between 20 to 25% of the total static weight of tractor by varying the hitch height.
7. The automatic variable hitch mechanism enabled the test tractor to operate at higher tractive efficiency without compromising the longitudinal stability within the effect of the specified range of hitch height.